AD NUMBER

AD880416

LIMITATION CHANGES

TO:

Approved for public release; distribution is unlimited.

FROM:

Distribution authorized to U.S. Gov't. agencies and their contractors; Critical Technology; NOV 1970. Other requests shall be referred to Army Aviation Materiel Laboratory, Fort Eustis, VA. This document contains export-controlled technical data.

AUTHORITY

usaamrdl ltr, 23 jun 1971

AD

USAAVLABS TECHNICAL REPORT 70-65

STUDY OF THE PERFORMANCE OF ADHESIVE BONDED JOINTS

FINAL REPORT

By

Harold K. Shen

John L. Rutherford

November 1970

U. S. ARMY AVIATION MATERIEL LABORATORIES
FORT EUSTIS, VIRGINIA

CONTRACT DAAJ02-69-C-0094
KEARFOTT DIVISION
SINGER-GENERAL PRECISION, INC.
LITTLE FALLS, NEW JERSEY

147

DISCLAIMERS

The findings in this report are not to be construed as an official Department of the Army position unless so designated by other authorized documents.

When Government drawings, specifications, or other data are used for any purpose other than in connection with a definitely related Government procurement operation, the United States Government thereby incurs no responsibility nor any obligation whatsoever; and the fact that the Government may have formulated, furnished, or in any way supplied the said drawings, specifications, or other data is not to be regarded by implication or otherwise as in any manner licensing the holder or any other person or corporation, or conveying any rights or permission, to manufacture, use, or sell any patented invention that may in any way be related thereto.

DISPOSITION INSTRUCTIONS

Destroy this report when no longer needed. Do not return it to the originator.

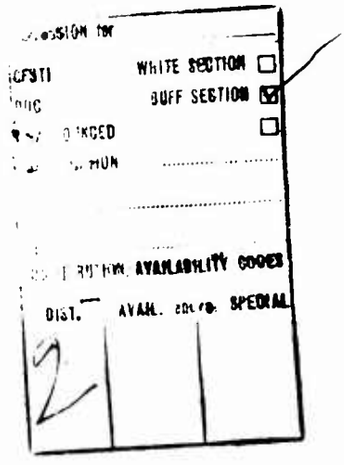

DEPARTMENT OF THE ARMY
HEADQUARTERS US ARMY AVIATION MATERIEL LABORATORIES
FORT EUSTIS, VIRGINIA 23604

This program was carried out under Contract DAAJ02-69-C-0094 with Singer-General Precision, Inc.

The information contained in this report is a result of research conducted to study the behavior and performance of adhesive bonded joints when subjected to tensile and shear loading conditions and service variables. Through selected experimental investigation and using high-sensitivity capacitance-type extensometers, tensile modulus, shear modulus, elastic limit, yield stress, fracture stress, and viscoelastic strain were determined for various combinations of adhesives, adherend materials, and service conditions.

This report has been reviewed by the U.S. Army Aviation Materiel Laboratories and is considered to be technically sound. It is published for the exchange of information and the stimulation of future research.

Task 1F162204A17001
Contract DAAJ02-69-C-0094
USAAVLABS Technical Report 70-65
November 1970

STUDY OF THE PERFORMANCE OF ADHESIVE BONDED JOINTS

Final Report RC 70-3

By

Harold K. Shen
John L. Rutherford

Prepared by

Research Center
Kearfott Division
Singer-General Precision, Inc.
Little Falls, New Jersey

for

U.S. ARMY AVIATION MATERIEL LABORATORIES
FORT EUSTIS, VIRGINIA

ABSTRACT

The purpose of this work was to observe the effects of selected experimental and material variables on the performance of metal/metal adhesive bonded joints. Three adhesives were used: FM1000, EC2214 and Metlbond 329 with aluminum and titanium adherends. The major experimental variables were test temperature and strain rate. Material variables included composition of adhesive, adherend material, bond-line thickness and tapered bond-lines. The following properties were determined for tensile and shear loading: modulus, microyield stress, precision elastic limit, viscoelastic flow, and fracture behavior. Lap shear properties were also measured. The strains were determined using a high sensitivity capacitance-type extensometer.

It was found that the tapered bond-lines did not degrade the properties; in fact, the viscoelastic flow was considerably reduced. The adhesives at 72°F, and higher, were elastic only up to about 5 to 15 percent of the fracture stress. The elastic limits were lower and the viscoelastic flow was higher for shear loading than for tension. Raising the test temperature and lowering the strain rate produce similar effects. Temperature cycles below the curing temperature did not influence the room-temperature properties. Poor bonding procedures and out-of-date adhesives provided the most damaging effects on the properties.

FOREWORD

The work reported here was performed in the Research Center, Kearfott Division, Singer-General Precision, Inc., at Little Falls, New Jersey, under Contract DAAJ02-69-C-0094, Task 1F162204A17001. It was sponsored by the Structures Division, U.S. Army Aviation Materiel Laboratories, Fort Eustis, Virginia, with Mr. Thomas Mazza serving as project monitor. This final report covers work performed from 12 June 1969 through 12 June 1970.

The project was conducted under the supervision of Dr. John L. Rutherford, Program Manager, with Dr. Harold K. Shen serving as Principal Investigator. The following people also contributed to the program: Messrs. Laverne Dunham, Thomas Magnini, and Andrew Skurna. All machining and adherend refinishing was the responsibility of Mr. Charles Bing, Manager, Model Shop.

TABLE OF CONTENTS

LIST OF ILLUSTRATIONS

LIST OF ILLUSTRATIONS (cont'd)

LIST OF TABLES

LIST OF TABLES (cont'd)

LIST OF TABLES (cont'd)

INTRODUCTION

The objectives of this research program were to: provide a better understanding of adhesive bonded joints, obtain information needed to improve present technology in the design of bonded structures, and evaluate the effects and interaction of adhesive material variables and service test variables on bonded joints. To accomplish these, microstrain techniques were used to determine the mechanical properties of metal/metal bonded joints as a function of a number of experimental and material variables. Microstrain analysis employs high sensitivity capacitance-type extensometers capable of resolving extensions of the order of 5×10^{-7} inches and angles of twist of 6×10^{-8} radians.

EXPERIMENTAL PROCEDURES

TEST MATERIALS

In this program, two adherend materials were used: 7075 aluminum alloy in the T 6 condition and titanium - 6 aluminum - 4 vanadium in the full hard condition. Three adhesives were studied:

1. Metlbond 329, Narmco Materials Division, Whittaker Corporation. This is a 100-percent-solids, modified epoxy adhesive film supported on a synthetic fabric carrier. Since it is symmetric, it is not necessary to orient the film with respect to the adherends. Metlbond 329 provides for load-bearing metal-to-metal and sandwich applications capable of long-time operation at temperatures ranging from -423° to 450°F.

2. EC2214, 3M Company. This is a one-part, 100-percent-solids, thermosetting liquid adhesive which gives off no volatile by-products during cure. It has high impact, peel and bend strengths with a service temperature range of -70° to 200°F.

3. FM1000, Bloomingdale Department, American Cyanamid Company. This adhesive is a white, elastomeric unsupported film designed for structural bonding of all metals, sandwich construction, wood and plastics. A primer is not required except where processing requires "tacking" of the film in place.

HIGH SENSITIVITY EXTENSOMETER

In order to measure strains of a few percent in a specimen whose gage length may be as small as 0.005 inch (the adhesive in a bonded joint, for example), it is necessary to have an extensometer that can resolve deformations as small as 10^{-6} or 10^{-7} inches. Such an instrument has been developed and is in daily use in the Research Center [1,2,3]. The basic instrumentation was originally conceived for deformation studies of metals. A description of that extensometer is presented here.

- It has the highest theoretical (10^{-8}) and practical (10^{-7}) extension sensitivity of all available gages.
- Since the extensometer is mounted on the specimen, it does not record any deformations in the loading assembly.
- This extensometer measures bulk behavior, and does not modify or alter the surface structure of the specimens.

- Sensitivities of 2×10^{-7} inches are routinely obtained, even after large prestrains (25 percent strain with a 1-inch gage length).
- The present extensometer has been used at temperatures between 4.2° and 473°K. A design has been worked out for an extensometer capable of operating up to about 1000°K.
- By matching the coefficients of expansion of the specimen and the extensometer material, temperature fluctuations as large as ±0.1°K do not influence the results.
- The capacitance bridge output is easily recorded.
- Present extensometers can be used with specimen diameters ranging from 0.060 to 1.250 inches and lengths from 0.002 to 3 inches.

The extensometer consists of two parallel copper plates, in close proximity, which are mounted concentrically on the tensile specimen (a schematic diagram is shown in Figure 1). A suitable circuit determines the capacitance of the system, which is a measure of the separation of the plates according to the formula

$$C = \frac{\alpha K A}{D}$$

where

C = capacitance

α = a constant

K = dielectric constant of medium between plates

A = area of smaller plate

D = distance between plates

Thus a change in the distance between the plates means a change in the capacitance, so that any changes in the length of the test section can be recorded. The extensometer forms one leg of a capacitance bridge which is balanced at the beginning of the test. As the specimen is extended, the capacitance of that leg decreases, thereby unbalancing the bridge. The bridge out-of-balance voltage is amplified and fed to the X-axis of an X-Y recorder.

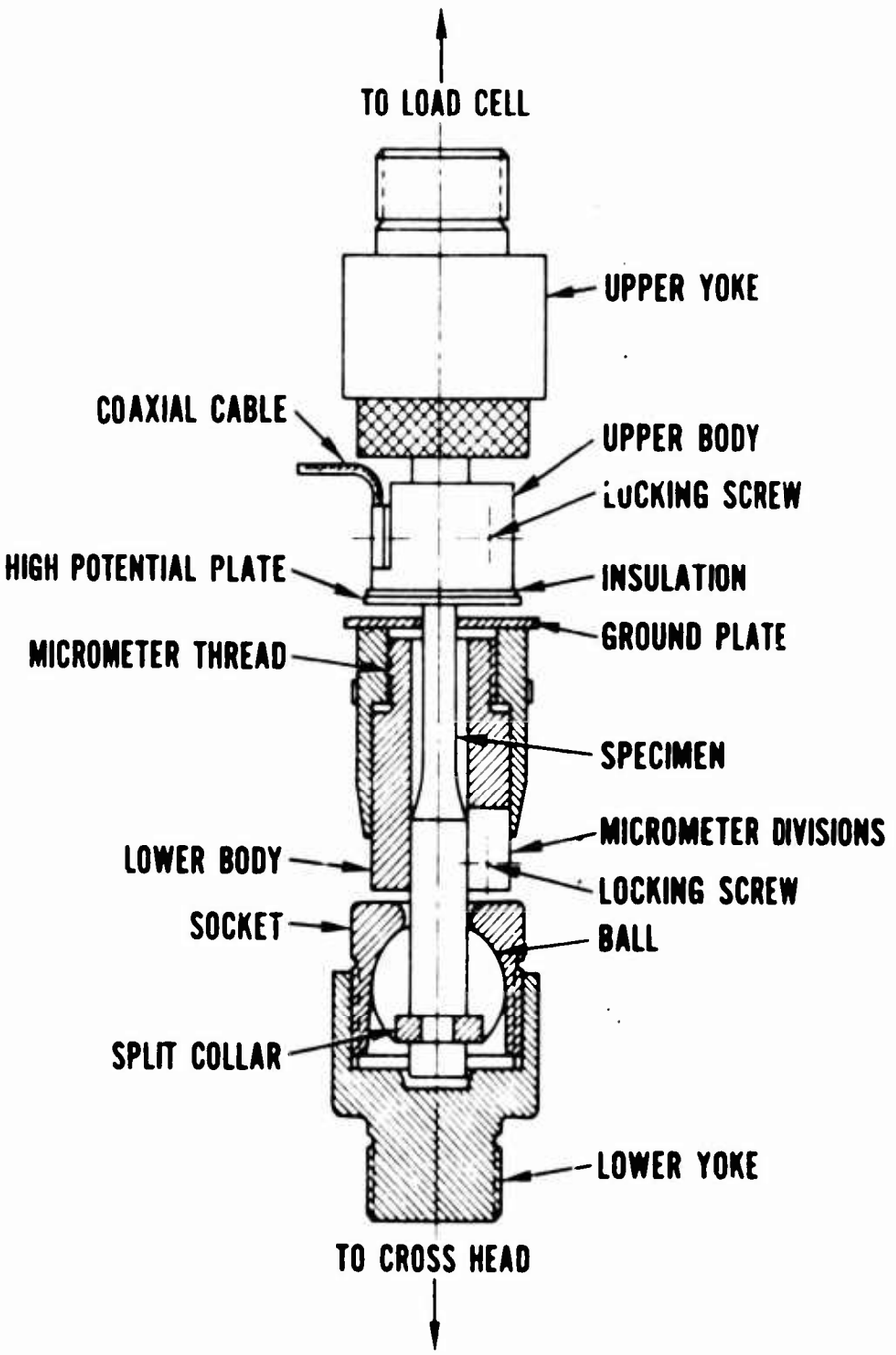

Figure 1. Capacitance-Type Extensometer.

To calibrate the extensometer, one plate is mounted on a precision micrometer thread so that it can be moved accurately a small distance. The response of the pen on the X-axis gives the sensitivity, which may be as high as 5×10^{-7} inches per division (20 divisions per inch of graph paper). The sensitivity is controlled through three variables: initial plate separation (usually about 0.025 inch), voltage range of X-axis on recorder, and amplification of bridge out-of-balance voltage (Robertshaw Fulton Proximity Meter). Other things being equal, the smaller the gap, the greater the sensitivity, since a given displacement represents a larger percentage of change in a small gap than in a large gap.

During the development of the capacitance extensometer and the evaluation of alternate methods, consideration was given to the amount of bending introduced during tensile testing. Misalignment was established with the use of both bonded resistance strain gages and a Huggenberger mechanical strain gage placed at different points around the circumference of a tensile specimen. The amount of bending was reported as the variation in reading of the gages for different stress levels. Combinations of chains and universal joints were first used and were found to introduce strain differences of 10 percent and higher. The minimum amount of bending (about 5 percent) resulted when a ball-and-socket joint was mounted on each end of the specimen. It was found that a small (bias) load had to be maintained at all times to preserve a[illegible]ity.

ADHEREND PREPARATION

All the adherends and bonding fixtures used in this program were machined from 7075 aluminum in the T-6 condition and Ti-6Al-4V as heat treated. The tensile specimens were in the form of a butt joint made with adherends having a circular cross section and a diameter at the epoxy/adherend interface of 0.500 inch. A schematic view of an adherend and the gripping assembly is shown in Figure 2. The machining specifications for the adherends are as follows: (1) the adhesive face to be flat within one light band of helium (5876 Å); (2) the adhesive face to be perpendicular to the surface of the 0.500-inch diameter within 0.00005 inch Total Indicated Reading (T.I.R.); (3) the 0.500-inch diameter to be round within 0.00005 inch and to match the mating adherend diameter within 0.00005 inch T.I.R.; (4) the adhesive face surface to have a roughness of 4 to 5 microinches (arithmetic average, using the standard cutoff width of 0.030 inch) with the stylus traverse made in several directions; (5) the adhesive face circumference to have a sharp edge with a maximum radius of 0.002 inch. The several machining processes have been organized so as to meet these specifications.

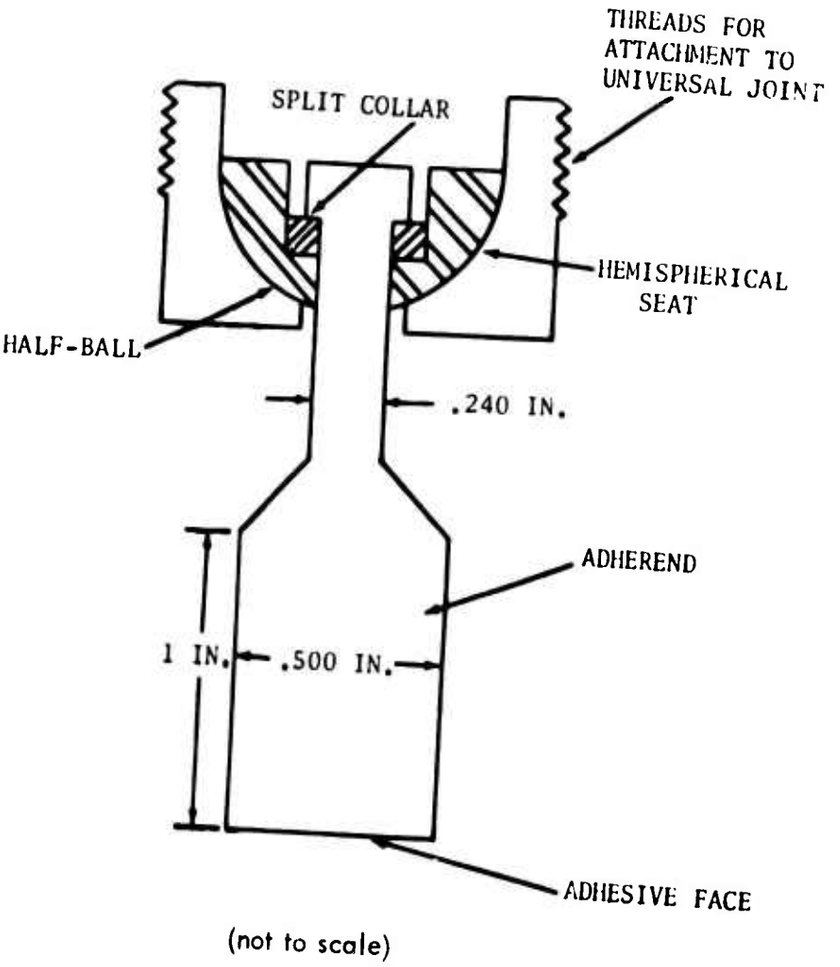

Figure 2. Tensile Adherend Gripping Assembly.

For shear tests, napkin-ring type adherends were used. At the adhesive face, these adherends are right circular hollow cylinders, having a 3-inch outside diameter and a wall thickness of 0.125 inch. The opposite ends of the adherends have wall thicknesses of 1 inch for attaching to the torsion test apparatus. The machining specification for the shear adherends was the same as for the tensile specimens with these additional requirements: the adhesive face to be perpendicular to the surface of the inside diameter within a T.I.R. of 50×10^{-6} inches and the inside and outside diameters of the adhesive face to be concentric to within 10^{-4} inch T.I.R.

There were three major reasons for selecting this type of shear test:

1. With tests such as these, the loading mode is pure shear; that is, there are no tensile forces acting on the joint. With more commonly used lap shear tests, cleavage loading is always present due to elastic or plastic deformation of the metal adherends. Thus the lap shear test data are difficult to interpret in terms of shear characteristics.

2. Pure shear tests do not involve dimensional changes in the specimen. This is in contrast to tensile tests where the material is elongated in one direction and tends to contract laterally to maintain constant volume (Poisson's ratio). In tensile tests and lap shear tests using metallic adherends bonded together, the difference in Poisson's ratio between the metal and the adhesive material influences the deformation characteristics of the adhesive. That is, when the joint is strained in tension, the adhesive material is not free to contract laterally according to its own Poisson's ratio because it is constrained to follow the Poisson contraction of the adherend. This constraint on the adhesive material is present in both tensile tests and lap shear tests. In napkin-ring tests, where the only deformation is pure shear, the absence of dimensional changes eliminates any effects resulting from differences in the Poisson's ratio between the adherend and the adhesive material.

3. In all torsion tests, the strain is a function of the radial distance from the axis of rotation. The strain is zero at the axis of rotation and increases to a maximum at the perimeter of the specimen. With this variable strain, it is difficult to calculate the shear modulus. Thus, a thin-walled tube is used where the wall thickness is small compared to the diameter of the tube. The strain changes so little across this wall that it can be considered uniform.

The lap shear adherends were carefully machined to 1 inch by 6 inches in the various thicknesses.

Two adherend cleaning methods were used prior to bonding: one for aluminum and the other for titanium. These two were selected after evaluating other procedures. The cleaning method for aluminum was developed by the Forest Products Laboratory, University of Wisconsin:

1. Degrease.
2. Dip in chromic acid solution at 150° ± 5°F for 10 minutes.
   sodium dichromate - 1 part/weight
   distilled water - 20 parts/weight
   concentrated sulfuric acid - 10 parts/weight
3. Rinse the metal thoroughly in cold, running distilled or deionized water.
4. Oven dry at 145° ± 5°F for about 10 minutes or air dry.

For titanium adherends, a procedure developed by the American Cyanamid Company was used:

1. Wipe with methyl ethyl ketone.
2. Degrease with trichloroethylene vapor.
3. Pickle in the following water solution at room temperature for 4 minutes:
   nitric acid - 15% by weight
   hydrofluoric acid - 3% by weight
4. Rinse in tap water at room temperature.
5. Immerse in the following water solution at room temperature for 2 minutes:
   trisodium phosphate - 50 grams/liter of solution
   potassium fluoride - 20 grams/liter of solution
   hydrofluoric acid (50% solution) 26 milliliters/liter of solution
6. Rinse in tap water at room temperature.
7. Soak in 150°F tap water for 15 minutes.
8. Spray with distilled water and air dry.

One of the methods for observing the surface finish of the tensile and shear adherends was a Talysurf profile. In this method, a stylus is drawn across the surface and the vertical displacement is recorded on a strip chart. A diamond stylus with a tip radius of 10^{-4} inch was employed; the stroke length was 0.5 inch. The strip chart moved at a rate 20 times faster than the stylus, giving an effective linear

magnification of 20. The sensitivity of the vertical travel was 10×10^{-6} inches per division of chart paper. On all adherends Talysurf profiles were made in two directions, at right angles to each other. A typical trace on an as-lapped adherend is shown in Figure 3. To ensure that the cleaning procedures used prior to bonding did not cause the flatness and roughness to exceed the above tolerances, Talysurf measurements were made on each adherend at regular intervals. If the Talysurf profiles indicated that the flatness or roughness tolerances were exceeded, the adherend was refinished by lapping. A typical profile of a specimen damaged by the cleaning solutions is shown in Figure 4.

SPECIMEN PREPARATION

The test specimens were bonded immediately after cleaning. Very careful fixturing was used to guarantee concentricity and axiality of the three types of specimens. In each case, the fixtures were made of the same material as the adherends so as to minimize differential strains due to different coefficients of thermal expansion.

The tensile specimens were prepared in a V-block assembly. Two V-blocks were mounted on a base with a removable end plate; one V-block has two spring clips for holding the adherend. To obtain a constant joint thickness using this fixture, the following procedure is employed: a precision shim (having a thickness equal to the desired bond-line thickness) is placed on the end plate, and one of the adherends is placed in the V-block in firm contact with the shim and held in place with the spring clips. The other adherend is then placed in the second V-block and pressed against the first adherend. A U-type clamp is used to hold this adherend in position. The base plate and shim are then removed as was the adherend held in position with the spring clips. The adherend still clamped in the V-block is then coated with the adhesive. The uncoated adherend is replaced in the spring clamp V-block and positioned about 1/16 inch away from the coated surface. The end plate is replaced in position (without the shim) and slowly tightened down. This procedure results in a joint having the proper bond-line thickness. Excess adhesive is wiped away from the joint immediately after assembly. The adherends are held this way until the curing cycle is completed.

The shear specimens were bonded using a specially designed central arbor. Figure 5 is a photograph of two napkin-ring type adherends and the central bonding arbor used to fixture them during the cure cycle. The arbor consists of a metal shaft surrounded by a Teflon ring (a) at the position of the adhesive line. Three steel pins (b) located at 120° intervals are press-fitted into the shaft through the Teflon ring to provide the arbor with a dimensionally stable diameter. During cure, these pins seat against the inner surface of the adherends at the bond line

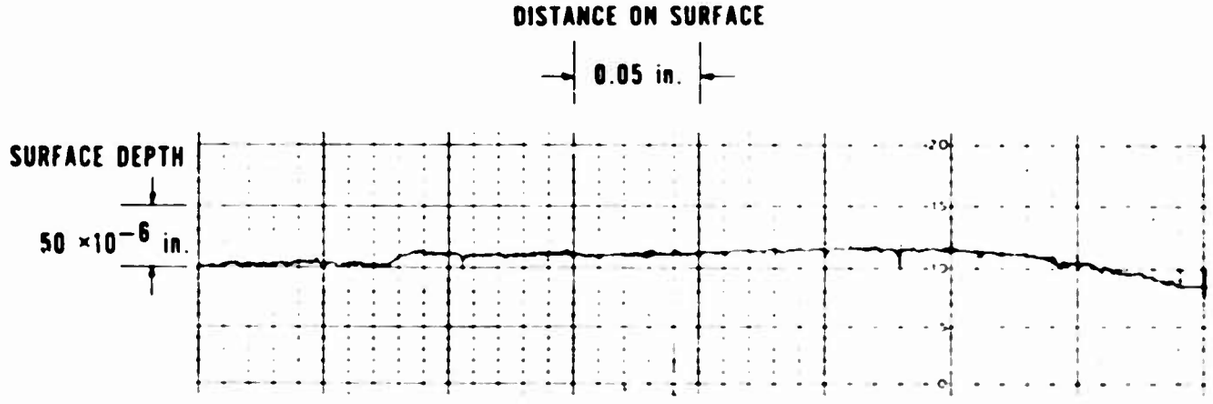

Figure 3. Talysurf Profile of Tensile Adherend After Lapping.

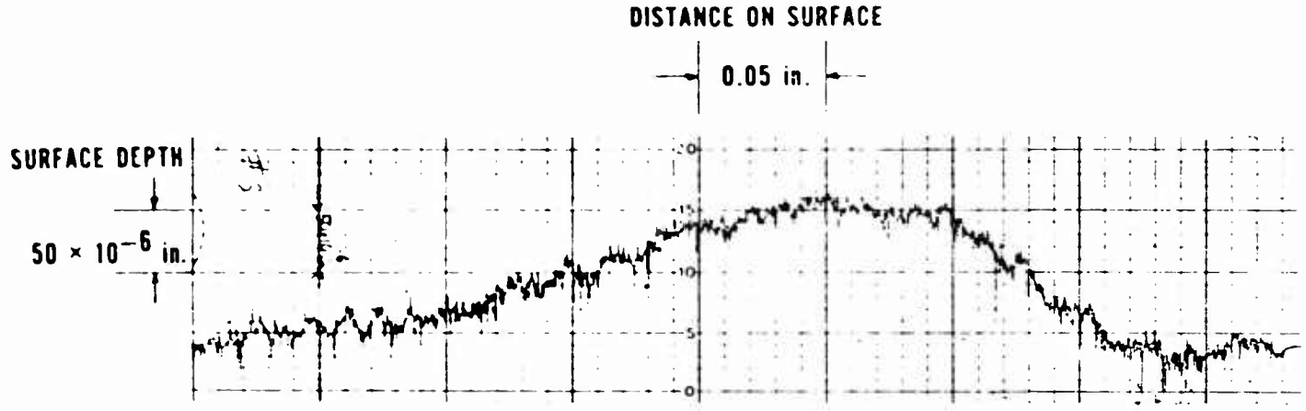

Figure 4. Talysurf Profile of Tensile Adherend After Several Bonding and Cleaning Cycles.

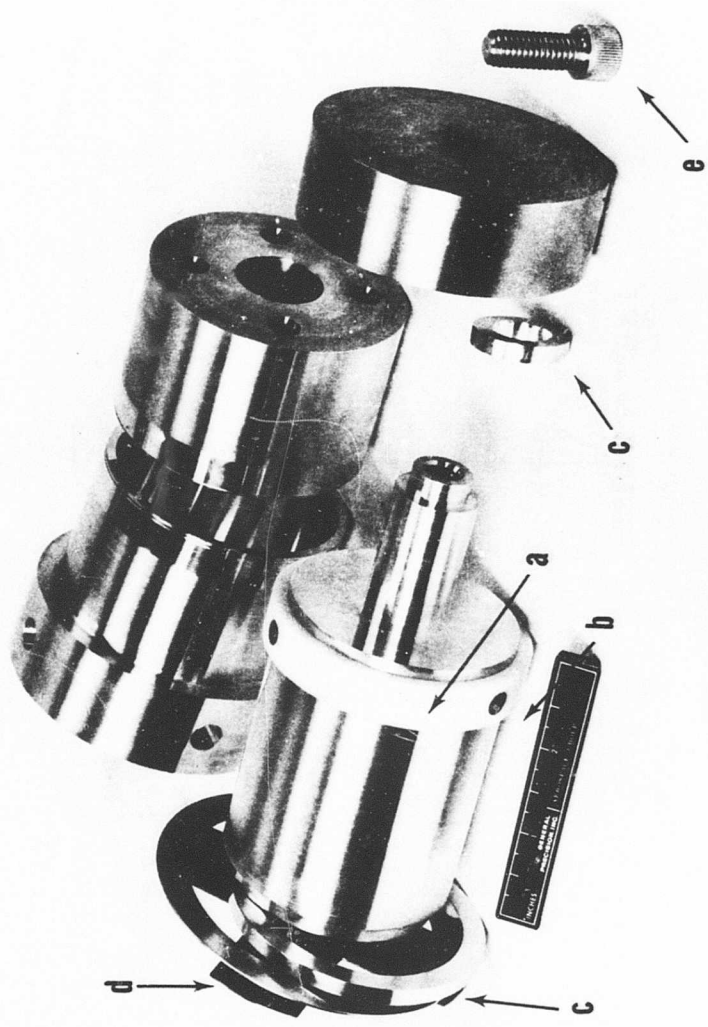

Figure 5. Shear Adherends and Bonding Fixture.

and maintain concentricity of the adherends with respect to each other. The Teflon ring serves to prevent bonding of the arbor to the adherends, and also keeps the inner diameter of the adherend free of adhesive. Close-fitting slip rings (c) are located at both ends of the arbor, thus providing axiality of the adhesive-bonded adherends. Since both axiality and concentricity of the adherends is insured, the adherend faces (which have been carefully machined perpendicular to the axis of the adherends) remain parallel to each other and thus provide a uniform bond thickness. The bond-line thickness obtained is constant to within ±0.0005 inch for the majority of joints prepared in this manner. For cast adhesives, joint thickness is established by holding the adherends apart with gage blocks located between pins (not shown) which have been press-fitted into the adherends. A leaf spring (d) bolted to the end of the arbor maintains pressure during the cure, preventing movement of the gage blocks. Gage blocks are not used for sheet adhesives, the bond thickness being determined by both the initial sheet thickness and the pressure applied through the leaf spring. The pressure is continuously adjustable to 25 psi by controlling the position of the bolt (e). Higher pressure can be attained by using a stiffer spring.

After completion of the cure, the adherends are removed from the fixture in an arbor press. Since adhesion between the arbor and adherends occurs only at the steel pins, the adherends are easily dismounted.

The bond-line thickness for both tensile and shear specimens is determined by measuring the distance between pairs of diamond-shaped indentations located on the adherends. These indentations are formed with a micro-hardness tester and spaced at 90° intervals on the adherends behind the grooves. The separation of the marks is measured first with the clean adherends butted together, and again after bonding. The precision of this measurement is of the order of 0.5×10^{-4} inches.

The lap shear specimens were made in a Carver Hydraulic Press using a fixture designed to produce aligned specimens with a uniform bond-line thickness. Each lap shear specimen was prepared individually. Finger-type specimens that must be cut apart after bonding were not used.

The cure cycles for the three adhesives are shown in Table 1 and are identical for both aluminum and titanium adherends.

SHEAR TESTS

The shear tests [2,3] use napkin-ring type adherends as described above. The shear specimen consists of two relatively thin-walled tubes bonded together end to end; they are loaded by rotating one adherend relative to the other about an axis

TABLE I . CURE CYCLES FOR ALUMINUM AND TITANIUM ADHEREND SPECIMENS

	FM1000	EC2214	Metlbond 329
Temperature (°F)	350	250	350
Time (hr)	2	2/3	2
Pre-Heat Temperature (°F)	160	160	160
Rate of Heating (°F/min)	≈6	≈4	≈6
Shear Bonding Pressure (psi)	26	0	26
Tensile Bonding Pressure (psi)	≈150	0	≈150

coincident with the longitudinal axis of the specimen. The torsion testing apparatus is shown schematically in Figure 6. A central axle supports the bonded shear specimen by means of close-fitting bushings. One adherend is bolted to an end plate; the other adherend has a torsion sprocket fastened to it. Torque is applied to this latter adherend through two chains on opposite points of the torsion sprocket. Two chains eliminate any bending moments on the specimen. The apparatus is attached to the cross-head of an Instron Testing Machine, and the loading chains are connected to the load cell in the top of the Instron. The capacitance-type extensometer is mounted straddling the adhesive bonded joint so that one capacitor plate is stationary along with the fixed adherend while the other plate moves as the second adherend rotates. The resultant change in plate separation introduces a new capacitance value which is calibrated in terms of angle of twist. A second extensometer, not shown in Figure 6, is mounted on one of the adherends for use as a load cell. It records the deformation in the adherend as a shear stress. Load-extension curves are drawn on an X-Y recorder, with the output from the extensometer that measures the angle of twist fed to the X-axis while the "load cell" extensometer signal is put into the Y-axis.

For measuring the angle of twist, the extensometer is attached to split rings which fit into grooves in the adherends near the adhesive bonded joint. The grooves serve to locate the split rings, in a reproducible manner, at a distance of 0.030 inch from each adherend face. Thus the amount of adherend deformation contributing to the observed extension is limited to a gage length of 0.060 inch, representing a significant improvement over multiple joint designs in which the large adherend deformation obscured the results. Here, for a typical choice of adherend material and adhesive system, the adherend deformation represents less than 15% of the total deformation and may be accurately accounted for through calibration procedures.

The standard test procedure is to record load-extension curves for load-unload cycles starting at very low maximum stress values. Load cycles are repeated at increasing maximum stress values until the specimen fractures. Such procedures are necessary to reveal the precision elastic limit, microyield stress, viscoelastic behavior, etc. When necessary, the procedures were modified to accommodate the test objectives.

The standard cross-head speed for shear tests was 0.5 in./min. To observe strain rate effects, two other speeds were used: 2.0 and 0.05 in./min. For the standard bond-line thickness of 0.008 in., these cross-head speeds represent strain rates of 2.9×10^{-1}, 7.2×10^{-2} and 7.2×10^{-3} per minute, in order of decreasing speeds.

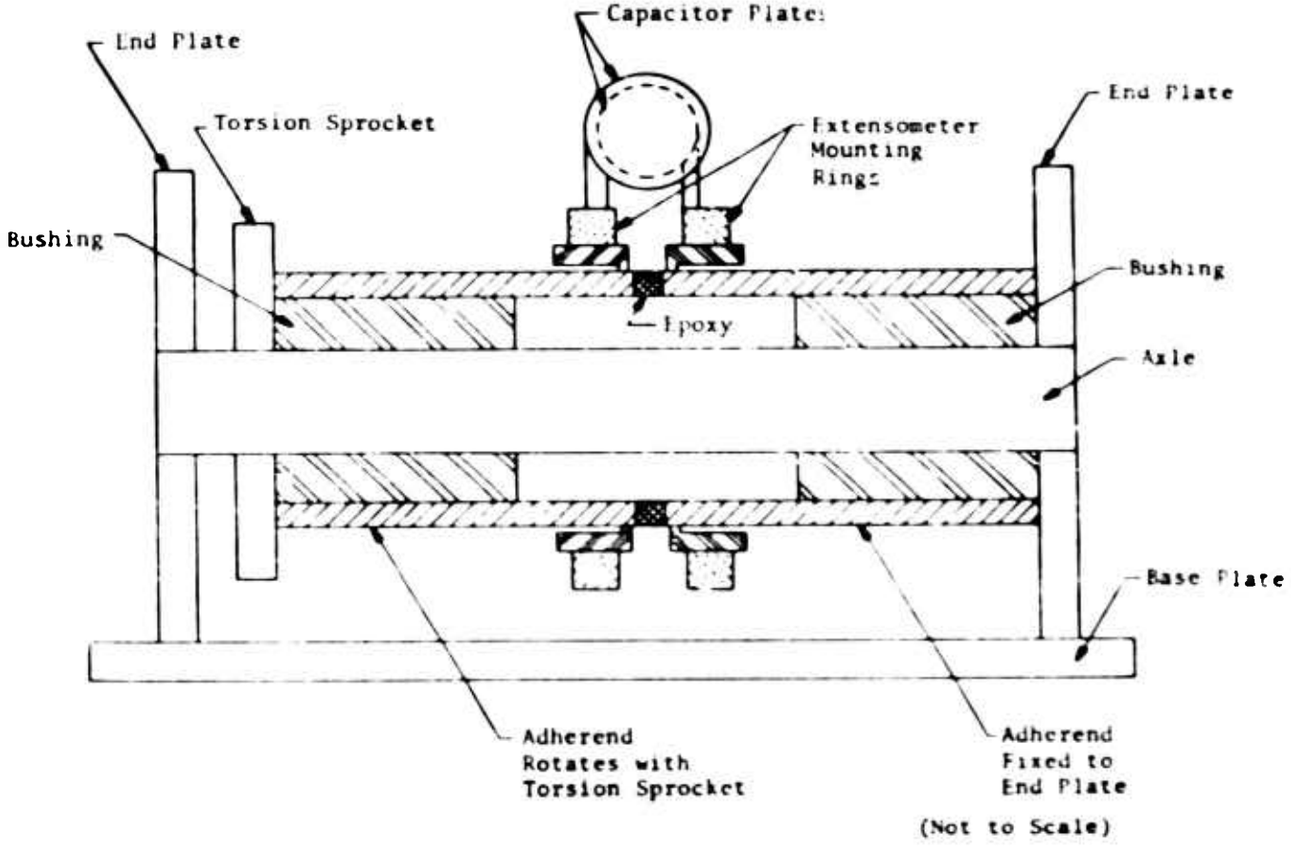

Figure 6. Torsion Testing Apparatus.

The entire torsion apparatus fits inside an environmental chamber so that tests may be made at temperatures ranging from -100° to 375°F. High-temperature testing uses an air atmosphere, while the low-temperature work is done in carbon dioxide gas. Temperature is controlled to ± 2°F, and a thermocouple is attached to the specimen to record its temperature. This same environmental chamber was used for the tensile and lap shear tests.

The shear modulus calculation starts with the torque T applied to the bonded joint

$$T = PD$$

where P is half the output of the adherend load cell (the load in each chain) and D is the torsion sprocket diameter. The shear stress applied to the adhesive joint is

$$\tau = TC/J$$

where C is the radial distance to the center line of the joint and J is the polar moment of inertia given by

$$J = \pi/32 \, (d_o^4 - d_i^4)$$

where d_i and d_o are the inner and outer diameters of the adherends. The width of the adherend face is 0.125 inch, sufficiently small compared to the 1.5-inch radius of the adherends that the shear stress across it may be considered constant.

Substituting for T and J in the equation for τ,

$$\tau = \frac{PDC}{\pi/32 \, (d_o^4 - d_i^4)}$$

The shear strain γ is related to the angle of twist, $\Delta\theta$, by

$$\gamma = C/L \; \Delta\theta$$

where L is the gage length of the specimen (bond-line thickness). For small displacements, $\Delta\theta$ is approximated by $\Delta s/r$ (the displacement measured with the extensometer divided by the radial distance to the center of the extensometer).

The shear modulus G is given by

$$G = \tau/\gamma$$

Substituting, this becomes

$$G = \frac{PDLr}{\pi/32\,(d_o^4 - d_i^4)\;\Delta s}$$

Putting in the numerical values from the equipment,

$$G = 8.06\,PL/\Delta s$$

TENSILE TESTS

As described above, the tensile specimen consists of two ½-inch-diameter metal rods adhesive bonded end to end. Each adherend is gripped in a ball-and-socket joint as shown in Figure 2. Previous studies have shown that such an arrangement minimizes any bending in the specimen during application of the load. A small bias load, about 10 to 20 pounds, is always maintained on the specimen to preserve alignment in the tensile assembly. Similar to the shear tests, the tensile specimen is subjected to load-unload cycles at increasing maximum stress values until fracture occurs. With these tensile tests [1,3], the applied load is measured by the Instron load cell whose signal output is fed to the Y-axis of the recorder. The tensile deformation is measured using a capacitance-type extensometer that straddles the adhesive bonded joint. This also requires that the recorded data be corrected for the adherend deformation included in the extensometer output (this correction is of the order of 15 percent for a typical specimen).

For standard tensile tests, a cross-head speed of 0.02 in./min was used; with a bond-line thickness of 0.008 inch, this was a strain rate of 7.5×10^{-3}/min. For strain rate effects, two other cross-head speeds were used: 0.1 and 0.002 in./min, corresponding to strain rates of 3.75×10^{-2} and 7.5×10^{-4}/min, respectively.

LAP SHEAR TESTS

All lap shear tests were made in the environmental chamber mounted in the Instron Testing Machine. Wedge-type grips were used with spacers so that the test alignment was axial. The standard cross-head speed was 0.5 in./min for all the tests; additional speeds of 0.05 and 2.0 in./min were also to be used to observe any strain rate effects. All specimens were taken directly to fracture.

DATA TO BE REPORTED

The following data, where applicable, were recorded for each test:

1. Specimen Number - Specimens are identified by a code using a combination of letters and numbers, where the first three letters identify the adhesive, the adherend, and the type of test (F for FM1000, E for EC2214, M for Metlbond 329, T for titanium, A for aluminum, S for shear, T for tensile and L for lap shear). The next element is either a pair of angles separated by a slash or one or two digits. The angles are the tapers of each adherend bonding face (see Test Program) used for nonuniform bond-line thicknesses, while the digits identify a particular pair of adherends used for bond lines of uniform thickness. The number following the dash is the test sequence.

2. Bond-Line Thickness - When one value is given, it refers to the uniformly thick bond. If two values are reported, they are the minimum and maximum thicknesses of the tapered bond line.

3. Effective Tensile Modulus - This term is used when discussing the tensile modulus of adhesives in the thin-film form between two adherends. This is in recognition of the fact that the observed modulus is for a material under severe constraint. When the epoxy is bonded to a metal adherend, it is not free to deform according to its own Poisson's ratio, but must conform to that of the adherend which generally has a lower value for the Poisson's ratio. By restricting the lateral contraction of the epoxy, the tensile modulus is effectively increased. Thus, the measured value in these thin-film tests is an effective modulus rather than the modulus found in the material when it is free to deform according to its own dictates.

4. Shear Modulus - The shear modulus is the ratio of the stress to strain, within the elastic limit, when the strain is measured as the displacement per unit length caused by shear stress per unit area. In napkin-ring tests, the only deformation is pure shear (as opposed to tensile or lap shear tests), and thus any effects resulting from differences in the Poisson's ratio between the adherend and the adhesive material are eliminated.

5. Precision Elastic Limit - The precision elastic limit is the maximum stress to which a specimen may be loaded and still behave elastically, with the deformation remaining a single-valued function of the load. The word precision is used since very small deviations from elastic behavior may be observed. Generally, the elastic limit depends on the sensitivity with which the stress-strain relationships are observed.

6. Microyield Stress - This is the lowest stress level, during a load-unload cycle, which results in the first permanent strain at the bias stress. Only the strain that persists several minutes after unloading is considered permanent.

7 Mode of Fracture - There are two possible modes of failure in thin-film epoxy adhesive joints: cohesive and adhesive. In cohesive failure, the epoxy itself fractures. This type of failure can be recognized by the presence of a layer of adhesive on each of the adherends. Another term for this fracture is "center-of-bond" failure. Adhesive failure occurs when the fracture is at the interface between the adhesive and the adherend, i.e., the adhesive/adherend bond fails. This is generally characterized by what appears to be a clean metallic surface after fracture. However, close examination may reveal a microscopically thin layer of epoxy remaining on the adherend surface. The results are presented as percentage of cohesive failure.

8. Fracture Stress - The fracture stress is that stress at which the joint fails. It is calculated by dividing the load at fracture by the cross-sectional area of the adhesive bond.

9. Viscoelastic Strain (ϵ_1) - Upon completion of a load-unload cycle from a stress level above the microyield point, there is a set remaining in the specimen. In fact, this is the major method for determining that the yield point has been exceeded. Very often the set disappears with time; that is, the specimen slowly returns to its original length. The value reported here is the set in the bonded joint immediately upon unloading to the bias stress (the minimum load maintained to preserve axiality in the loading assembly). When discussing viscoelastic, recovered or permanent strain, it is necessary to report the maximum stress level used in that load-unload cycle.

10. Recovered Strain (ϵ_2) - This is the amount of strain that is recovered within two minutes after unloading; it is viscoelastic recovery.

11. Permanent Strain (ϵ_3) - The strain remaining in the specimen after the 2-minute recovery ($\epsilon_3 = \epsilon_1 - \epsilon_2$). These 3 viscoelastic strain parameters are shown in Figure 7. For shear strains, the symbols γ_1, γ_2 and γ_3 are used.

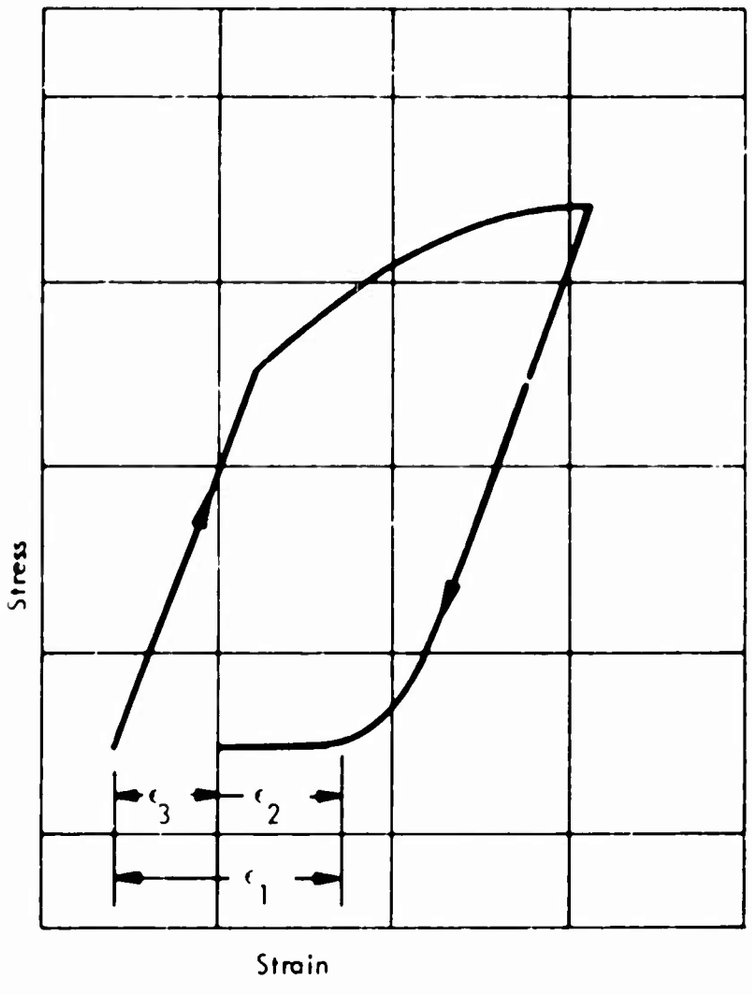

Figure 7. Viscoelastic Strain Parameters.

TEST PROGRAM

The test program was divided into nine phases. It is summarized in Table II and described in more detail below.

Phase I - Base-Line Data

The objectives of this phase were to: establish the base-line values of the standard tests for comparison with subsequent tests having different test conditions; examine six different bond-line tapers so as to select three for use in the balance of the program; select the best adherend thickness for lap shear tests.

The standard tests were made with FM1000 on aluminum adherends at the intermediate cross-head speeds (0.5 in./min for shear and 0.02 in./min for tension) at room temperature with a 0.008-inch-thick bond line.

Six different tapered bond-line thicknesses were investigated for shear tests (Figure 8):

1. an included angle of 22 minutes with the bond center plane normal to the longitudinal axis of the specimen (designated as 11'/11')
2. an included angle of 44 minutes with the bond center plane normal to the longitudinal axis of the specimen (designated as 22'/22')
3. an included angle of 22 minutes with the bond center plane tilted 11 minutes from normal to the longitudinal axis of the specimen (designated as 22'/0)
4. an included angle of 11 minutes with the bond center plane tilted 5.5 minutes from normal to the longitudinal axis of the specimen (designated as 11'/0)
5. an included angle of 0° with the bond center plane tilted 11 minutes from normal to the longitudinal axis of the specimen (designated as $11'_A/11'_C$)
6. an included angle of 0° with the bond center plane tilted 22 minutes from normal to the longitudinal axis of the specimen (designated as $22'_A/22'_C$)

TABLE II. SUMMARY OF TEST PROGRAM

Phase	Program Elements	EXPERIMENTAL VARIABLES														NUMBER OF SPECIMENS									
		Adhesive			Adherend		Cross-Head Speed +			Temperature (°F)			Bond-Line Thickness			Shear				Tension				Lap Shear	Total
		FM1000	2214	329	Al	Ti	High	Std	Low	75°	-65°	160°	Std	.004	.020	Std	•1	•2	•3	Std.	•4	•5	•6		
I	Base-Line Data	X			X			X		X			X			2	4	4	4	2	4	4	4	6	34
II	Adherend Material	X				X		X		X			X			2	2	2	2	2	2	2	2	2	18
III a	Cryogenic	X				X		X			X		X			2	2	2	2	2	2	2	2	2	36
III b		X			X			X			X		X			2	2	2	2	2	2	2	2	2	
IV a	Strain Rate	X			X				X	X			X			2	2	2	2	2	2	2	2	2	36
IV b		X			X		X			X			X			2	2	2	2	2	2	2	2	2	
V	Cryogenic Strain Rate	X			X		X				X		X			2	2	2	2	2	2	2	2	2	18
VI a	Bond-Line Thickness		X		X			X		X				X		2	2	2	2	2	2	2	2	2	36
VI b			X		X			X		X					X	2	2	2	2	2	2	2	2	2	
VII a	High Temperature			X	X			X		X			X			2	2	2	2	2	2		2	2	36
VII b				X	X			X				X	X			2	2	2	2	2	2		2	2	
VIII	High Temp. Strain Rate			X	X				X			X	X			2	2	2	2	2	2		2	2	18
IX	Ageing Environ.	X				X		X		X			X							12					12

+ See text (Experimental Procedures)

• Tapered bond-lines; see Phase I results

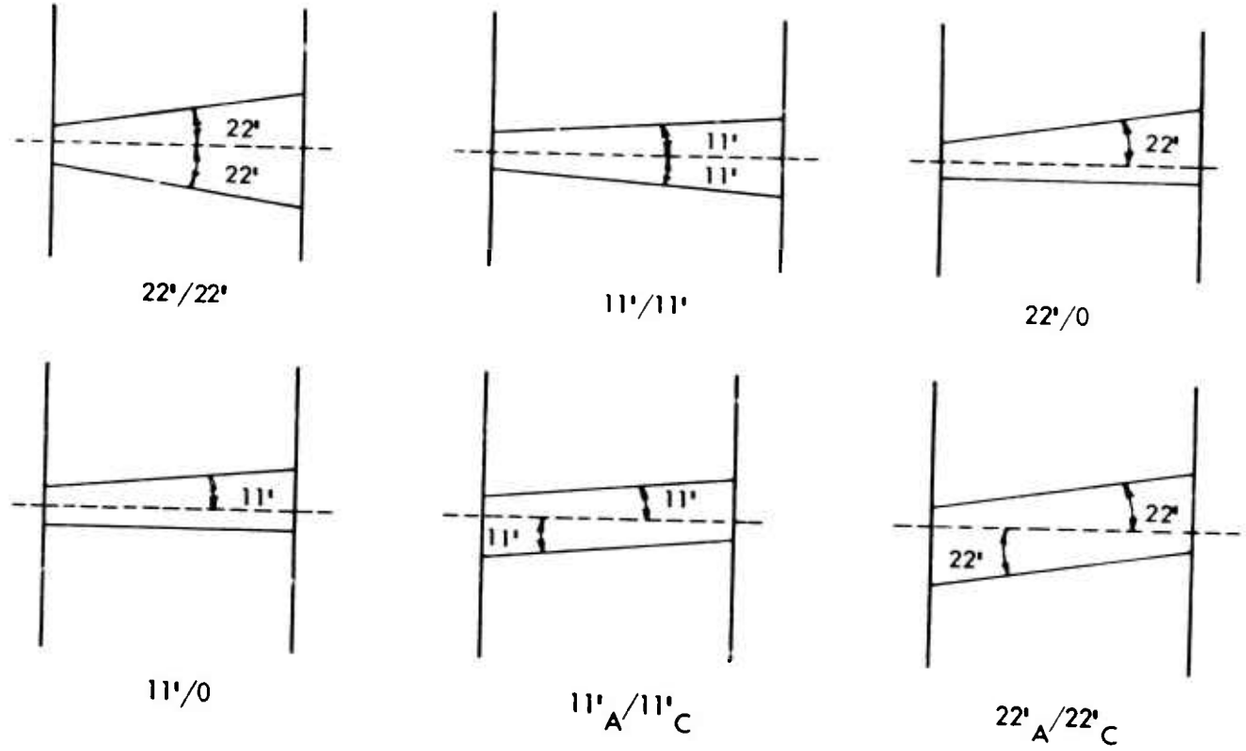

Figure 8. Nonuniform Bond-Line Configurations for Shear Tests.

Six different tapered bond-line thicknesses were investigated for tensile tests (Figure 9):

1. an included angle of 4° with the bond center plane normal to the longitudinal axis of the specimen (designated as $2^{\circ}/2^{\circ}$)
2. an included angle of 2° with the bond center plane normal to the longitudinal axis of the specimen (designated as $1^{\circ}/1^{\circ}$)
3. an included angle of 2° with the bond center plane tilted 1° from the normal to the longitudinal axis of the specimen (designated as $2^{\circ}/0^{\circ}$)
4. an included angle of 1° with the bond center plane tilted $\frac{1}{2}^{\circ}$ from the normal to the longitudinal axis of the specimen (designated as $1^{\circ}/0^{\circ}$)
5. an included angle of 0° with the bond center plane tilted at an angle of 2° from the normal to the longitudinal axis of the specimen (designated as $2^{\circ}_{A}/2^{\circ}_{C}$)
6. an included angle of 0° with the bond center plane tilted at an angle of 1° from the normal to the longitudinal axis of the specimen (designated as $1^{\circ}_{A}/1^{\circ}_{C}$)

From each group of 6 tapered bond lines, 3 were to be selected for use in Phases II through VIII.

For the lap shear tests, aluminum adherends were used in 4 thicknesses: 0.088, 0.062, 0.048 and 0.032 inch. Following evaluation of the results, one thickness was to be used for all subsequent lap shear tests.

Phase II - Adherend Material

To determine the effect of an adherend having a higher modulus of elasticity, the tests made in Phase I were repeated using Ti-6Al-4V adherends. Only 8 shear, 8 tensile, and 2 lap shear tests were made using the thickness values selected in Phase I.

Phase III - Cryogenic

The low-temperature characteristics of FM1000 were measured at -65°F using both aluminum and titanium adherends. All other experimental variables were the same as in Phase II.

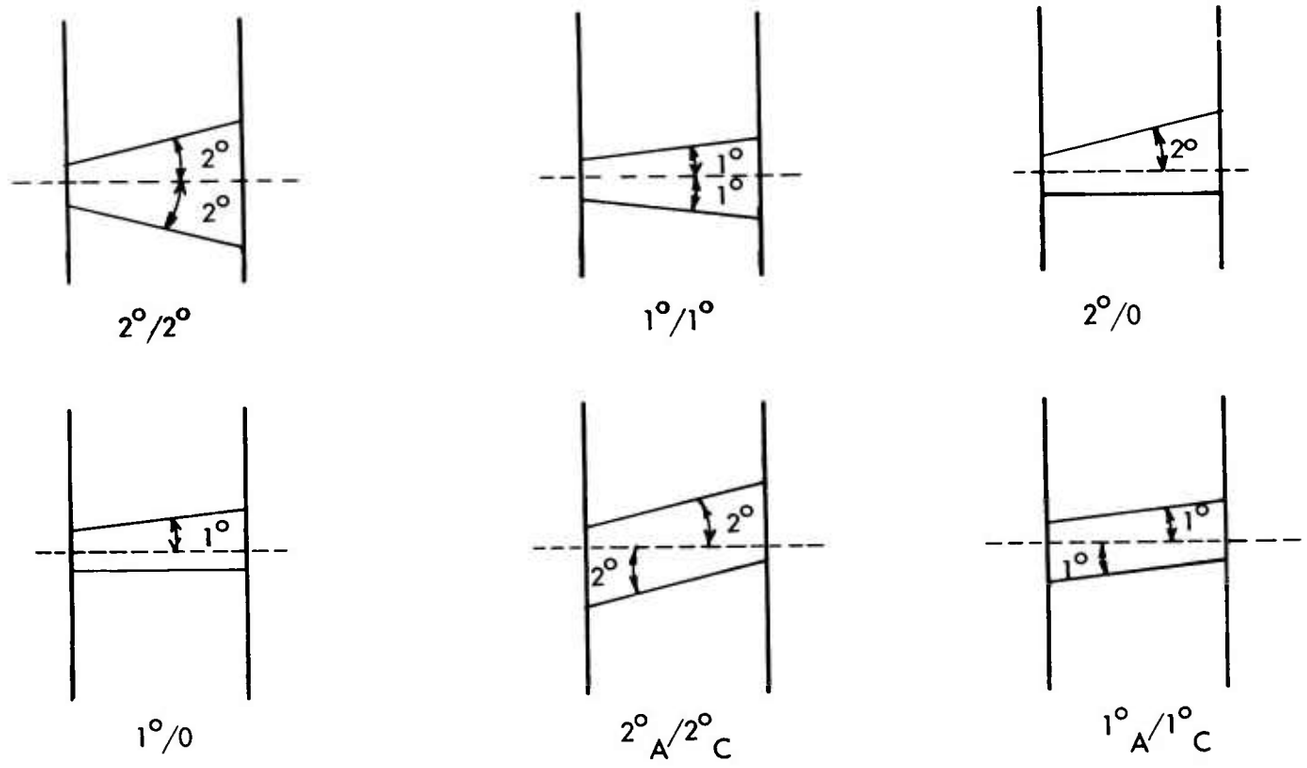

(not drawn to scale)

Figure 9. Nonuniform Bond-Line Configurations for Tensile Tests.

Phase IV - Strain Rate

Tests were made with FM1000 on both aluminum and titanium adherends at high and low cross-head speeds (2.0 and 0.05 in./min for shear; 0.1 and 0.002 in./min for tension).

Phase V - Cryogenic/Strain Rate

Since low test temperatures and high strain rates both are known to increase modulus values, they were combined in this phase. Tests were made with FM1000 on aluminum adherends at -65°F using cross-head speeds of 2.0 in./min for shear and 0.1 in./min for tension.

Phase VI - Bond-Line Thickness

Earlier work had shown that some mechanical properties depended on the thickness of the bond line. To evaluate this effect, shear, tensile and lap shear tests were made using thicknesses of 0.004 and 0.020 inch. Since FM1000 has an optimum bond-line thickness (0.008 inch), an alternate adhesive was selected, EC2214. This is a paste-type adhesive having no carrier cloth so that a thickness-dependence study could be made.

Phase VII - High Temperature

Adhesive properties were measured at 160°F using a high-temperature adhesive, Metlbond 329, with aluminum adherends. For comparison, another set of specimens was tested at room temperature; all other variables were kept constant.

Phase VIII - High Temperature/Strain Rate

To observe the combined influence of two factors that tend to lower the modulus values, tests were made on Metlbond 329, with aluminum adherends, at 160°F with the lowest strain rates (cross-head speeds of 0.05 in./min for shear and 0.002 in./min for tension).

Phase IX - Ageing/Environment

At the beginning of the program, tensile tests were made with fresh FM1000 on aluminum adherends. That batch of adhesive was stored until the end of the program, and new specimens were prepared and tested using the old adhesive.

RESULTS AND DISCUSSION

The test results and discussion are presented by phases. Each phase is introduced by a brief summary of the experimental variables, followed by three sections for the tensile, shear and lap shear tests. The results are given in tabular form and typical stress-strain curves are shown (the fracture point is indicated by an X at the end of the curve). It should be noted that the results presented here are for those specimens considered to be acceptable in terms of bond-line thickness and uniformity and having reasonable values for the fracture stress. Many specimens were rejected out-of-hand because the bond-line thickness was not correct or because it varied in random fashion. The test results for specimens having very low fracture stresses were discarded, for premature fracture was considered strong evidence of an improperly bonded specimen.

The test results for each phase are summarized in separate tables. To report experimental scatter values, the maximum and minimum variations from the average value are averaged. For the viscoelastic strain measurements (ϵ_1, ϵ_2, γ_1, γ_2), only approximate values are given because these stress level-dependent measurements were not all made at the same stress value. In some cases only one value is included in the summary table.

PHASE I, BASE-LINE DATA

The basic data, to be used for comparison with the other phases, were accumulated for FM1000 adhesive on aluminum adherends at room temperature with the standard cross-head speeds: tensile - 0.02 in./min, shear - 0.5 in./min, and lap shear - 0.5 in./min.

Tensile Tests

The results from the tensile tests of Phase I are presented in Table III, including the 6 tapered bond lines (see Figure 9). Table IV is a summary of the results with the experimental scatter. A typical tensile stress-strain curve is shown in Figure 10 (curve A). The elastic effective tensile modulus (E*) is calculated from the load-extension X-Y traces using the bond-line thickness as the gage length for determining the strain and the cross-sectional area of the adherend for the stress. For specimens with a tapered bond-line configuration, the gage length was taken to be the average thickness.

TABLE III. TENSILE, FM1000, ALUMINUM, PHASE I

Specimen Number	Average Bond-Line Thickness (10^{-3} in.)	Cross-Head Speed (in./min)	Test Temp. ($^{\circ}$F)	Elastic Tensile Modulus (10^5 psi)	Precision Elastic Limit (psi)	Microyield Stress (psi)	Fracture Stress σ_F (psi)	Fracture Mode (% cohesive)
FAT10-1	10.0	0.02	72	5.3	1020	2000	11000	100
FAT3-9	7.7	"	"	5.5	1120	2040	9995	60
FAT2°/2°-1	14.5-49.5	"	"	5.8	770	1170	12000	60
FAT2°/2°-2	5.5-41.0	"	"	5.2	1020	2280	9200	60
FAT1°/1°-1	4.6-22.1	"	"	5.0	640	1270	11700	85
FAT1°/1°-2	18.0-35.5	"	"	4.9	765	1530	12400	50
FAT2°/0°-1	7.7-25.2	"	"	4.9	610	714	9200	100
FAT2°/0°-2	8.6-26.1	"	"	7.5	894	1210	11000	80
FAT1°/0°-1	8.0-16.8	"	"	4.6	890	1530	11000	60
FAT1°/0°-2	8.4-17.2	"	"	5.7	765	1270	10400	90
$FAT2^{\circ}_{A}/2^{\circ}_{C}$-1	9.1	"	"	3.6	640	1500	9900	80
$FAT2^{\circ}_{A}/2^{\circ}_{C}$-2	8.0	"	"	3.0	764	1530	9200	80
$FAT1^{\circ}_{A}/1^{\circ}_{C}$-1	8.4	"	"	4.0	1020	2140	10200	80
$FAT1^{\circ}_{A}/1^{\circ}_{C}$-2	8.2	"	"	5.3	1520	2160	9830	75

TABLE III - Continued

Specimen Number	Average Bond-Line Thickness (10^{-3} in.)	Cross-Head Speed (in./min)	Test Temp. (°F)	ϵ_1 (10^{-3})	ϵ_2 (10^{-3})	ϵ_3 (10^{-3})	Stress Level (% σ_F)
FAT10-1	10.0	0.02	72	0.35	0	0.35	70
				1.35	0	1.35	90
FAT3-9	7.7	"	"	-	-	-	70
				0.90	0	0.90	90
FAT2°/2°-1	14.5-49.5	"	"	0.54	0	0.54	70
				0.95	0	0.95	85
FAT2°/2°-2	5.5-41.0	"	"	0.30	0.18	0.12	70
				1.60	0.50	1.10	90
FAT1°/1°-1	4.6-22.1	"	"	0.35	0	0.35	70
				1.05	0.3	0.75	90
FAT1°/1°-2	18.0-35.5	"	"	0.64	0	0.64	70
				0.80	0	0.80	90
FAT1°/1°-3	13.0-30.5	"	"	0.25	0.15	0.10	62
FAT2°/0°-1	7.7-25.2	"	"	1.0	0.5	0.5	67
				5.0	1.5	3.5	95
FAT2°/0°-2	8.6-26.1	"	"	0.15	0.07	0.08	70
				0.53	0.20	0.33	90

TABLE III - Continued

Specimen Number	Average Bond-Line Thickness (10^{-3} in.)	Cross-Head Speed (in./min)	Test Temp. (°F)	ϵ_1 (10^{-3})	ϵ_2 (10^{-3})	ϵ_3 (10^{-3})	Stress Level (% σ_F)
FAT1°/0°-1	8.0-16.8	0.02	72	0.14	0	0.14	60
				2.40	0.90	1.50	90
FAT1°/0°-2	8.4-17.2	"	"	1.00	0.68	0.32	75
$FAT2^{\circ}_{A}/2^{\circ}_{C}$-1	9.1	"	"	0.35	0.18	0.17	67
				2.70	0.80	1.90	90
$FAT2^{\circ}_{A}/2^{\circ}_{C}$-2	8.0	"	"	0.50	0	0.50	67
				1.25	0.70	0.55	90
$FAT1^{\circ}_{A}/1^{\circ}_{C}$-1	8.4	"	"	0.80	0.40	0.40	70
				2.60	0.80	1.80	90
$FAT1^{\circ}_{A}/1^{\circ}_{C}$-2	8.2	"	"	0.40	0.40	0	70
				2.50	1.20	1.30	91

TABLE IV. TENSILE SUMMARY, FM1000, ALUMINUM, PHASE I

Bondline Configuration	Cross-Head Speed (in./min)	Test Temp. ($^{\circ}$F)	Elastic Tensile Modulus (10^5 psi)	Precision Elastic Limit (psi)	Microyield Stress (psi)	Fracture Stress σ_F (psi)	ϵ_1 (10^{-3})	ϵ_2 (10^{-3})	Stress Level (%σ_F)
0/0	0.02	72	5.4±.1	1070±50	2020±20	10500±500	1.13±.23	0	90
$2^{\circ}/2^{\circ}$	"	"	5.5±.3	895±125	1725±555	10600±1400	1.27±.33	0.25±.25	≈ 80
$1^{\circ}/1^{\circ}$	"	"	5.0±.05	724±56	1530±180	11900±333	0.93±.08	0.15±.15	≈ 75
$2^{\circ}/0^{\circ}$	"	"	6.2±1.3	752±142	962±248	10100±900	0.58±.58	0.29±.29	≈68.5
$1^{\circ}/0^{\circ}$	"	"	5.2±.6	827±63	1400±130	10700±300	1.70±.7	0.79±.11	≈ 75
$2^{\circ}_A/2^{\circ}_C$	"	"	3.3±1.5	702±62	1515±15	9550±350	2.00±.7	0.75±.05	≈ 80
$1^{\circ}_A/1^{\circ}_C$	"	"	4.7±.7	1270±250	2150±10	10015±185	2.55±.05	1.00±.2	≈ 80

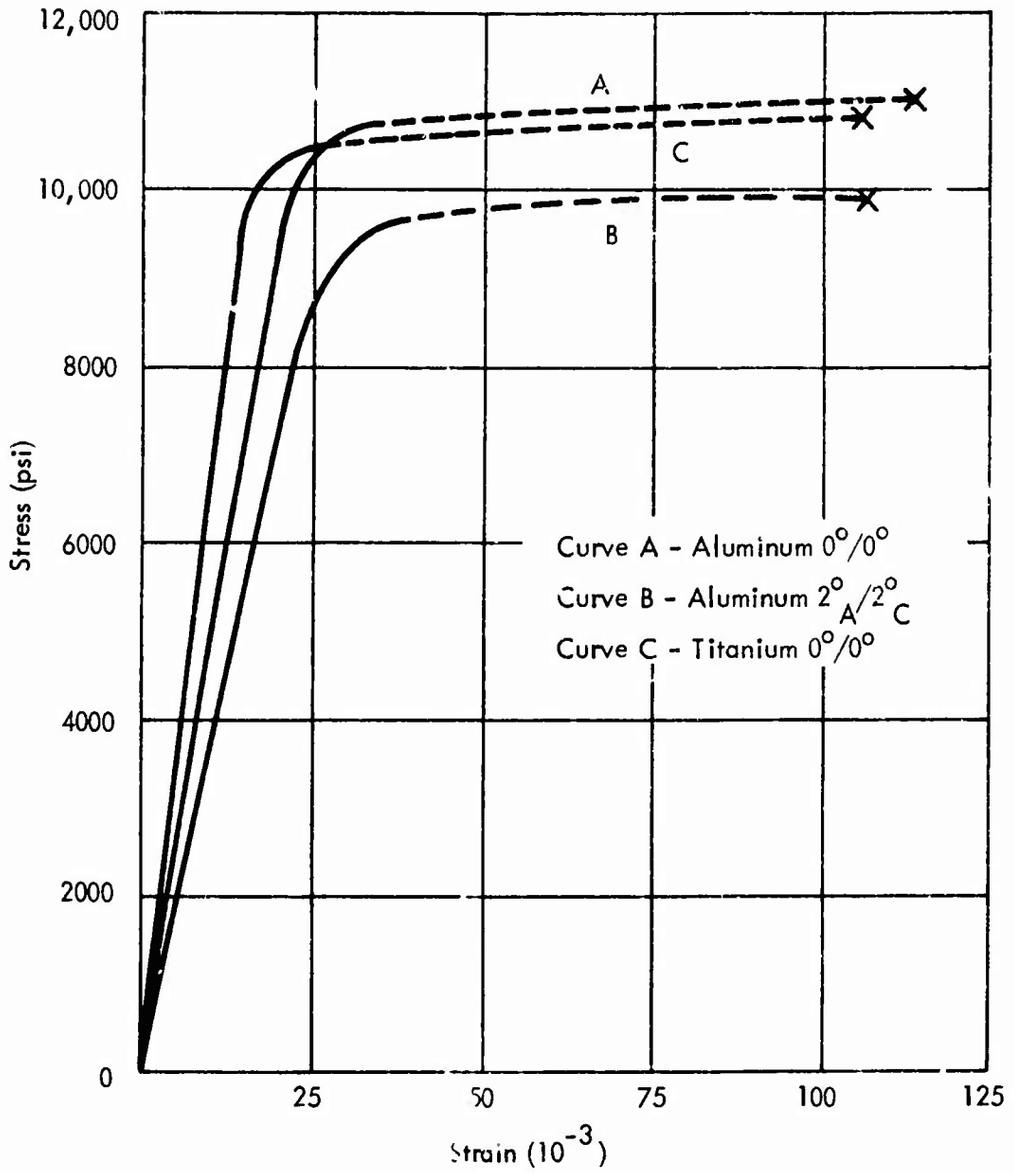

Figure 10. Tensile Tests, FM 1000, 72°F, Cross-Head Speed - 0.02 in./min.

Due to the large experimental scatter, it was difficult to determine the influence of nonuniform bond-line configuration on the elastic effective tensile modulus, within the experimental scatter there was no effect due to nonuniformity. Similar observations were made for the precision elastic limit, the microyield stress, the fracture stress, and the fracture mode. However, the strain at unloading, ϵ_1, was diminished when nonuniform bond lines were used. Comparing the uniform bond-line value of 1.13×10^{-3} for ϵ_1 to that for the $2^o/0^o$ value of 0.58×10^{-3}, it can be seen that there is a 49 percent decrease. For the other two selected configurations, the decrease was somewhat smaller.

One striking feature of the results is the deviation from elastic behavior at very low stress levels. The average precision elastic limit (P.E.L.) for all bond-line configurations was 870 psi, which is only 8 percent of the average fracture stress (10,500 psi). The P.E.L. is the first deviation from elastic loading; in this work it was in the form of a hysteresis loop. When the specimen was unloaded, there was no change in the length, but energy had been dissipated during the load-unload cycle. The P.E.L. was largely independent of the tapered bond-line configuration. The first permanent set (microyield stress) was found at an average value of 1580 psi. Thus, at only 15 percent of the average fracture stress, the bonded joint undergoes permanent damage. During load-unload cycles at higher maximum stress levels, proportionately greater damage was incurred. Above the microyield stress, viscoelastic flow was usually observed. The tapered joints had only a negligible influence on the microyield stress. For a quantitative description of viscoelastic behavior, three strain parameters are used as described in the section "Data To Be Reported" (also see Figure 7). The total strain remaining in the specimen at the instant unloading is finished is designated as ϵ_1. In all cases ϵ_1 was greater, the higher the maximum stress used in the load-unload cycle. For example, in Table III, specimen number FAT10-1 had a value of 0.35×10^{-3} for ϵ_1 when the stress was 70 percent of the fracture stress. When a cycle was made at 90 percent of the fracture stress, ϵ_1 was 1.35×10^{-3}. Thus, the strain upon unloading was greater by a factor of 4 for an increase of only 29 percent (7700 to 9900 psi) in the maximum stress. Sometimes the strain (ϵ_1) in the specimen at the instant of unloading would persist for long times (of the order of tens of minutes); in other cases, the specimen would recover some of that strain almost immediately.

For each load-unload cycle, the length of the specimen was monitored for 2 minutes after unloading. Experience has shown that the major part of the recovery after unloading occurs within 2 minutes. The columns of Tables III and IV labeled ϵ_2 show the strain recovered within that 2-minute waiting period. ϵ_3 is the difference between ϵ_1 and ϵ_2 and is called permanent strain; the word permanent means only that it exists after the 2-minute recovery time. Whether ϵ_3 would be found after several hours or days was not determined. For all specimens, the higher the maximum stress, the greater the amount of recovery and also the larger the amount of total

strain at unloading. It appears that for stresses below about 65 to 70 percent of the fracture stress, there is no recovery after unloading. Recovery occurs during the unloading process; most of the load-extension recordings do not have straight-line unloading that is typical of elastic behavior.

It appears that the viscoelastic strain, ϵ_1, was greatest for the two configurations ($2^{\circ}_A/2^{\circ}_C$ and $1^{\circ}_A/1^{\circ}_C$) whose normal to the bond center plane is not parallel to the longitudinal axis of the specimen. These are the two bond-line tapers that introduce the greatest amount of shear during the tensile loading. The values shown for columns ϵ_1 and ϵ_2 and stress level in Table IV are averages for all the data reported in Table III; it should be remembered that ϵ_1 and ϵ_2 depend on the stress level (percent σ_F) to which the load-unload cycle was made.

The fracture stresses averaged 10,500 psi for all specimen configurations. The highest values were for the $1^{\circ}/1^{\circ}$ tapered joint, while the lowest were for the $2^{\circ}_A/2^{\circ}_C$ configuration. In general, the tapered bond lines had only a negligible influence on the values of the fracture stress. For the $2^{\circ}_A/2^{\circ}_C$ and $1^{\circ}_A/1^{\circ}_C$ configurations (see Figure 9), the bond center plane is parallel to the two adherend faces, but all three of these planes are tilted. Thus, there is introduced a shearing action in addition to the tensile force. This may account for the observation that the lowest fracture stress was found for the $2^{\circ}_A/2^{\circ}_C$ taper in which the center plane tilt is 2°, the largest tested. A typical stress-strain curve is shown in Figure 10 (curve B) for a $2^{\circ}_A/2^{\circ}_C$ configuration. The fracture mode was characterized as percent cohesive (center of bond) using a visual estimating procedure. On the average, the fractures were about 80 percent cohesive in nature.

As discussed at the beginning of this section, many specimens were discarded because of fracture at very low stress levels. Examination of these specimens showed that the standard cleaning procedures had not been followed or that the adhesive had spoiled or that there were many voids in the joint. Thus, it appears that the bonding procedures are much more important in controlling the fracture stresses than is the introduction of nonuniform bond-line thickness.

Based on the results shown in Tables III and IV, three taper configurations were selected for use in the balance of the program:

1. an included angle of 4° with the bond center plane normal to the longitudinal axis of the specimen (designated as $2^{\circ}/2^{\circ}$)
2. an included angle of 2° with the bond center plane normal to the longitudinal axis of the specimen (designated as $1^{\circ}/1^{\circ}$)
3. an included angle of 2° with the bond center plane tilted 1° from the normal to the longitudinal axis of the specimen (designated as $2^{\circ}/0^{\circ}$)

The first two of these are symmetrical about a plane whose normal is parallel to the longitudinal axis of the specimen. The center plane of the third configuration is tilted 1° and the taper is not symmetrical as are the first two taper configurations (see top three sketches of Figure 9).

Shear Tests

At the beginning of the program it was extremely difficult to obtain satisfactory results with the tapered bond-line shear specimens. In order to obtain good results for at least 14 tests, over 42 specimens were made and evaluated. Results for 16 of the satisfactory tests are presented in Table V. The shear modulus (G) was calculated as described in the section "Shear Tests," using the average bond-line thickness as the gage length. A summary of these results, along with the experimental scatter, is presented in Table VI. A typical shear stress-strain curve is shown in Figure 11.

Deviations from elastic behavior occurred at very low stress levels. Taking the average for all specimens, the precision elastic limit was about 320 psi, which is only 3.4 percent of the average fracture stress (τ_F = 9500 psi). The average value for the stress necessary for the first permanent strain (microyield stress, τ_{mys}) was 620 psi, or 6.5 percent of the average fracture stress. These percentages are lower than those observed for the tensile tests (P.E.L. = 0.08 σ_F and σ_{mys} = 0.15 σ_F). With shear tests, the fracture mode was less cohesive (center of bond) in nature than was the case for the tensile tests. In these latter specimens the typical failure was 80 percent cohesive, while for the shear tests the average was only 33 percent cohesive. There was no strong correlation between mode of failure and failure stress. There were too few specimens having 100 percent cohesive failures to establish a limiting value in the total absence of any adhesive failure. Thus, it is not possible to say whether the fracture stress is established by localized adhesive failure, with the path of the propagating crack determining the specific mode of failure (cohesive vs adhesive).

In association with the low stress values for the onset of nonelastic behavior, the viscoelastic strain values were very high. These parameters, γ_1, γ_2 and γ_3, are the shear equivalent of those shown in Figure 7. In comparison to tensile tests, the viscoelastic flow occurred at lower stress levels and in greater quantity for comparable fractions of the fracture stress. Viscoelastic flow in shear occurred at stresses as low as 15 percent of the fracture stress. As the maximum stress for a load-unload cycle was raised, the viscoelastic strain increased rapidly. For specimen number FAS22'/0-5, the strain at unloading, γ_1, increased from 0.3×10^{-3} at 0.15 τ_F to 148.0×10^{-3} at 0.85 τ_F. To a great extent, the strain γ_1 was not permanent in the shear specimens. Averaging all the results for columns γ_1 and γ_2 in Table V shows

TABLE V. SHEAR, FM1000, ALUMINUM, PHASE I

Specimen Number	Average Bond-Line Thickness (10^{-3} in.)	Cross-Head Speed (in./min)	Test Temp. (°F)	Elastic Shear Modulus (10^5 psi)	Precision Elastic Limit (psi)	Microyield Stress (psi)	Fracture Stress τ_F (psi)	Fracture Mode (% cohesive)
FAS11-3	7.0	0.5	72	1.0	270	690	9700	0
FAS11-4	7.1	"	"	1.1	223	810	9300	10
FAS11-5	7.1	"	"	1.4	198	407	11400	60
FAS11-9	7.2	"	"	1.3	194	680	9900	0
FAS22'/22'-1	8.5-46.9	"	"	1.6	182	530	6450	10
FAS22'/22'-2	7.6-46.0	"	"	1.3	194	640	7000	10
FAS11'/11'-1	8.7-27.9	"	"	1.5	430	457	10600	50
FAS11'/11'-2	5.8-25.0	"	"	1.5	198	392	10700	50
FAS22'/0-5	4.7-23.9	"	"	1.3	515	710	7860	50
FAS22'/0-6	4.1-23.3	"	"	1.6	420	620	8330	0
FAS11'/0-1	9.4-19.0	"	"	1.6	290	680	9500	0
FAS11'/0-2	10.3-19.9	"	"	1.3	272	770	7300	0
$FAS22'_A/22'_C$-2	9.3	"	"	3.7	550	737	10700	70
$FAS22'_A/22'_C$-3	10.1	"	"	2.5	209	870	11600	60
$FAS11'_A/11'_C$-1	7.3	"	"	1.1	340	505	12400	50
$FAS11'_A/11'_C$-2	6.8	"	"	1.2	386	640	11600	85

TABLE V - Continued

Specimen Number	Average Bond-Line Thickness (10^{-3} in.)	Cross-Head Speed (in./min)	Test Temp. (°F)	γ_1 (10^{-3})	γ_2 (10^{-3})	γ_3 (10^{-3})	Stress Level (% τ_F)
FAS11-3	7.0	0.5	72	3.4	2.5	0.9	46
				20.0	2.6	17.4	52
FAS11-4	7.1	"	"	1.8	0.7	1.1	42
				100.0	10.0	90.0	65
FAS11-5	7.1	"	"	1.8	0	1.8	35
				13.5	0.8	12.7	43
FAS11-9	7.2	"	"	38.0	9.0	27	54
FAS22'/22'-1	8.5-46.9	"	"	3.0	3.0	0	50
				6.0	1.0	5.0	63
FAS22'/22'-2	7.6-46.0	"	"	0.40	0	0.40	50
				1.86	0.75	1.11	80
FAS11'/11'-1	8.7-27.9	"	"	2.1	0	2.1	54
				14.0	1.4	12.6	60
FAS11'/11'-2	5.8-25.0	"	"	1.2	0	1.2	50
				6.4	1.2	5.2	58
FAS22'/0-5	4.7-23.9	"	"	1.8	0	1.8	63
				148.0	-	-	85
FAS22'/0-6	4.1-23.3	"	"	0.5	0	0.5	57
				4.3	0.9	3.4	72

TABLE V - Continued

Specimen Number	Average Bond-Line Thickness (10^{-3} in.)	Cross-Head Speed (in./min)	Test Temp. (°F)	γ_1 (10^{-3})	γ_2 (10^{-3})	γ_3 (10^{-3})	Stress Level (% τ_F)
FAS11'/0-1	9.4-19.0	0.5	72	0.9	0	0.9	49
				3.4	0	3.4	63
FAS11'/0-2	10.3-19.9	"	"	2.0	0	2.0	66
				9.0	2.4	6.6	87
$FAS22'_A/22'_C$-2	9.3	"	"	2.1	0.8	1.3	30
$FAS22'_A/22'_C$-3	10.1	"	"	1.5	0	1.5	15
$FAS11'_A/11'_C$-1	7.3	"	"	2.3	0	2.3	21
$FAS11'_A/11'_C$-2	6.8	"	"	0.3	0	0.3	15

TABLE VI. SHEAR SUMMARY, FM1000, ALUMINUM, PHASE I

Bond-Line Configuration	Cross-Head Speed (in./min)	Test Temp. (^{o}F)	Elastic Shear Modulus (10^5 psi)	Precision Elastic Limit (psi)	Microyield Stress (psi)	Fracture Stress τ_F (psi)	γ_1 (10^{-3})	γ_2 (10^{-3})	Stress Level (% τ_F)
0/0	0.5	72	1.2±.2	220±38	648±200	10070±735	20.0	2.6	52*
22'/22'	"	"	1.5±.2	188±6	585±55	6725±275	3.0	3.0	50*
11'/11'	"	"	1.5±0	314±116	425±32	10650±50	2.1	0	54*
22'/0	"	"	1.5±.2	468±48	665±45	8095±235	1.8	0	63*
11'/0	"	"	1.5±.2	281±9	725±45	8400±1100	0.9	0	49*
$22'_A/22'_C$	"	"	2.1±.7	402±129	756±76	10830±510	2.1	0.8	30*
$11'_A/11'_C$	"	"	1.2±.1	363±23	573±68	12000±400	2.3	0	21*

* one datum point

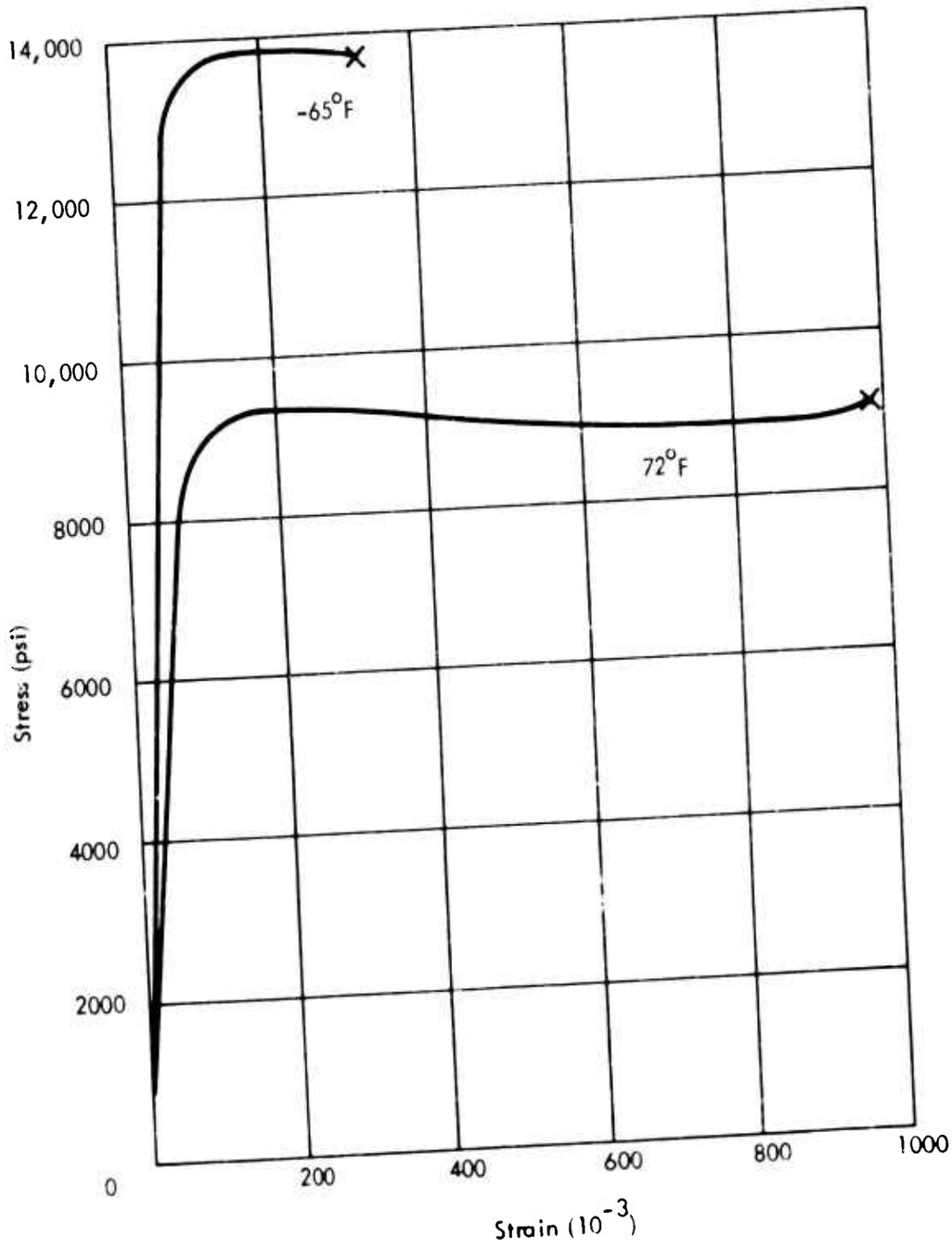

Figure 11. Shear Tests, FM1000, Aluminum, Cross-Head Speed - 0.5 in./min, 0°/0°.

that the recovered strain γ_2 is about 69 percent of γ_1. For the comparable case in tensile tests, the recovered strain ϵ_2 was only 31 percent of the total strain at unloading (ϵ_1). These comparisons cannot be rigorously made because of the different types of loading and also because they were made from results at different stress levels. The tensile data were for load-unload cycles at about 80 percent of the fracture stress, while for the shear tests the numbers were for stresses averaging 47 percent of the fracture stress. However, this difference in stress level merely emphasizes the observations; for if ϵ_1, ϵ_2 and ϵ_3 data were shown for tensile tests at 0.47 σ_F, there would be practically no viscoelastic flow. With tensile tests, the stress threshold for viscoelasticity recovery, ϵ_2, was of the order of 0.6 σ_F.

Specimens made with nonuniform bond-line configurations had shear modulus values 25 percent higher than those of the uniform bond-line thickness. The nonuniformity slightly increased the precision elastic limit and had only a negligible effect on the microyield stress and the fracture behavior (stress and mode). There was a strong effect of tapered joints on the viscoelastic strain, γ_1. At a stress level of 50 percent τ_F, γ_1 was 20×10^{-3}. Nonuniform joints at the same stress level had values for γ_1 of only 0.9×10^{-3} to 3.0×10^{-3}, a decrease of 90 percent.

Based on the test results shown in Tables V and VI, three taper configurations were selected for use in the balance of the program:

1. an included angle of 22 minutes with the bond center plane normal to the longitudinal axis of the specimen (designated as 11'/11')
2. an included angle of 44 minutes with the bond center plane normal to the longitudinal axis of the specimen (designated as 22'/22')
3. an included angle of 22 minutes with the bond center plane tilted 11 minutes from normal to the longitudinal axis of the specimen (designated as 22'/0)

The first two of these are symmetrical about a plane whose normal is parallel to the longitudinal axis of the specimen. The center plane of the third configuration is tilted 11 minutes and the taper is not symmetrical as are the first two taper configurations (see top three sketches of Figure 8).

Based on these observations of tensile and shear properties and on those from succeeding phases, it appears that the deviations from elasticity (precision elastic limit and microyield stress) are associated with the tendency for viscoelastic flow. If for any reason the viscoelasticity can be suppressed, then the elastic range of the material can be extended. Lowering the test temperature (see Phases III and V) eliminates the viscoelastic flow so that the adhesive is elastic up to the point of fracture. Within the strain rate range used in Phase IV, a higher cross-head speed diminishes the

viscoelastic flow so that elasticity continues to a higher stress level. Raising the temperature, Phases VII and VIII, promotes viscoelasticity with an attendant decrease in the elastic behavior. The use of tapered bond-line configurations markedly reduced the viscoelastic flow propensity (except for the cryogenic tests). This was probably due to the introduction of more complex stress states that interfered with the molecular viscoelastic flow mechanisms; for example, creating a compressive stress in addition to that for pure shear, or adding a shear component to a pure tensile stress.

As will be shown in later phases, the use of tapered bond-line configurations had the effect of lowering the values of the effective tensile and shear modulus. In homogeneous materials, measured in bulk, the modulus values are uniform throughout the sample. However, in thin film form, or when the adherends modify the properties, adhesives may not have constant modulus values. Consider a tensile specimen being loaded at a uniform rate. The stress is the same throughout the sample and is given by the load divided by cross-sectional area. However, the strain in the adhesive bond is not uniform; it varies inversely as the thickness. For the thinnest part of a tapered joint, the strain will be the greatest because the elongation is the same at all points. Since the modulus is defined as the ratio of stress to strain, increasing the denominator results in a lower modulus. Another factor that depresses modulus values is viscoelasticity. This contributes strain for a given stress that is additional to that of the elastic strain. It is not clear whether the onset of viscoelasticity is a strain or a stress threshold. However, in a tensile test with a tapered bond line, deviations from elasticity would be expected to occur at the thinnest portions first. For all calculations of modulus, an average bond-line thickness was used which raised the calculated modulus for the thin sections and lowered it for the thick sections.

Of course, another factor that influences the modulus of a material is a change in response due to alteration of the method of loading. In a shear test, the molecular chains uncoil, stretch or move in a certain fashion. If a compressive stress is superimposed (as with tapered bond lines), the chains will react differently. Whatever the mechanisms of that reaction are, they have the net effect of providing more strain (for a given stress) and producing a lower modulus than is the case for a pure shear test.

Lap Shear Tests

To determine the optimum adherend thickness for lap shear specimens, 12 sets of 7075-T6 aluminum adherends were bonded with FM1000. Adherend dimensions were 6 by 1 inches with four thicknesses (0.032, 0.048, 0.062, 0.088 inch). The specimens were taken directly to fracture at room temperature using a cross-head

speed of 0.5 in./min, with results as shown in Table VII. A summary of the results is presented in Table VIII. The adherend thickness of 0.062 inch was selected for all additional lap shear tests in the other phases of the program. It was chosen because it produced the highest fracture stress and because it had the best fracture characteristics.

PHASE II, ADHEREND MATERIAL

The tests made in this phase differed from those of Phase I in three respects: all adherends were made of a heat-treated titanium alloy (Ti-6Al-4V), only three tapered bond-line configurations were used for tensile tests and three for shear tests, and only one adherend thickness was used for lap shear tests. The curing cycle was the same for the titanium adherends as for aluminum adherends.

Tensile Tests

More than 30 specimens were prepared to obtain the 13 successfully tested and reported in Table IX. The results are summarized in Table X, which also shows the experimental scatter. A typical stress-strain curve is shown in Figure 10 (curve C). It was expected that the effective tensile modulus of an adhesive would increase when used with a higher modulus adherend material. In this comparison, the adherends used in Phase I (aluminum) had a Young's modulus of 10×10^6 psi, while in Phase II the adherends (titanium) had a modulus of 17×10^6 psi. Referring to Table IV, the average adhesive modulus for the uniform and selected tapered bond lines was 5.0×10^5 psi. From Table X, for titanium adherends, the average adhesive modulus was 5.9×10^5 psi, an increase of 18 percent. A stiffer adherend material seemed to have a greater effect on the uniform bond-line properties than on the tapered joints. From Tables III and IX, it can be seen that the increase for uniform specimens is about 11 percent.

The precision elastic limit and the microyield stress were about the same for the Phase II tests as for Phase I. The fracture stress values were not appreciably altered by using titanium adherends, and the fracture mode was also about 80 percent cohesive in nature. The viscoelastic behavior was essentially the same in Phase II as in Phase I. The recovered ϵ_2 was about 50 percent of ϵ_1 on the average, compared to 31 percent of ϵ_1 for the Phase I tests.

Introducing the tapered bond lines does not influence the effective tensile modulus, within the experimental scatter. Tapered bond lines do appear to lower the precision elastic limit and the microyield stress values. With the exception of the $1^o/1^o$ configuration, the strain at unloading, ϵ_1, is diminished. There was no effect on the fracture stress or mode due to tapered joints.

TABLE VII. LAP SHEAR, FM1000, ALUMINUM, PHASE I

Specimen Number	Adherend Thickness (10^{-3} in.)	Bond-Line Thickness (10^{-3} in.)	Fracture Stress (psi)	Fracture Mode (% Cohesive)
FAL-1	88	7.0	5900	50
FAL-2	88	4.0	7100	50
FAL-3	88	6.5	6700	50
FAL-4	62	8.0	7450	100
FAL-5	62	8.0	6450	100
FAL-6	62	8.0	6350	100
FAL-7	32	5.5	N.A.	adherend failed
FAL-8	32	6.0	N.A.	adherend failed
FAL-9	32	6.0	N.A.	adherend failed
FAL-10	48	2.0	6100	70
FAL-11	48	3.0	5950	70
FAL-12	48	2.0	6100	70

TABLE VIII. LAP SHEAR SUMMARY, FM1000, ALUMINUM, PHASE I

Adherend Thickness (10^{-3} in.)	Fracture Stress (psi)	Fracture Mode
88	6570 ± 600	adhesive/cohesive
62	6750 ± 550	cohesive
48	6050 ± 75	cohesive/adhesive
32	adherends failed	-

TABLE IX. TENSILE, FM1000, TITANIUM, PHASE II

Specimen Number	Average Bond-Line Thickness (10^{-3} in.)	Cross-Head Speed (in./min)	Test Temp. (^{o}F)	Elastic Tensile Modulus (10^{5} psi)	Precision Elastic Limit (psi)	Microyield Stress (psi)	Fracture Stress σ_F (psi)	Fracture Mode (% cohesive)
FTT9-1	7.5	0.02	72	6.0	1280	2960	8800	75
FTT1-1	3.4	"	"	6.4	640	2160	8900	70
FTT12-3	7.9	"	"	5.5	1780	4040	10700	75
FTT2°/2°-1	6.4-41.4	"	"	5.6	510	1400	9400	85
FTT2°/2°-2	10.5-45.5	"	"	5.6	1280	2040	11200	80
FTT1°/1°-1	7.7-25.2	"	"	6.1	304	612	9800	70
FTT1°/1°-2	7.5-25.0	"	"	5.3	604	1430	11200	90
FTT2°/0°-3	6.9-24.4	"	"	5.9	407	1400	9950	80
FTT2°/0°-4	7.3-24.8	"	"	6.4	920	1650	10800	100

TABLE IX - Continued

Specimen Number	Average Bond-Line Thickness (10^{-3} in.)	Cross-Head Speed (in./min)	Test Temp. (°F)	ϵ_1 (10^{-3})	ϵ_2 (10^{-3})	ϵ_3 (10^{-3})	Stress Level (% σ_F)
FTT9-1	7.5	0.02	72	1.60	0.80	0.20	84
FTT1-1	3.4	"	"	1.10	0.50	0.60	86
FTT9-2	8.1	"	"	1.60	-	-	86
FTT12-3	7.9	"	"	0.65	0.05	0.60	76
FTT2°/2°-1	6.4-41.4	"	"	0.90	0.60	0.30	87
FTT2°/2°-2	10.5-45.5	"	"	0.30	0.10	0.20	78
FTT2°/2°-3	6.1-41.1	"	"	1.40	0.70	0.70	85
FTT1°/1°-1	7.7-25.2	"	"	0.90	0.35	0.55	63
FTT1°/1°-2	7.5-25.0	"	"	2.30	1.20	1.10	81
FTT1°/1°-3	7.4-24.9	"	"	1.40	0.80	0.60	81
FTT2°/0°-2	9.9-27.4	"	"	1.60	1.00	0.60	87
FTT2°/0°-3	6.9-24.4	"	"	1.32	0.72	0.60	82
FTT2°/0°-4	7.3-24.8	"	"	1.02	0.48	0.54	80

TABLE X. TENSILE SUMMARY, FM1000, TITANIUM, PHASE II

Bond-Line Configuration	Cross-Head Speed (in./min)	Test Temp. (°F)	Elastic Tensile Modulus (10^5 psi)	Precision Elastic Limit (psi)	Microyield Stress (psi)	Fracture Stress σ_F (psi)	ϵ_1 (10^{-3})	ϵ_2 (10^{-3})	Stress Level (% σ_F)
0/0	0.02	72	6.0 ±.5	1230±570	2870±635	9460±920	1.24±.48	0.45±0.27	≈ 82
2°/2°	"	"	5.6±0	895±385	1720±320	10300±900	0.86±0.55	0.46±0.25	≈ 82
1°/1°	"	"	5.7 ± .4	450±150	1020± 410	10500±700	1.85± .45	1.0±.2	81
2°/0°	"	"	6.2± 2.0	660±260	1530± 130	10375±430	1.17±.15	0.60±.12	81

Shear Tests

The test results for the shear specimens are shown in Table XI and summarized in Table XII. A typical shear stress-strain curve for these experimental conditions is shown in Figure 12. There was no significant change in the shear modulus when titanium adherends were used as compared to aluminum adherends. Using the average values of Table VI (including the selected tapers) and Table XII, the comparative modulus values are 1.43 and 1.48 x 10^5 psi. Also, comparing the results configuration-by-configuration does not reveal any large differences.

Deviations from elastic behavior occurred at very low stresses as in Phase I. For these Phase II tests, the average precision elastic limit was 3.4 percent of the fracture stress and the microyield stress was 6.5 percent. Fracture stresses were somewhat lower than with the aluminum adherends, with the 22'/22' specimens having significantly lower values for τ_F. The fracture modes averaged about 75 percent cohesive with the exception of the same 22'/22' specimens. The other mechanical property values for these two specimens were in close agreement with the other specimens in this phase. Viscoelastic flow was similarly prevalent here as in the specimens of Phase I, although the recovered strain γ_2 was slightly lower with titanium adherends than with aluminum adherends.

As with the Phase I shear results, introducing nonuniform bond-line configurations increases the effective shear modulus by about 25 percent; likewise, the strain at unloading, γ_1, was markedly reduced (about 90 percent for similar stress levels). In contrast to the Phase I shear results, the tapered bond lines resulted in a lowering of the precision elastic limit, the microyield stress and the fracture stress.

It is not surprising that the shear modulus is the same for joints made with aluminum adherends as with titanium adherends. With this method of pure shear loading, there are no dimensional changes in the adherends when they are loaded. In the absence of size changes, there is no Poisson contraction and the modulus of elasticity is not invoked. In tensile tests, the adherends deform at different rates depending upon their modulus values. Since the adhesive is forced to deform along with the adherend, it has a foreign modulus imposed upon it. Thus, the tensile modulus of an adhesive is affected by the adherend properties. In these shear tests the adherend modulus values do not participate, so the adhesive modulus in shear is the same for titanium adherends as it is for aluminum adherends.

TABLE XI. SHEAR, FM1000, TITANIUM, PHASE II

Specimen Number	Average Bond-Line Thickness (10^{-3} in.)	Cross-Head Speed (in./min)	Test Temp. (°F)	Elastic Shear Modulus (10^5 psi)	Precision Elastic Limit (psi)	Microyield Stress (psi)	Fracture Stress τ_F (psi)	Fracture Mode (% cohesive)
FTS8-2	7.6	0.5	72	1.2	370	640	8940	60
FTS8-3	7.2	"	"	1.1	213	650	9700	60
FTS1-1	7.9	"	"	1.3	272	710	11250	100
FTS22'/22'-1	11.0-49.4	"	"	1.5	<310	462	4850	10
FTS22'/22'-2	7.3-45.7	"	"	1.4	174	264	5000	60
FTS11'/11'-1	9.4-28.6	"	"	1.6	230	600	8350	80
FTS11'/11'-2	10.0-29.2	"	"	1.5	233	497	9100	90
FTS22'/0-2	5-24.2	"	"	1.6	330	562	7850	70
FTS22'/0-3	10-29.2	"	"	1.5	262	544	8250	70

TABLE XI - Continued

Specimen Number	Average Bond-Line Thickness (10^{-3} in.)	Cross-Head Speed (in./min)	Test Temp. (°F)	γ_1 (10^{-3})	γ_2 (10^{-3})	γ_3 (10^{-3})	Stress Level (% τ_F)
FTS8-2	7.6	0.5	72	12.5	7.0	5.5	50
FTS8-3	7.2	"	"	14.5	3.8	10.7	50
FTS1-1	7.9	"	"	0.7	0	0.7	21
FTS22'/22'-1	11.0-49.4	"	"	3.0	2.0	1.0	30
FTS22'/22'-2	7.3-45.7	"	"	2.0	1.3	0.7	50
FTS11'/11'-1	9.4-28.6	"	"	1.4	0.3	1.1	51
FTS11'/11'-2	10.0-29.2	"	"	9.0	2.2	6.8	67
FTS22'/0-2	5-24.2	"	"	0.9	0	0.9	53
				9.9	2.5	7.4	78
FTS22'/0-3	10-29.2	"	"	1.0	0	1.0	55
				2.5	0.5	2.0	76

TABLE XII. SHEAR SUMMARY, FM1000, TITANIUM, PHASE II

Bond-Line Configuration	Cross-Head Speed (in./min)	Test Temp. (^{o}F)	Elastic Shear Modulus (10^5 psi)	Precision Elastic Limit (psi)	Microyield Stress (psi)	Fracture Stress τ_F (psi)	γ_1 (10^{-3})	γ_2 (10^{-3})	Stress Level (% τ_F)
0/0	0.5	72	1.2±.1	285±78	666±29	9960±1150	≈ 13.5	≈5.4	≈ 50
22'/22'	"	"	1.5±.1	242±58	363±99	4925±75	≈ 1.9	≈ 1.0	≈ 25
11'/11'	"	"	1.6±.1	231±2	549±51	8725±375	1.7±.3	0.8±.5	51
22'/0	"	"	1.6±.1	296±34	553±9	8050±200	1.0±.1	0	54

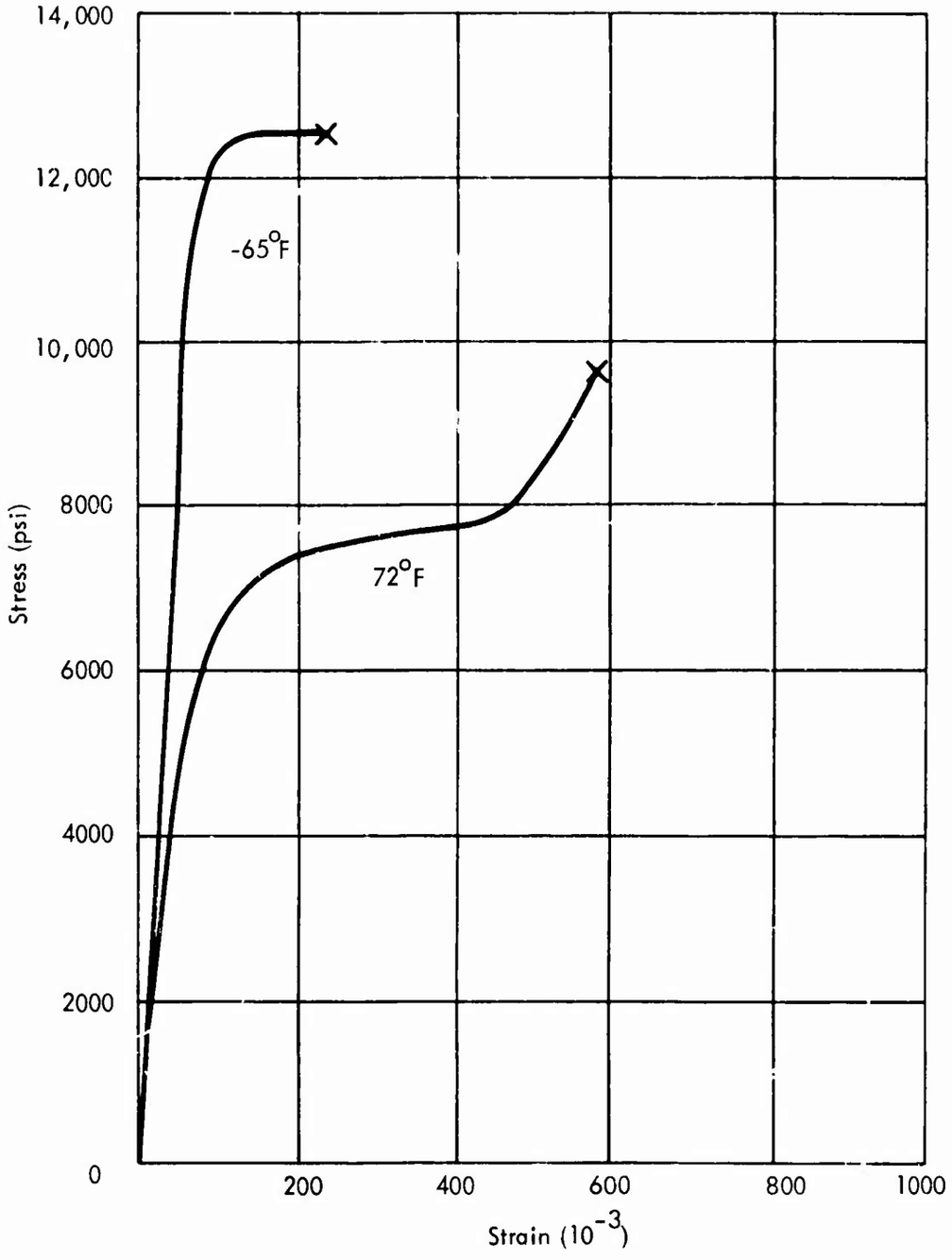

Figure 12. Shear Tests, FM1000, Titanium, Cross-Head Speed - 0.5 in./min, 0°/0°.

Lap Shear Tests

The results for the lap shear tests using titanium adherends 0.051 inch thick are shown in Table XIII. The average fracture stress was 7075 ± 550 psi, which is slightly higher than the average value of 6750 ± 550 psi for aluminum adherends. With the best Phase I specimens the failure was 100 percent cohesive; with these tests it averaged 75 percent cohesive and 25 percent adhesive.

PHASE II, CRYOGENIC

The major experimental variable change in this phase was that of the test temperature. Tests were made at -65°F with both titanium (Part a) and aluminum (Part b) adherends, with all other conditions as in Phases I and II.

Tensile Tests

The test results are presented in Table XIV and summarized in Table XV for both titanium and aluminum specimens. A typical stress-strain curve for low-temperature tensile tests of FM1000 on titanium adherends is shown in Figure 13.

Referring to the Part a (Table II) results for titanium adherends, the elastic tensile modulus was increased about 45 percent, from average values 5.0×10^5 psi at room temperature to 7.3×10^5 psi at -65°F. The fracture stress was raised to an average value of 15,000 psi, an increase of 39 percent over the room-temperature value. In general, the fractures were slightly more cohesive in nature at the lowest test temperature of -65°F - an average of 90 percent versus 75 percent for room temperature. The most significant property changes as a result of testing at low temperatures were associated with viscoelasticity. In contrast to the large instantaneous strains (ϵ_1) at room temperature (Table X), averaging 1.23×10^{-3} at about 80 percent of the fracture stress, these specimens showed no viscoelastic flow even at stresses very close to the fracture stress. Also related to the lack of viscoelasticity was the 200 percent increase in the precision elastic limit from an average of 825 psi to 2500 psi at -65°F. The average microyield stress increased from 1750 psi to 5460 psi at the lower temperature, an increase of about 210 percent.

With the aluminum adherends, a greater cryogenic effect was observed. The average tensile modulus was raised from 5.0×10^5 psi to 7.15×10^5 psi, an increase of 43 percent caused by lowering the test temperature to -65°F. An increase of 330 percent was seen in the precision elastic limit, going from 870 psi to an average of 3750 psi. In this case the P.E.L. occurred at 22 percent of the fracture stress, while at room temperature it was seen at 8 percent of σ_F. The microyield stress showed a similar effect - about a 400 percent increase in absolute value - and it was at 47 percent of the fracture stress. At the low test temperature, the fracture stress

TABLE XIII. LAP SHEAR, FM1000, TITANIUM, PHASE II

Specimen Number	Adherend Thickness (10^{-3} in.)	Bond-Line Thickness (10^{-3} in.)	Fracture Stress (psi)	Fracture Mode (% cohesive)
FTL-1	51	5	6700	80
FTL-2	51	5	7500	80
FTL-3	51	5	7250	80
FTL-4	51	2	7200	70
FTL-5	51	3	6400	70
FTL-6	51	4	7400	70

TABLE XIV. TENSILE, FM1000, TITANIUM AND ALUMINUM, PHASE III

Specimen Number	Average Bond-Line Thickness (10^{-3} in.)	Cross-Head Speed (in./min)	Test Temp. (°F)	Elastic Tensile Modulus (10^5 psi)	Precision Elastic Limit (psi)	Microyield Stress (psi)	Fracture Stress σ_F (psi)	Fracture Mode (% cohesive)
FTT9-3	9.3	0.02	-65	7.6	4600	7150	17350	95
FTT9-4	8.2	"	"	7.6	1760	4200	14000	50
FTT2°/2°-4	3.8-38.8	"	"	7.9	1780	4600	14000	90
FTT2°/2°-5	2.6-37.6	"	"	7.2	1730	4850	15800	100
FTT1°/1°-4	5.1-22.6	"	"	6.2	2020	5100	12000	80
FTT1°/1°-5	5.1-22.6	"	"	6.9	1530	6100	13400	95
FTT2°/0°-5	4.1-21.6	"	"	7.6	4600	7150	17350	95
FTT2°/0°-6	4.0-21.5	"	"	7.1	1780	4780	16500	100
FAT1-4	8.5	"	"	6.2	4070	6100	14200	100
FAT2-1	9.6	"	"	7.0	5100	10700	12800	70
FAT3-1	10.0	"	"	7.3	2800	6100	19250	70
FAT2°/2°-7	6.8-41.8	"	"	6.3	5100	7640	15300	90
FAT2°/2°-8	7.8-42.8	"	"	6.1	3030	7160	17800	80

TABLE XIV - Continued

Specimen Number	Average Bond-Line Thickness (10^{-3} in.)	Cross-Head Speed (in./min)	Test Temp. (°F)	Elastic Tensile Modulus (10^5 psi)	Precision Elastic Limit (psi)	Microyield Stress (psi)	Fracture Stress σ_F (psi)	Fracture Mode (% cohesive)
FAT1°/1°-10	9.3-26.8	0.02	-65	6.7	6100	9200	17800	75
FAT1°/1°-11	8.4-25.9	"	"	8.9	2800	4600	17300	10
FAT2°/0-5	10.4-27.9	"	"	7.4	3220	6120	18900	50
FAT2°/0-6	7.0-24.5	"	"	8.2	3800	14300	19100	70

TABLE XIV - Continued

Specimen Number	Average Bond-Line Thickness (10^{-3} in.)	Cross-Head Speed (in./min)	Test Temp. (°F)	ϵ_1 (10^{-3})	ϵ_2 (10^{-3})	ϵ_3 (10^{-3})	Stress Level (% σ_F)
FTT9-3	9.3	0.02	-65	0.1	0.1	0	90
FTT9-4	8.2	"	"	nil			
FTT2°/2°-4	3.8-38.8	"	"	"			
FTT2°/2°-5	2.6-37.6	"	"	"			
FTT1°/1°-4	5.1-22.6	"	"	"			
FTT1°/1°-5	5.1-22.6	"	"	"			
FTT2°/0°-5	4.1-21.6	"	"	"			
FTT2°/0°-6	4.0-21.5	"	"	"			
FAT1-4	8.5	"	"	"			
FAT2-1	9.6	"	"	"			
FAT3-1	10.0	"	"	"			
FAT2°/2°-7	6.8-41.8	"	"	"			
FAT2°/2°-8	7.8-42.8	"	"	"			

TABLE XIV - Continued

Specimen Number	Average Bond-Line Thickness (10^{-3} in.)	Cross-Head Speed (in./min)	Test Temp. (°F)	ϵ_1 (10^{-3})	ϵ_2 (10^{-3})	ϵ_3 (10^{-3})	Stress Level (% σ_F)
FAT1°/1°-10	9.3-26.8	0.02	-65	nil			
FAT1°/1°-11	8.4-25.9	"	"	"			
FAT2°/0-5	10.4-27.9	"	"	"			
FAT2°/0-6	7.0-24.5	"	"	"			

TABLE XV. TENSILE SUMMARY, FM1000, TITANIUM AND ALUMINUM, PHASE III

Bond-Line Configuration	Cross-Head Speed (in./min)	Test Temp. (°F)	Elastic Tensile Modulus (10^5 psi)	Precision Elastic Limit (psi)	Microyield Stress (psi)	Fracture Stress σ_F (psi)	ϵ_1 (10^{-3})	ϵ_2 (10^{-3})	Stress Level (% σ_F)
0/0 (Ti)	0.02	-65	7.6±0	3180±1420	5675±1475	15675±1675	nil		
2°/2° (Ti)	"	"	7.6±0.4	1755±25	4725±125	14900±900	"		
1°/1° (Ti)	"	"	6.6±0.4	1775±245	5600±500	12700±700	"		
2°/0° (Ti)	"	"	7.4±0.3	3190±1410	5965±1185	16925±425	"		
0/0 (Al)	"	"	6.8±0.6	3990±1150	7633±2044	15400±2550	"		
2°/2° (Al)	"	"	6.2±0.1	4065±1035	7400±240	16550±1250	"		
1°/1° (Al)	"	"	7.8±1.1	4450±1650	6900±2300	17550±250	"		
2°/0° (Al)	"	"	7.8±0.4	3510±290	10210±4090	19000±100	"		

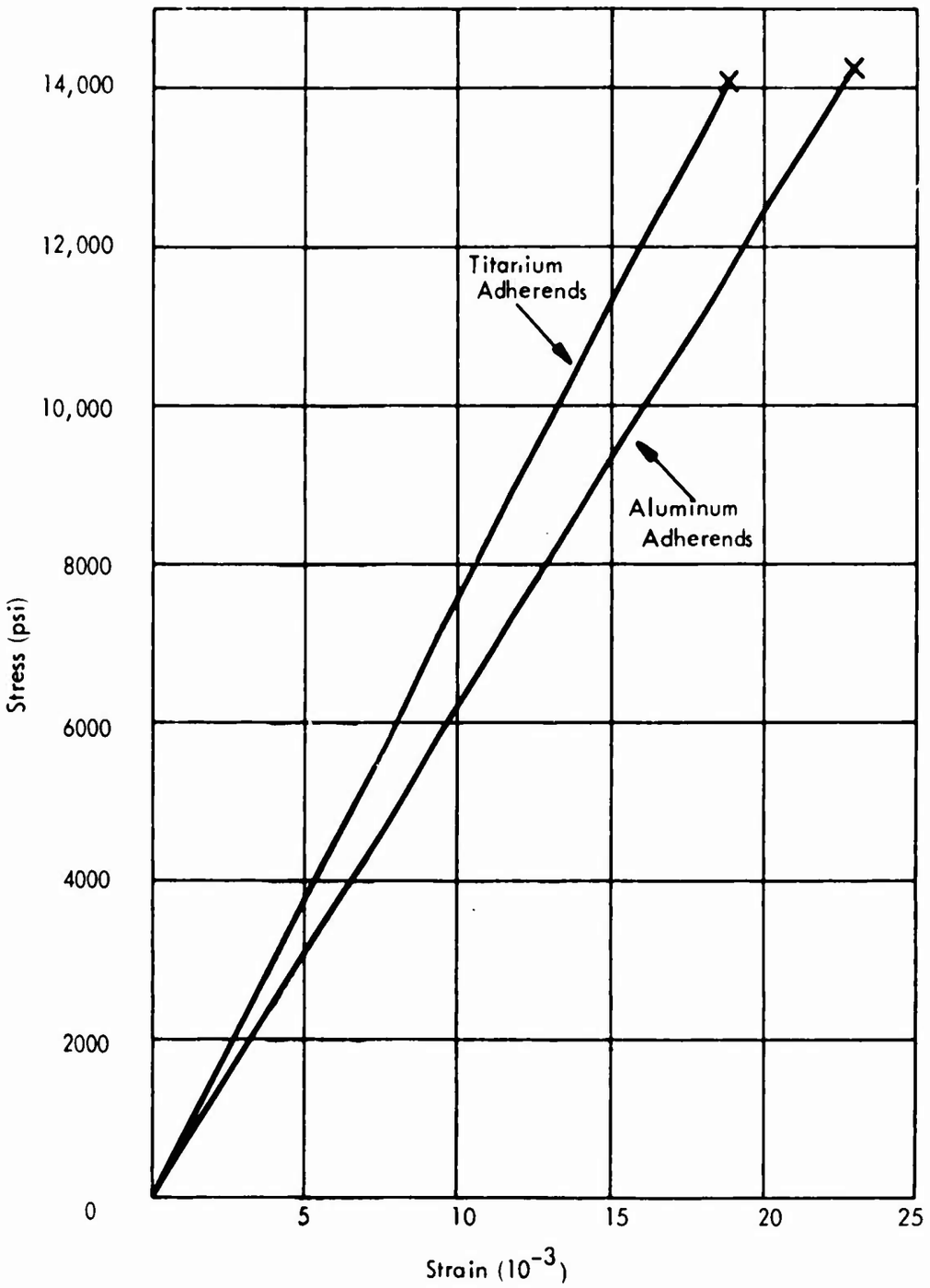

Figure 13. Tensile Tests, FM1000, -65°F, Cross-Head Speed - 0.02 in./min, 0°/0°.

averaged 17,120 psi, compared to a room-temperature value of 10,800 psi. As with the titanium specimens, there was no viscoelastic flow at any stress level for the specimens made with aluminum adherends. A typical -65°F stress-strain curve for FM1000 on aluminum adherends is shown in Figure 13.

Generally speaking, the most significant effect of low temperature was in the viscoelastic behavior. No viscoelastic flow was observed at any stress levels, and the precision elastic limit and microyield stress values were increased 200 to 400 percent. The increases in the modulus values and fracture values were more modest in comparison.

For the specimens made with titanium adherends, there was little effect due to the tapered bond-line configurations. In the case of aluminum adherends, there was a slight increase in the elastic tensile modulus, the precision elastic limit, and the microyield stress.

Shear Tests

Thirty-two specimens were prepared and tested for the shear portion of this phase in order to obtain the 16 satisfactory tests reported in Tables XVI and XVII. A typical stress-strain curve for a -65°F shear test using titanium adherends is shown in Figure 12.

With regard to the specimens made with titanium adherends (Part a, Table II), the elastic shear modulus increased 34 percent at the low test temperature. The fracture stress increased from an average value of 7900 psi at 72°F to 13,400 psi at -65°F, an increase of almost 70 percent. However, the fracture mode changed from principally cohesive in nature to completely adhesive failure. The effect of the low temperature was more pronounced for those properties associated with viscoelastic behavior. As with the tensile tests, there was no viscoelastic flow at any stress level, even very close to the fracture stress. The precision elastic limit showed a massive increase (650 percent), going from an average of 264 psi at 72°F to 1860 psi at -65°F. The microyield stress was raised from 530 psi to 3120 psi, an increase of 500 percent. These low-temperature values of the P.E.L. and the τ_{mys} were, respectively, 14 and 23 percent of the fracture stress τ_F. At room temperature, the P.E.L. and τ_{mys} were 3.1 and 6.7 percent of τ_F, respectively.

Specimens made with aluminum adherends showed similar low-temperature behavior, but the changes were not so pronounced. The elastic shear modulus increased 38 percent to an average value of 13,260 psi. The precision elastic limit was raised from 320 psi to 525 psi, an increase of only 64 percent; this value was 4 percent of the fracture stress. The microyield stress, at 1470 psi, was 11 percent of τ_F. At room temperature, these values were 3.4 and 6.5 percent of the fracture stress, respectively. Fracture behavior changed, on the average, from 33 percent

TABLE XVI. SHEAR, FM1000, TITANIUM AND ALUMINUM, PHASE III

Specimen Number	Average Bond-Line Thickness (10^{-3} in.)	Cross-Head Speed (in./min)	Test Temp. (^{o}F)	Elastic Shear Modulus (10^{5} psi)	Precision Elastic Limit (psi)	Microyield Stress (psi)	Fracture Stress τ_F (psi)	Fracture Mode (% cohesive)
FTS4-1	8.0	0.5	-65	1.9	1690	3500	14300	95
FTS1-3	7.2	"	"	1.7	1530	N.A.	12600	85
FTS22'/22'-3	9.9-48.3	"	"	2.0	1570	2900	12100	0
FTS22'/22'-4	10.1-48.5	"	"	1.8	1940	3100	12600	0
FTS11'/11'-3	10-29.2	"	"	1.9	2200	3200	13200	0
FTS11'/11'-4	10.4-29.6	"	"	2.0	1550	2700	14000	0
FTS22'/0-4	5.6-24.8	"	"	2.1	2330	3600	14100	0
FTS22'/0-5	5.3-24.5	"	"	2.2	1870	2450	14400	0
FAS11-6	7.5	"	"	2.0	450	700	15800	0
FAS12-1	14.0	"	"	1.6	890	1300	13800	0
FAS22'/22'-6	2.5-40.9	"	"	2.5	485	1730	14600	0
FAS22'/22'-X2	26-64.4	"	"	1.8	475	1460	14000	0
FAS11'/11'-3	6.8-26.0	"	"	2.0	395	1940	12100	0
FAS11'/11'-4	11.8-31.0	"	"	1.6	835	2140	12700	0
FAS22'/0-1	9.1-28.3	"	"	1.8	466	780	9100	0
FAS22'/0-3	4.1-23.3	"	"	1.8	204	1740	14000	0

TABLE XVI - Continued

Specimen Number	Average Bond-Line Thickness (10^{-3} in.)	Cross-Head Speed (in./min)	Test Temp. (°F)	ϵ_1 (10^{-3})	ϵ_2 (10^{-3})	ϵ_3 (10^{-3})	Stress Level (% σ_F)
FTS4-1	8.0	0.5	-65	nil			
FTS1-3	7.2	"	"	"			
FTS22'/22'-3	9.9-48.3	"	"	"			
FTS22'/22'-4	10.1-48.5	"	"	"			
FTS11'/11'-3	10-29.2	"	"	"			
FTS11'/11'-4	10.4-29.6	"	"	"			
FTS22'/0-4	5.6-24.8	"	"	"			
FTS22'/0-5	5.3-24.5	"	"	"			
FAS11-6	7.5	"	"	"			
FAS12-1	14.0	"	"	"			
FAS22'/22'-6	2.5-40.9	"	"	"			
FAS22'/22'-X2	26-64.4	"	"	"			
FAS11'/11'-3	6.8-26.0	"	"	"			
FAS11'/11'-4	11.8-31.0	"	"	"			
FAS22'/0-1	9.1-28.3	"	"	"			
FAS22'/0-3	4.1-23.3	"	"	"			

TABLE XVII. SHEAR SUMMARY, FM1000, TITANIUM AND ALUMINUM, PHASE III

Bond-Line Configuration	Cross-Head Speed (in./min)	Test Temp. (°F)	Elastic Shear Modulus (10^5 psi)	Precision Elastic Limit (psi)	Microyield Stress (psi)	Fracture Stress τ_F (psi)	γ_1 (10^{-3})	γ_2 (10^{-3})	Stress Level (% τ_F)
0/0 (Ti)	0.5	-65	1.8±0.1	1610± 80	3500	13450±850	nil		
22°/22° (Ti)	"	"	1.9±0.1	1755± 185	3000± 100	12350±250	"		
11°/11° (Ti)	"	"	2.0±0.1	1875±325	2950± 250	13600±400	"		
22°/0 (Ti)	"	"	2.2±0.1	2100±230	3025±575	14250±150	"		
0/0 (Al)	"	"	1.8±0.2	670± 220	1000± 300	14800±1000	"		
22°/22° (Al)	"	"	2.2±0.4	480± 5	1595± 135	14300±300	"		
11°/11° (Al)	"	"	1.8±0.2	615± 220	2040± 100	12400± 300	"		
22°/0 (Al)	"	"	1.8±0	335± 131	1260± 480	11550±2450	"		

cohesive at room temperature to 100 percent adhesive at -65°F. Lowering the temperature raised the fracture stress from 9500 psi to 13,260 psi, an increase of 40 percent. No viscoelastic flow was seen at any stress levels at -65°F as compared to an average strain at unloading (γ_1) of 5.2×10^{-3} at 72°F.

Introducing tapered bond-line configurations in the titanium specimens changed some of the properties. The elastic shear modulus was increased as was the P.E.L., while the τ_{mys} appeared to decrease. Although the fracture stress did not change much, the fracture mode changed from 90 percent cohesive with a uniform bond line to total adhesive failure in the tapered joints. There was very little effect on the aluminum bonded specimens due to the tapered adhesive joints.

Lap Shear Tests

Lap shear specimens made of titanium and aluminum were tested at -65°F; the results are shown in Table XVIII. The titanium specimens fractured at an average stress of 8430 psi, which is 19 percent higher than the room-temperature value. A similar change was observed with the aluminum specimens: the average fracture stress at -65°F (7950 psi) was 18 percent higher than the value at room temperature (6750 psi).

PHASE IV, STRAIN RATE

The tests performed in this phase were similar to those of Phase I except that different cross-head speeds were used: for tension, 0.1 and 0.002 in place of 0.02 in./min; for shear, 2.0 and 0.05 in place of 0.5 in./min; for lap shear, 2.0, 0.1, 0.05 and 0.002 in place of 0.5 in./min.

Tensile Tests

The tensile test results for the low and high cross-head speeds are presented in Table XIX and summarized in Table XX. These data are to be compared with those of Tables III and IV. The results for the tests at the low cross-head speed of 0.002 in./min were very close to those of the Phase I tests. There was no appreciable change in the tensile modulus, the precision elastic limit, the microyield stress, the fracture mode or the viscoelastic flow parameters. Only the fracture stress was different: it decreased from 10,700 psi (average) to 9100 psi at the lower cross-head speed. Thus, lowering the strain rate by a factor of 10 did not significantly change the tensile properties. However, raising the strain rate by a factor of 5 did have an effect on the mechanical properties. At the higher cross-head speed (0.1 in./min), the effective tensile modulus was raised, on the average, 22 percent from 5.0×10^5 psi to 6.1×10^5 psi. All the parameters associated with viscoelasticity

TABLE XVIII. LAP SHEAR, FM1000, TITANIUM AND ALUMINUM, PHASE III*

Specimen Number	Bond-Line Thickness (10^{-3} in.)	Cross-Head Speed (in./min)	Fracture Stress (psi)	Fracture Mode (% cohesive)
FAL27 (Al)	7.0	0.5	8800	0
FAL28 (Al)	5.0	"	7100	0
FTL11 (Ti)	4.0	0.5	7970	50
FTL12 (Ti)	4.0	"	8900	50
FTL7 (Ti)	3.5	0.02	6500	100
FTL8 (Ti)	4.0	"	6750	100

* All tests made at -65°F

TABLE XIX. TENSILE, FM1000, ALUMINUM, PHASE IV

Specimen Number	Average Bond-Line Thickness (10^{-3} in.)	Cross-Head Speed (in./min)	Test Temp. (°F)	Elastic Tensile Modulus (10^5 psi)	Precision Elastic Limit (psi)	Microyield Stress (psi)	Fracture Stress σ_F (psi)	Fracture Mode (% cohesive)
FAT10-4	5.8	0.002	72	4.4	890	1730	8980	80
FAT1-3	9.2	"	"	4.7	816	1780	7100	70
FAT2°/2°-5	2 - 37	"	"	4.9	~250	1270	9000	60
FAT2°/2°-6	3.3-38.3	"	"	4.7	1150	1800	9180	60
FAT1°/1°-6	9.3-26.8	"	"	5.3	765	1530	9200	70
FAT1°/1°-8	15.4-32.9	"	"	5.4	815	1270	9400	60
FAT2°/0°-3	4.8-22.3	"	"	4.7	770	1400	10600	70
FAT2°/0°-9	9.9-27.4	"	"	5.5	1040	1780	9380	60
FAT1-2	8.4	0.1	72	5.7	~1200	1530	11000	100
FAT10-5	7.2	"	"	4.9	1050	4100	10900	100
FAT2°/2°-3	7.9-42.9	"	"	5.3	1780	3550	10600	90
FAT2°/2°-4	5.5-40.5	"	"	6.4	1400	3550	10700	95

TABLE XIX - Continued

Specimen Number	Average Bond-Line Thickness (10^{-3} in.)	Cross-Head Speed (in./min)	Test Temp. (°F)	Elastic Tensile Modulus (10^5 psi)	Precision Elastic Limit (psi)	Microyield Stress (psi)	Fracture Stress σ_F (psi)	Fracture Mode (% cohesive)
FAT1°/1°-4	8.1-25.6	0.1	72	6.7	1530	3200	11200	90
FAT1°/1°-5	7.2-24.7	"	"	6.2	1270	3030	10200	90
FAT2°/0°-4	11.3-28.8	"	"	5.0	1530	3800	10400	100
FAT2°/0°-7	11 -28.5	"	"	8.3	2300	3200	10700	50

TABLE XIX - Continued

Specimen Number	Average Bond-Line Thickness (10^{-3} in.)	Cross-Head Speed (in./min)	Test Temp. (°F)	ϵ_1 (10^{-3})	ϵ_2 (10^{-3})	ϵ_3 (10^{-3})	Stress Level (% σ_F)
FAT10-4	5.8	0.002	72	1.20	0.20	1.00	94
FAT1-3	9.2	"	"	0.85	0.56	0.29	65
FAT2°/2°-5	2 - 37	"	"	0.40	0.15	0.25	75
FAT2°/2°-6	3.3-38.3	"	"	1.25	0.17	1.08	83
FAT1°/1°-6	9.3-26.8	"	"	3.0	0	3.0	69
FAT1°/1°-8	15.4-32.9	"	"	1.65	0.16	1.49	80
FAT2°/0°-3	4.8-22.3	"	"	1.95	0.32	1.66	92
FAT2°/0°-9	9.9-27.4	"	"	0.73	0	0.73	75
FAT1-2	8.4	0.1	72	0.54	0.37	0.17	84
FAT10-5	7.2	"	"	1.03	0	1.03	84
FAT2°/2°-4	5.5-40.5	"	"	0.24	0.24	0	86
FAT2°/2°-3	7.9-42.9	"	"	0.72	0.20	0.52	90

TABLE XIX - Continued

Specimen Number	Average Bond-Line Thickness (10^{-3} in.)	Cross-Head Speed (in./min)	Test Temp. (°F)	ϵ_1 (10^{-3})	ϵ_2 (10^{-3})	ϵ_3 (10^{-3})	Stress Level (% σ_F)
FAT1°/1°-4	8.1-25.6	0.1	72	0.36	0.36	0	90
FAT1°/1°-5	7.2-24.7	"	"	0.45	0.15	0.30	90
FAT2°/0°-4	11.3-28.8	"	"	0.56	0.56	0	90
FAT2°/0°-7	11-28.5	"	"	0.25	0.1	0.15	86

TABLE XX. TENSILE SUMMARY, FM1000, ALUMINUM, PHASE IV

Bond-Line Configuration	Cross-Head Speed (in./min)	Test Temp. (°F)	Elastic Tensile Modulus (10^5psi)	Precision Elastic Limit (psi)	Microyield Stress (psi)	Fracture Stress σ_F (psi)	ϵ_1 (10^{-3})	ϵ_2 (10^{-3})	Stress Level (%σ_F)
0/0	0.002	72	4.6±.2	853±37	1755±25	8040±940	1.02±.18	0.38±.18	≈ 80
2°/2°	"	"	4.8±.1	700±450	1535±265	9090±90	0.83±.43	0.16±.01	≈ 80
1°/1°	"	"	5.4±.1	790± 25	1400±130	9300±100	2.35±.75	0.08±.08	≈ 85
2°/0°	"	"	5.1±.4	905±135	1590±190	9990±610	1.34±.61	0.16±.16	≈ 80
0/0	0.1	72	5.3±.4	1125±75	2815±1285	10950±50	0.79±.25	0.19±.19	84
2°/2°	"	"	5.9±.6	1590±190	3550± 0	10650±50	0.48±.24	0.22±.02	≈ 88
1°/1°	"	"	6.4±.3	1400±130	3115± 85	10700±500	0.40±.04	0.26±.1	90
2°/0°	"	"	6.7±1.7	1915±385	3500±300	10550±150	0.40±.15	0.33±.23	≈ 88

were changed to reflect the shorter times available for the viscoelastic mechanisms to operate. Accordingly, the P.E.L. and the σ_{mys} were increased while the strains, ϵ_1 and ϵ_2, were decreased. The fracture stress remained about the same, but the fracture mode became more cohesive at the highest strain rate. The precision elastic limit nearly doubled in value so that at 0.1 in./min the P.E.L. was 14 percent of σ_F instead of 8 percent of σ_F at the standard strain rate. Likewise, the microyield stress was increased to 30 percent of the fracture stress compared to 15 percent from the Phase I tests. The strain at unloading, ϵ_1, averaged 1.48×10^{-3} at the standard strain rate; at the higher cross-head speed, this value dropped to 0.52×10^{-3}. There was a similar decrease in ϵ_2. At the high strain rate, the recovered strain (ϵ_2) was about 50 percent of ϵ_1; at the standard strain rate, ϵ_2 was about 0.31 ϵ_1.

The effect of bond-line configuration was indeterminate for some properties because any changes were within the experimental scatter. However, at the low strain rate, it appears that: the modulus was increased slightly; there was little effect on the P.E.L., the σ_{mys}, and the fracture behavior; the viscoelastic flow, ϵ_1, was raised. This latter observation may have been somewhat in error because of the possibility of instrument drift during the long loading-unloading times encountered at a cross-head speed of 0.002 in./min. The same generalizations can be made for the results at 0.1 in./min with one exception: the strain at unloading, ϵ_1, was diminished about 45 percent when tapered bond-line configurations were used.

Shear Tests

The effects due to changing the strain rate were minimal for the shear tests. The most significant change was in the elastic shear modulus at the highest cross-head speed; this was an increase of 26 percent. All the test data are reported in Table XXI and summarized in Table XXII. In the Phase I work, it was shown that the strain at unloading, ϵ_1, was about 15 to 30 times greater in the uniform bond line than in the tapered joints. Similar observations were made here for the two alternate cross-head speeds. The variations in ϵ_1 due to the nonuniform configurations ranged from a factor of 7 for the low strain rate to about 19 for the high strain rate. Changing the strain rate did not alter this marked effect caused by introducing a tapered bond line.

The tapered bond-line configurations raised the elastic shear modulus values above that of the uniform bond-line case, with the effect being more pronounced at the higher strain rate. The other strength values and the fracture behavior were not appreciably altered by the tapered bond lines. For both strain rates there was a marked decrease in the viscoelastic flow. The strain at unloading, γ_1, decreased about 85 percent at the high strain rate when tapered bond lines were used.

TABLE XXI. SHEAR, FM1000, ALUMINUM, PHASE IV

Specimen Number	Average Bond-Line Thickness (10^{-3} in.)	Cross-Head Speed (in./min)	Test Temp. (°F)	Elastic Shear Modulus (10^5 psi)	Precision Elastic Limit (psi)	Microyield Stress (psi)	Fracture Stress τ_F (psi)	Fracture Mode (% cohesive)
FAS12-2	10.1	0.05	72	1.4	252	368	10300	30
FAS11-8	7.2	"	"	1.5	350	496	8150	0
FAS22'/22'-3	9.8-48.2	"	"	1.2	360	570	7600	0
FAS22'/22'-4	10.2-48.6	"	"	1.5	272	575	7130	10
FAS11'/11'-6	10.3-29.5	"	"	1.7	282	388	10100	80
FAS11'/11'-7	12-31.2	"	"	1.7	242	435	7860	10
FAS22' /0-4	6-25.2	"	"	1.4	290	780	8800	10
FAS22'/0-13	4.8-24	"	"	1.8	243	485	4950	0
FAS11-7	10.6	2.0	72	1.8	<250	342	9700	0
FAS12-3	12.0	"	"	1.4	310	504	12200	20
FAS10-1	11.1	"	"	1.3	233	613	8540	0
FAS22'/22'-X1	25-63.4	"	"	1.8	388	1320	9200	10
FAS22'/22'-X4	9-47.4	"	"	2.1	447	700	8800	15

TABLE XXI - Continued

Specimen Number	Average Bond-Line Thickness (10^{-3} in.)	Cross-Head Speed (in./min)	Test Temp. (°F)	Elastic Shear Modulus (10^5 psi)	Precision Elastic Limit (psi)	Microyield Stress (psi)	Fracture Stress τ_F (psi)	Fracture Mode (% cohesive)
FAS11'/11'-X1	11.5-30.7	2.0	72	1.4	<213	873	7200	0
FAS11'/11'-X4	9.5-28.7	"	"	1.9	320	806	9900	15
FAS22'/0-14	8.2-27.4	"	"	2.0	388	640	8000	30
FAS22'/0-15	15.3-34.5	"	"	2.0	<440	852	6400	0

TABLE XXI - Continued

Specimen Number	Average Bond-Line Thickness (10^{-3} in.)	Cross-Head Speed (in./min)	Test Temp. (°F)	γ_1 (10^{-3})	γ_2 (10^{-3})	γ_3 (10^{-3})	Stress Level (% τ_F)
FAS12-2	10.1	0.05	72	28.0	4.0	24.0	47
FAS11-8	7.2	"	"	13.2	3.0	12.9	60
FAS22'/22'-3	9.8-48.2	"	"	0.4	0	0.4	63
FAS22'/22'-4	10.2-48.6	"	"	1.6	0	1.6	68
FAS11'/11'-6	10.3-29.5	"	"	5.6	1.4	4.2	58
FAS11'/11'-7	12-31.2	"	"	2.2	0	2.2	62
FAS22'/0-4	6-25.2	"	"	0.2	0	0.2	38
FAS22'/0-13	4.8-24	"	"	1.8	0	1.8	80
FAS11-7	10.6	2.0	72	24.6	1.4	23.2	54
FAS12-3	12.0	"	"	52.0	7.0	45.0	55
FAS10-1	11.1	"	"	9.5	1.9	7.6	66
FAS22'/22'-X1	25-63.4	"	"	1.0	0	1.0	66
FAS22'/22'-X4	9-47.4	"	"	2.5	0.9	1.6	68

TABLE XXI - Continued

Specimen Number	Average Bond-Line Thickness (10^{-3} in.)	Cross-Head Speed (in./min)	Test Temp. (°F)	γ_1 (10^{-3})	γ_2 (10^{-3})	γ_3 (10^{-3})	Stress Level (% τ_F)
FAS11'/11'-X1	11.5-30.7	2.0	72	1.3	0.3	1.0	69
FAS11'/11'-X4	9.5-28.7	"	"	1.7	0.6	1.1	63
FAS22'/0-14	8.2-27.4	"	"	1.0	0	1.0	60
FAS22'/0-15	15.3-34.5	"	"	0.9	0	0.9	68

TABLE XXII. SHEAR SUMMARY, FM1000, ALUMINUM, PHASE IV

Bond-Line Configuration	Cross-Head Speed (in./min)	Test Temp. (°F)	Elastic Shear Modulus (10^5 psi)	Precision Elastic Limit (psi)	Microyield Stress (psi)	Fracture Stress τ_F (psi)	γ_1 (10^{-3})	γ_2 (10^{-3})	Stress Level (% τ_F)
0/0	0.05	72	1.5±.1	301±49	432±64	9225±1075	20.6±7.4	3.5±.5	≈ 54
22'/22'	"	"	1.4±.2	316±44	573±3	7365±235	1.0±.6	0	≈ 65
11'/11'	"	"	1.7±0	262±20	412±23	8980±1120	3.9±1.7	0.7±.7	≈ 60
22'/0	"	"	1.6±.2	267±24	633±147	6875±1925	1.0±.8	0	≈ 60
0/0	2.0	72	1.5±.2	264±30	486±135	10146±1830	38.3±13.7	3.4±2.4	55
22'/22'	"	"	2.0±.2	418±30	1010±310	9000±200	1.8±.8	0.45±.45	≈ 67
11'/11'	"	"	1.7±.3	267±54	840±33	8550±1350	1.5±.2	0.5±.2	≈ 66
22'/0	"	"	2.0±0	414±26	746±106	7200±800	1.0±.1	0	≈ 64

Lap Shear Tests

Although the test program called for only two alternate cross-head speeds in this phase, four speeds were used - 2.0, 0.1, 0.05 and 0.002 in./min. The results, shown in Table XXIII, are to be compared to those of Phase I (Table VIII). The highest cross-head speed produced the largest fracture stresses. As the strain rate decreased, the fracture stress also decreased. Under the standard test condition (Phase I), the average fracture stress was 6750 psi, somewhat less than the comparable value of 7300 psi for the 2.0 in./min cross-head speed.

PHASE V, CRYOGENIC/STRAIN RATE

Tests made in this phase differed from those of Phases I, III and IV in that they were made at the highest strain rate and the lowest temperature. The purpose was to evaluate strain rate effects at -65°F. Each of these experimental variations was studied separately in Phase III (low test temperature) and Phase IV (high strain rate). Thus, the results presented here must be compared to those of Tables III through VIII and XIV through XXIII.

Tensile Tests

The test results for FM1000 on aluminum adherends at -65°F using a cross-head speed of 0.1 in./min are shown in Table XXIV. A summary of the results is presented in Table XXV. This combination of high strain rate and low test temperature produced the highest average values for the effective tensile modulus in the entire FM1000 program. Recapitulating, the average effective tensile modulus for the standard cross-head speed at room temperature was 5.0×10^5 psi; lowering the test temperature to -65°F raised this value to 7.15×10^5 psi (Table XV); increasing the strain rate brought the value up to 6.1×10^5 psi (Table XX). When the two changes were made simultaneously (Tables XXIV and XXV), the average effective tensile modulus was 8.6×10^5 psi. The fracture stress in this phase averaged 17,900 psi, a value only slightly greater than that of Phase III (cryogenic). The P.E.L. value was comparable to that of the cryogenic tests (3750 psi vs 3420 psi here). However, the microyield stress values in this series of tests averaged 10,100 psi, by far the highest seen in the program. This σ_{mys} was 56 percent of the fracture stress. The mode of failure was not much different from those of Phases I, III and IV. As in the earlier cryogenic tests, there was no viscoelastic flow at any stress level.

The major effect of the nonuniform bond lines was to increase the elastic tensile modulus by about 12 percent. There was also a slight decrease in the precision elastic limit, while the other properties did not change very much.

TABLE XXIII. LAP SHEAR, FM1000, ALUMINUM, PHASE IV

Specimen Number	Bond-Line Thickness (10^{-3} in.)	Cross-Head Speed (in./min)	Fracture Stress (psi)	Fracture Mode (% cohesive)
FAL-21	9.0	2.0	7000	30
FAL-22	7.0	2.0	7600	50
FAL-13	4.0	0.1	6500	0
FAL-14	3.0	0.1	6900	0
FAL-23	11.0	0.05	5700	20
FAL-24	6.5	0.05	6400	0
FAL-15	3.0	0.002	5600	0
FAL-16	2.0	0.002	5700	0

TABLE XXIV. TENSILE, FM1000, ALUMINUM, PHASE V

Specimen Number	Average Bond-Line Thickness (10^{-3} in.)	Cross-Head Speed (in./min)	Test Temp. ($^{\circ}$F)	Elastic Tensile Modulus (10^5 psi)	Precision Elastic Limit (psi)	Microyield Stress (psi)	Fracture Stress σ_F (psi)	Fracture Mode (% cohesive)
FAT1-6	9.8	0.1	-65	7.3	6100	12700	19000	95
FAT3-3	9.2	"	"	8.5	3050	8100	16600	90
FAT2°/2°-9	6.0-41	"	"	9.6	3600	12100	17800	70
FAT2°/2°-10	8.6-43.6	"	"	7.7	2300	≈ 7900	19000	90
FAT1°/1°-12	8.5	"	"	9.3	2500	6100	16300	70
FAT1°/1°-13	7.1-24.6	"	"	9.0	2600		20800	50
FAT1°/1°-14	8.5-26.0	"	"	8.8	3060	8200	18400	85
FAT2°/0°-8	11.9-29.4	"	"	10.5	2680	12700	18900	90
FAT2°/0°-10	9.4-26.9	"	"	6.9	4100	~13000	15000	40

TABLE XXIV - Continued

Specimen Number	Average Bond-Line Thickness (10^{-3} in.)	Cross-Head Speed (in./min)	Test Temp. (^{o}F)	ϵ_1 (10^{-3})	ϵ_2 (10^{-3})	ϵ_3 (10^{-3})	Stress Level (% σ_F)
FAT1-6	9.8	0.1	-65	nil			
FAT3-3	9.2	"	"	"			
FAT2°/2°-9	6.0-41	"	"	"			
FAT2°/2°-10	8.6-43.6	"	"	"			
FAT1°/1°-12	8.5	"	"	"			
FAT1°/1°-13	7.1-24.6	"	"	"			
FAT1°/1°-14	8.5-26.0	"	"	"			
FAT2°/0°-8	11.9-29.4	"	"	"			
FAT2°/0°-10	9.4-26.9	"	"	"			

TABLE XXV. TENSILE SUMMARY, FM1000, ALUMINUM, PHASE V

Bond-Line Configuration	Cross-Head Speed (in./min)	Test Temp. (°F)	Elastic Tensile Modulus (10^5 psi)	Precision Elastic Limit (psi)	Microyield Stress (psi)	Fracture Stress σ_F (psi)	ϵ_1 (10^{-3})	ϵ_2 (10^{-3})	Stress Level (% σ_F)
0/0	0.1	-65	7.9±0.6	4575±1525	10400±2300	17800±1200	nil		
2°/2°	"	"	8.7±1.0	2950±650	10000±2100	18400±600	"		
1°/1°	"	"	9.0±0.2	2780±280	7200± 1100	18500±2250	"		
2°/0	"	"	8.7±1.8	3390±710	12850±150	16950±1950	"		

Shear Tests

These shear tests combined low temperature and high strain rate with results as given in Tables XXVI and XXVII. The average base-line shear modulus (Table VI) for this system was 1.43×10^5 psi. Increasing the cross-head speed raised the modulus to 1.8×10^5 psi; dropping the test temperature raised the modulus to 1.9×10^5 psi. Making both these changes together (high strain rate, low test temperature) produced the highest shear modulus seen - an average of 2.15×10^5 psi (an increase of 50 percent over the Phase I value). The P.E.L. showed a 100 percent increase over the Phase I value. The fracture stress was most greatly influenced by the test temperature and not very strongly by a higher strain rate. The fracture stresses of this Phase V work were essentially the same value as for the cryogenic phase (III). As with the tensile tests, the property showing the largest effect was the microyield stress. The average base-line τ_{mys} was 620 psi; lowering the test temperature increased that to 1470 psi. Then combining the low temperature with the high strain rate, the microyield stress was 2370 psi (18 percent of the fracture stress). In Phase I, τ_{mys} was 6.5 percent of τ_F. Viscoelastic flow was not observed at any stress level during the experiments of this phase.

The shear modulus was increased about 16 percent when tapered bond-line configurations were used. Another effect caused by the nonuniform joints was an apparent lowering of the microyield stress and the fracture stress.

Lap Shear Tests

These lap shear tests were made at three cross-head speeds - 2.0, 0.1 and 0.02 in./min at -65°F. The results are shown in Table XXVIII and should be compared with those of Tables VII and VIII from Phase I. The average base-line fracture stress value was 6750 psi. Lowering the test temperature increased the fracture stresses at all cross-head speeds. Strain rate had a much smaller influence on the fracture stress. Referring to Table XXVIII, the greatest average fracture stress was 8200 psi. At -65°F, all the specimens showed complete adhesive failure, listed as zero percent cohesive.

That the low test temperature had a stronger influence on the properties than did the strain rate is consistent with the observations of the tensile and shear parts of this phase.

TABLE XXVI. SHEAR, FM1000, ALUMINUM, PHASE V

Specimen Number	Average Bond-Line Thickness (10^{-3} in.)	Cross-Head Speed (in./min)	Test Temp. (°F)	Elastic Shear Modulus (10^5 psi)	Precision Elastic Limit (psi)	Microyield Stress (psi)	Fracture Stress τ_F (psi)	Fracture Mode (% cohesive)
FAS11-15	7.7	2	-65	1.7	630	2900	14600	0
FAS11-13	7.6	"	"	2.1	785	3700	13700	0
FAS22'/22'-X3	7-45.4	"	"	2.2	580	2700	12300	0
FAS22'/22'-7	5-43.4	"	"	2.7	920	1950	12700	0
FAS11'/11'-5	12-31.2	"	"	2.2	565	1700	14300	10
FAS11'/11'-X2	19.5-38.7	"	"	2.2	680	1550	12900	10
FAS22'/0-7	5-24.2	"	"	1.8	835	1650	12900	0
FAS22'/0-8	13-32.2	"	"	2.2	600	2820	12250	0

TABLE XXVI - Continued

Specimen Number	Average Bond-Line Thickness (10^{-3} in.)	Cross-Head Speed (in./min)	Test Temp. (°F)	γ_1 (10^{-3})	γ_2 (10^{-3})	γ_3 (10^{-3})	Stress Level (% τ_F)
FAS11-15	7.7	2	-65	nil			
FAS11-13	7.6	"	"	"			
FAS22'/22'-X3	7-45.4	"	"	"			
FAS22'/22'-7	5-43.4	"	"	"			
FAS11'/11'-5	12-31.2	"	"	"			
FAS11'/11'-X2	19.5-38.7	"	"	2	0	2	83
FAS22'/0-7	5-24.2	"	"	nil			
FAS22'/0-8	13-32.2	"	"	"			

TABLE XXVII. SHEAR SUMMARY, FM1000, ALUMINUM, PHASE V

Bond-Line Configuration	Cross-Head Speed (in./min)	Test Temp. (°F)	Elastic Shear Modulus (10^5 psi)	Precision Elastic Limit (psi)	Microyield Stress (psi)	Fracture Stress τ_F (psi)	γ_1 (10^{-3})	γ_2 (10^{-3})	Stress Level (% τ_F)
0/0	2	-65	1.9±.2	708±77	3300±400	14150±450	nil		
22'/22'	"	"	2.5±.3	750±170	2325±375	12500±200	"		
11'/11'	"	"	2.2±0	623±57	1625±75	13600±700	some		
22'/0	"	"	2.0±0.2	718±118	2235±585	12575±325	nil		

TABLE XXVIII. LAP SHEAR, FM1000, ALUMINUM, PHASE V *

Specimen Number	Bond-Line Thickness (10^{-3} in.)	Cross-Head Speed (in./min)	Fracture Stress (psi)	Fracture Mode (% cohesive)
FAL-25	7.0	2.0	8800	0
FAL-26	8.0	2.0	7600	0
FAL-19	4.0	0.1	6100	0
FAL-20	3.0	0.1	8150	0
FAL-17	3.5	0.02	7550	0
FAL-18	3.5	0.02	7900	0

* All tests made at -65°F

PHASE VI, BOND-LINE THICKNESS

To study the effect of bond-line thickness, it was necessary to use a paste-type adhesive in place of the sheet adhesive having a carrier cloth (FM1000). With FM1000 there is one optimum thickness (0.008 in.) that must be used. EC2214 was selected as the paste-type adhesive for the thickness study because it is widely used in the aircraft industry. Standard tests were performed as in Phase I except that the adhesive/adherend system was EC2214/aluminum.

Tensile Tests

A large number of specimens were prepared and rejected because of unacceptable bond-line thicknesses. Finally, 9 specimens with thicknesses ranging from 0.0019 to 0.0054 in. were accepted for the thin bond-line configuration (0.004 in.), and 10 specimens with thicknesses of 0.0183 to 0.023 in. were accepted for the thick bond-line joints (0.020 in.). The results are shown in Table XXIX and summarized in Table XXX. A typical tensile stress-strain curve from these tests is shown in Figure 14.

Considering average values from Table XXX and the experimental scatter, there were no appreciable differences in properties between the thin bond lines and the thick bond lines for EC2214 adhesive on aluminum adherends. The average effective tensile modulus for all tests was 0.91×10^6 psi. In contrast, FM1000 on aluminum adherends had an average effective tensile modulus of 5.5×10^5 psi. The values for the P.E.L. and the σ_{mys} for EC2214 were nearly double those for FM1000. The fracture stresses and modes of failure were comparable for EC2214 and FM1000. Viscoelastic flow was readily observed in all specimens.

Using tapered bond-line configurations with EC2214 caused a change in the viscoelastic parameters. At similar stress levels, ϵ_1, for the thin bond lines, averaged 1.8×10^{-3} for uniform specimens. The average ϵ_1 for the thin tapered joints was 0.27×10^{-3}, a reduction of 85 percent. A similar effect, but not so pronounced, was seen in the thick bond-line specimens. Introduction of tapered bond lines had a mixed effect on the other mechanical properties, with consistent trends in evidence.

Shear Tests

Because of difficulties in preparing suitable specimens, a number were prepared and rejected. Finally, 8 were accepted having bond-line thicknesses between 0.0019 and 0.0056 in.; 9 were used with the thicknesses ranging from 0.021 to 0.0288 in.

TABLE XXIX. TENSILE, EC2214, ALUMINUM, PHASE VI

Specimen Number	Average Bond-Line Thickness (10^{-3} in.)	Cross-Head Speed (in./min)	Test Temp. (°F)	Elastic Tensile Modulus (10^6 psi)	Precision Elastic Limit (psi)	Microyield Stress (psi)	Fracture Stress σ_F (psi)	Fracture Mode (% cohesive)
EAT3-5	1.9	0.02	72	1.01	1270	4070	11500	100
EAT2-3	3.7	"	"	0.77	2040	5150	10450	100
EAT2-4	3.6	"	"	1.00			10950	100
EAT2°/2°-X2	3.2-38.2	"	"	0.90	1530	2800	9100	90
EAT2°/2°-X3	4.1-39.1	"	"	0.59	2040	5600	9450	97
EAT1°/1°-16	3.9-21.4	"	"	1.00	4500	6200	10200	100
EAT1°/1°-17	4.2-21.7	"	"	0.86	2560	5620	10950	100
EAT2°/0°-15	5.4-22.9	"	"	0.78	2800	4300	10450	100
EAT2°/0°-20	1.9-19.4	"	"	0.97	2040	4850	10700	50
EAT3-4	23.0	0.02	72	1.02	2300	4600	11500	90
EAT1-9	19.0	"	"	0.95	2540	4600	11500	90
EAT3-7	19.5	"	"	0.86	3560	5350	11200	100
EAT1-10	18.5	"	"	0.87	1520	4060	10200	100

TABLE XXIX - Continued

Specimen Number	Average Bond-Line Thickness (10^{-3} in.)	Cross-Head Speed (in./min)	Test Temp. (^{o}F)	Elastic Tensile Modulus (10^{6} psi)	Precision Elastic Limit (psi)	Microyield Stress (psi)	Fracture Stress σ_F (psi)	Fracture Mode (% cohesive)
EAT2°/2°-11	18.3-53.3	0.02	72	0.82	2040	5100	10700	100
EAT2°/2°-X4	21.8-56.8	"	"	1.08	2060	4840	9850	50
EAT1°/1°-12	21.4-38.9	"	"	0.97	1270	1830	10450	100
EAT1°/1°-15	20.1-37.6	"	"	1.07	2170	5600	10000	100
EAT2°/0°-17	20.5-38.0	"	"	0.95	3060	4590	10950	100
EAT2°/0°-21	18.6-36.1	"	"	0.89	2300	3050	9700	100

TABLE XXIX - Continued

Specimen Number	Average Bond-Line Thickness (10^{-3} in.)	Cross-Head Speed (in./min)	Test Temp. (°F)	ϵ_1 (10^{-3})	ϵ_2 (10^{-3})	ϵ_3 (10^{-3})	Stress Level (% σ_F)
EAT3-5	1.9	0.02	72	2.70	1.60	0.90	67
EAT2-3	3.7	"	"	0.90	0	0.90	80
EAT2-4	3.6	"	"				
EAT2°/2°-X2	3.2-38.2	"	"	0.14	0	0.14	80
EAT2°/2°-X3	4.1-39.1	"	"	0.42	0	0.42	80
EAT1°/1°-16	3.9-21.4	"	"	0.20	0	0.20	80
EAT1°/1°-17	4.2-21.7	"	"	0.14	0	0.14	83
EAT2°/0°-15	5.4-22.9	"	"	0.40	0	0.40	80
EAT2°/0°-20	1.9-19.4	"	"	0.15	0.10	0.05	67
				0.30	0.15	0.15	86
EAT3-4	23.0	"	"	0.38	0.13	0.25	67
EAT1-9	19.0	"	"	0.50	0.20	0.30	81
EAT3-7	19.5	"	"	0.42	0.14	0.28	68
EAT1-10	18.5	"	"	0.30	0.15	0.15	66

TABLE XXIX - Continued

Specimen Number	Average Bond-Line Thickness (10^{-3} in.)	Cross-Head Speed (in./min)	Test Temp. (°F)	ϵ_1 (10^{-3})	ϵ_2 (10^{-3})	ϵ_3 (10^{-3})	Stress Level (% σ_F)
EAT2°/2°-11	18.3-53.3	0.02	72	0.20	0.20	0	80
EAT2°/2°-X4	21.8-56.8	"	"	0.23	0.10	0.13	73
EAT1°/1°-12	21.4-38.9	"	"	0.30	0	0.30	80
EAT1°/1°-15	20.1-37.6	"	"	0.33	0.11	0.22	82
EAT2°/C-17	20.5-38.0	"	"	0.30	0	0.30	85
EAT2°/0-21	18.6-36.1	"	"	0.36	0.06	0.30	74

TABLE XXX. TENSILE SUMMARY, EC2214, ALUMINUM, PHASE VI

Bond-Line Configuration	Cross-Head Speed (in./min)	Test Temp. (^{o}F)	Elastic Tensile Modulus (10^{6} psi)	Precision Elastic Limit (psi)	Microyield Stress (psi)	Fracture Stress σ_F (psi)	ϵ_1 (10^{-3})	ϵ_2 (10^{-3})	Stress Level (% σ_F)
0/0 (Thin)	0.02	72	0.93±.10	1655±385	4610± 540	10966± 525	1.80±.9	0.8±.8	≈ 70
2°/2° (Thin)	"	"	0.75±.16	1785±255	4200± 1400	9275±175	0.28±.14	0	80
1°/1° (Thin)	"	"	0.93±.07	3530± 970	5910±290	10575±375	0.17±.03	0	≈ 82
2°/0 (Thin)	"	"	0.88±.1	2420±380	4575± 275	10575±125	0.35±.05	.08±.08	≈ 78
0/0 (Thick)	0.02	72	0.93±.07	2480±.020	4650± 645	11100± 650	0.4±.1	0.15±.02	≈ 70
2°/2° (Thick)	"	"	0.95±.13	2050± 10	4970± 130	10275±425	0.22±.02	0.15±.05	≈ 77
1°/1° (Thick)	"	"	1.02±.05	1720± 450	3715± 1885	10225±225	0.32±.02	0.06±.06	≈ 81
2°/0 (Thick)	"	"	0.92±.03	2680± 380	3820±770	10325±625	0.33±.03	0.03±.03	≈ 80

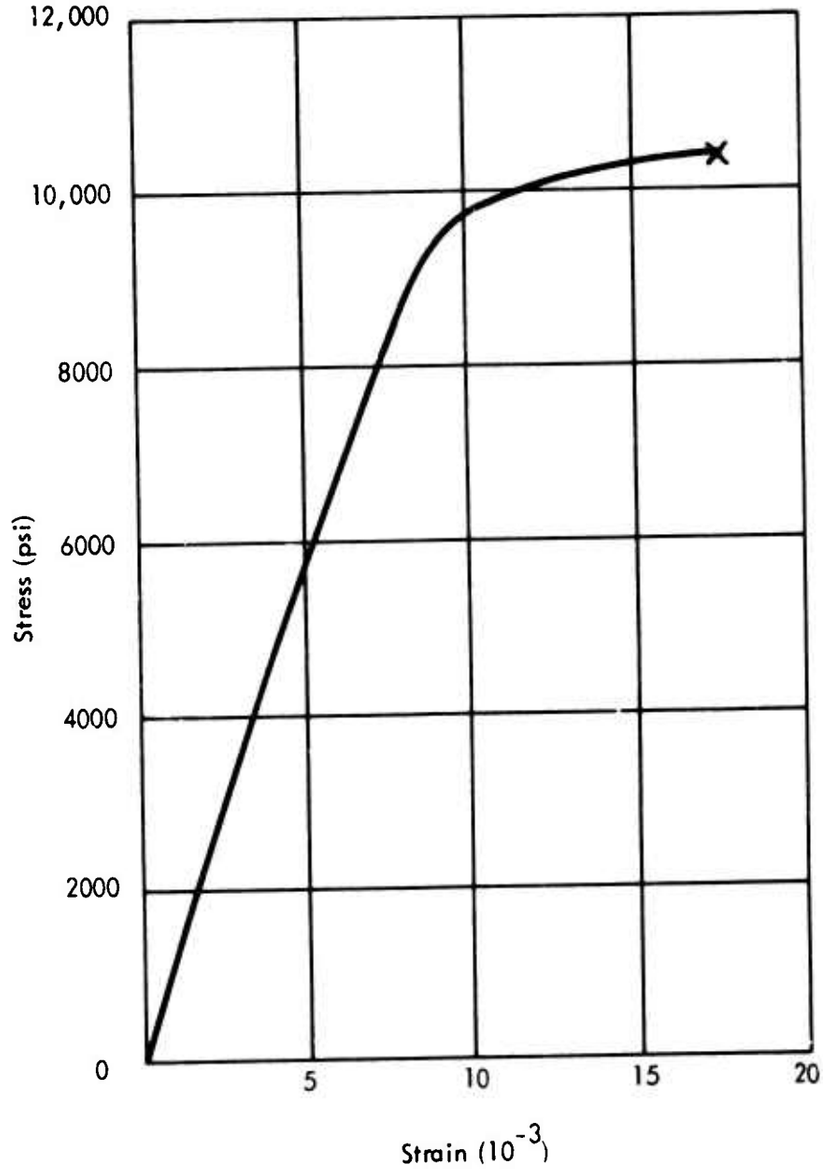

Figure 14. Tensile Test, EC2214, Aluminum, 72°F, Cross-Head Speed - 0.02 in./min, 0°/0°.

The nominal bond-line thicknesses were similar for both the tensile and shear specimens. The shear test results are listed in Table XXXI and summarized in Table XXXII. A typical stress-strain curve for these shear tests is shown in Figure 15.

Comparing the uniform bond-line properties for thin and thick bond lines, it was seen that the thicker specimens had somewhat lower values. The average shear modulus decreased about 6 percent with the thick bond lines. The thicker bond lines also caused the following decrease in average values: precision elastic limit, 28 percent; microyield stress, 28 percent; fracture stress, 8 percent. There was about a 23 percent increase in strain at unloading (γ_1) for the thick bond-line samples compared to that of the thin samples.

The effects due to introduction of the nonuniform bond-line thickness were not very strong; no trends could be observed. The one exception was the viscoelastic behavior, especially γ_1, the strain at unloading. For the thin bond-line samples, the tapered joints had an average value for γ_1 65 percent lower than for the uniform bond-line specimens. For the thick bond-line tests, the reduction was 77 percent.

The tensile modulus for EC2214 was shown to be only 17 percent of the value for FM1000. However, the shear modulus for EC2214 was 2-½ times greater than that for the FM1000 under similar test conditions.

Lap Shear Tests

The two thicknesses chosen for testing were nominally 0.006 and 0.014 in. Table XXXIII lists the results for these lap shear tests and includes one test for a specimen with a bond-line thickness of 0.022 in. The average fracture stress for the 0.006 in. bond-line joints was 5950 psi. Increasing the thickness to a nominal value of 0.014 in. did not materially affect that value. The specimen having a bond line of 0.022 in. had a lower fracture stress (4900 psi).

TABLE XXXI. SHEAR, EC2214, ALUMINUM, PHASE VI

Specimen Number	Average Bond-Line Thickness (10^{-3} in.)	Cross-Head Speed (in./min)	Test Temp. (°F)	Elastic Shear Modulus (10^5 psi)	Precision Elastic Limit (psi)	Microyield Stress (psi)	Fracture Stress τ_F (psi)	Fracture Mode (% cohesive)
EAS11-11	2.6	0.5	72	3.5	564	2140	8350	50
EAS12-7	4.9	"	"	3.1	576	1800	10700	75
EAS22'/22'-Y6	3.5-41.9	"	"	3.4	214	930	8530	20
EAS22'/22'-X9	5.6-44	"	"	2.3	388	1760	8420	50
EAS11'/11'-8	1.5-20.7	"	"	4.1	407	990	10000	80
EAS11'/11'-X5	3.1-22.3	"	"	3.5	272	1550	8920	50
EAS22'/0-10	2.2-21.4	"	"	2.9	368	864	10600	50
EAS22'/0-12	4.5-23.7	"	"	4.2	290	970	9130	100
EAS12-4	25	"	"	3.2	350	1360	9900	100
EAS10-2	28.1	"	"	2.8	242	1570	8250	100
EAS10-4	23.4	"	"	3.1	232	880	8550	0
EAS22'/22'-Y1	23.6-62.0	"	"	3.9	400	970	8000	20
EAS22'/22'-X8	24.3-62.7	"	"	3.0	175	577	8250	60

TABLE XXXI - Continued

Specimen Number	Average Bond-Line Thickness (10^{-3} in.)	Cross-Head Speed (in./min)	Test Temp. (°F)	Elastic Shear Modulus (10^5 psi)	Precision Elastic Limit (psi)	Microyield Stress (psi)	Fracture Stress τ_F (psi)	Fracture Mode (% cohesive)
EAS11'/11'-X3	23-42.2	0.5	72	2.1	310	680	8920	0
EAS11'/11'-X9	26.2-45.4	"	"	3.4	220	912	8630	50
EAS22'/0-11	21-40.2	"	"	4.1	276	490	8350	70
EAS22'/0-16	28.8-48.0	"	"	3.1	286	1340	8550	30

TABLE XXXI - Continued

Specimen Number	Average Bond-Line Thickness (10^{-3} in.)	Cross-Head Speed (in./min)	Test Temp. (°F)	γ_1 (10^{-3})	γ_2 (10^{-3})	γ_3 (10^{-3})	Stress Level (% τ_F)
EAS11-11	2.6	0.5	72	5.80	0	5.80	69
EAS12-7	4.9	"	"	6.40	1.6	4.80	72
EAS22'/22'-Y6	3.5-41.9	"	"	1.20	0.5	0.70	70
EAS22'/22'-X9	5.6-44	"	"	2.50	0.5	2.00	69
EAS11'/11'-8	1.5-20.7	"	"	1.92	0.96	0.96	55
EAS11'/11'-X5	3.1-22.3	"	"	2.10	0.40	1.70	65
EAS22'/0-10	2.2-21.4	"	"	2.30	0	2.30	61
EAS22'/0-12	4.5-23.7	"	"	2.50	0.80	1.70	63
EAS12-4	25	"	"	2.40	0.4	2.00	55
EAS10-2	28.1	"	"	6.00	1.5	4.50	75
EAS10-4	23.4	"	"	18.5	2.7	15.8	86
EAS22'/22'-Y1	23.6-62.0	"	"	2.50	0.7	1.80	69
EAS22'/22'-X8	24.3-62.7	"	"	1.80	0.3	1.50	59

TABLE XXXI - Continued

Specimen Number	Average Bond-Line Thickness (10^{-3} in.)	Cross-Head Speed (in./min)	Test Temp. (°F)	γ_1 (10^{-3})	γ_2 (10^{-3})	γ_3 (10^{-3})	Stress Level (% τ_F)
EAS11/11'-X3	23-42.2	0.5	72	3.50	1.0	2.50	80
EAS11'/11'-X9	26.2-45.4	"	"	1.35	0.3	1.05	54
EAS22'/0-11	21-40.2	"	"	1.56	0.5	1.06	63
EAS22'/0-16	28.8-48.0	"	"	1.76	0.5	1.26	65

TABLE XXXII. SHEAR SUMMARY, EC2214, ALUMINUM, PHASE VI

Bond-Line Configuration	Cross-Head Speed (in./min)	Test Temp. (°F)	Elastic Shear Modulus (10^5 psi)	Precision Elastic Limit (psi)	Microyield Stress (psi)	Fracture Stress τ_F (psi)	γ_1 (10^{-3})	γ_2 (10^{-3})	Stress Level (%τ_F)
0/0 (Thin)	0.5	72	3.3±.2	570±6	1970±170	9525±1175	6.1±.3	0.8±.8	≈ 71
22°/22° (Thin)	"	"	2.9±.6	301±87	1345±415	8475±55	1.9±.7	0.5±0	70
11°/11° (Thin)	"	"	3.8±.3	339±68	1270±280	9460±540	2.0±.08	0.68±.28	≈ 60
22°/0 (Thin)	"	"	3.6	329±39	917±53	9865±735	2.4±.1	0.4±.4	≈ 62
0/0 (Thick)	0.5	72	3.0±.2	275±50	1270±345	8900±825	9.0±8.1	1.5±1.2	≈ 72
22°/22° (Thick)	"	"	3.5±.4	290±110	774±196	8125±125	2.2±.3	0.5±.2	≈ 64
11°/11° (Thick)	"	"	2.8±.6	265±45	796±116	8775±145	2.43±1.07	0.65±.35	≈ 67
22°/0 (Thick)	"	"	3.6±.5	281±5	915±425	8450±100	1.66±.10	0.5±0	≈ 64

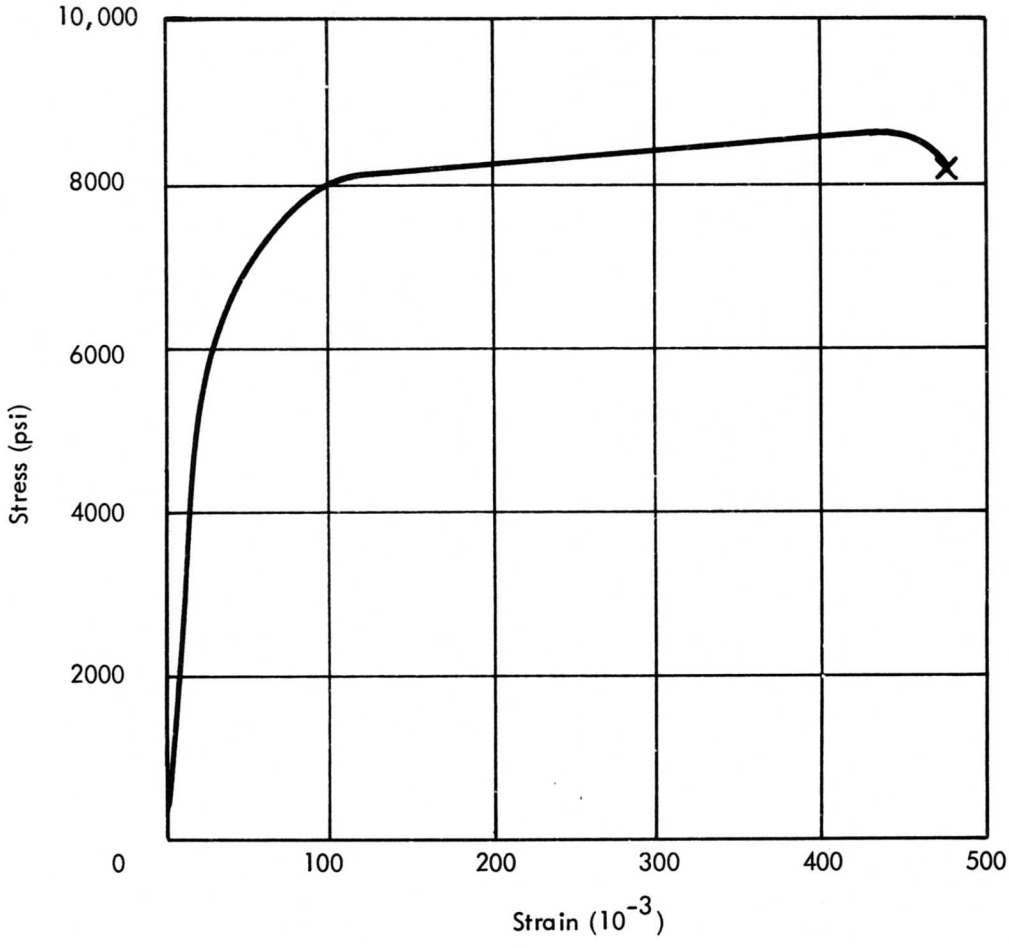

Figure 15. Shear Test, EC2214, Aluminum, 72°F, Cross-Head Speed - 0.5 in./min, 0°/0°.

TABLE XXXiII. LAP SHEAR, EC2214, ALUMINUM, PHASE VI

Specimen Number	Bond-Line Thickness (10^{-3} in.)	Fracture Stress (psi)	Fracture Mode (% cohesive)
EAL-1	5.0	6360	20
EAL-2	7.0	6000	20
EAL-4	7.0	5500	20
EAL-3	12.0	5800	20
EAL-5	15.0	5700	10
EAL-6	15.0	5800	10
EAL-7	22.0	4900	10

PHASES VII AND VIII, HIGH TEMPERATURE/STRAIN RATE

The specimens for these phases were Metlbond 329 on aluminum adherends. Phase VII was devoted to establishing the base-line properties for this system. Tests were made at room temperature using the standard cross-head speeds and bond-line thickness. In Phase VIII, similar specimens were used for tests at 160°F using the standard cross-head speeds as well as lower rates. The same nonuniform bond-line configurations were used here as were selected in Phase I.

Tensile Tests

The tensile test results for Phases VII and VIII are presented in Table XXXIV and summarized in Table XXXV. Typical stress-strain curves for tests at 72° and 160°F are shown in Figure 16. In general it can be said that raising the test temperature lowers the modulus and the strength levels and increases the viscoelastic flow. If the strain rate is lowered at 160°F, the same trends continue. Due to the relatively large experimental scatter, it is difficult to delineate the effects due to the introduction of nonuniform bond-line thicknesses. However, it can be said qualitatively that tapered bond lines raise the modulus; lower the P.E.L., the σ_{mys}, and the fracture stress; and diminish the viscoelastic flow slightly.

Considering average values for the various properties, the effects of higher test temperature and lower strain rate can be discussed. The average base-line modulus under standard conditions was 8.3×10^5 psi. Raising the test temperature to 160°F lowered this value to 6.5×10^5 psi. A further decrease was noted when the cross-head speed was reduced to 0.002 in./min - 5.95×10^5 psi. The absolute values for the precision elastic limit decreased as the temperature was raised and as the strain rate was lowered. In addition, for each of those two factors, the P.E.L. as fractions of the fracture stress also decreased in the order 39, 25 and 17 percent of σ_F. The same phenomenon was noted for the microyield stress. Average absolute values of σ_{mys} and as a fraction of σ_F were 2700 psi (58 percent), 2000 psi (40 percent) and 1450 psi (33 percent) for the test conditions, respectively. The fracture stress was not changed much by test temperature or strain rate, and the fractures were nearly all 100 percent cohesive in nature. The viscoelastic flow (ϵ_1) was increased about 47 percent due to raising the test temperature. Lowering the strain rate did not change this characteristic very much.

Shear Tests

Results for the shear tests of Phases VII and VIII are given in Tables XXXVI and XXXVII. Typical shear stress-strain curves for tests at 72° and 160°F are shown in Figure 17.

TABLE XXXIV. TENSILE, METLBOND 329, ALUMINUM, PHASE VII AND VIII

Specimen Number	Average Bond-Line Thickness (10^{-3} in.)	Cross-Head Speed (in./min)	Test Temp. (°F)	Elastic Tensile Modulus (10^5 psi)	Precision Elastic Limit (psi)	Microyield Stress (psi)	Fracture Stress σ_F (psi)	Fracture Mode (% cohesive)
MAT3-13	7.7	0.02	72	6.8	1270	2650	4280	100
MAT1-12	10.0	"	"	8.2	2500	3310	4800	100
MAT3-14	7.1	"	"	7.9	2500	3060	5020	100
MAT3-11	8.7	"	"	8.9	2800	3820	4940	100
MAT2°/2°-X1	14.3-49.3	"	"	8.5	1650	2550	6430	100
MAT2°/2°-X5	10.7-45.7	"	"	8.8	1910	2550	4500	100
MAT1°/1°-18	12.0-29.5	"	"	9.2	1790	2800	4070	100
MAT1°/1°-19	11.2-28.7	"	"	6.5	1920	2300	4230	100
MAT2°/0°-11	5.4-22.9	"	"	7.7	1780	2530	3800	100
MAT2°/0°-12	6.0-23.5	"	"	9.2	1150	2420	4870	100
MAT3-15	8.3	0.02	160	4.8	1270	2040	5800	100
MAT1-13	10.3	"	"	6.7	2300	3320	6130	100
MAT2°/2°-X6	9-44	"	"	7.7	1020	1660	4670	100
MAT2°/2°-X7	8.6-43.6	"	"	6.1	893	1400	4420	100

TABLE XXXIV - Continued

Specimen Number	Average Bond-Line Thickness (10^{-3} in.)	Cross-Head Speed (in./min)	Test Temp. (°F)	Elastic Tensile Modulus (10^5 psi)	Precision Elastic Limit (psi)	Microyield Stress (psi)	Fracture Stress σ_F (psi)	Fracture Mode (% cohesive)
MAT1°/1°-20	8.8-26.3	0.02	160	6.3	1070	2090	4000	100
MAT1°/1°-21	4.3-21.8	"	"	6.5	1560	2190	4840	100
MAT2°/0-14	4.7-22.2	"	"	8.3	1270	2040	5700	90
MAT2°/0-16	7.3-24.8	"	"	5.6	765	1270	5000	100
MAT3-15	7.9	0.002	160	4.1	765	2000	4080	50
MAT3-16	8.2	"		4.1	640	1400	4180	100
MAT2°/2°-12	6.5-41.5	"	"	5.4	510	1020	4340	100
MAT2°/2°-13	3.2-38.2	"	"	7.5	1020	1780	4070	100
MAT1°/1°-22	8.2-25.7	"	"	6.2	1280	2040	4950	100
MAT1°/1°-23	12.0-29.5	"	"	7.6	750	1250	4850	100
MAT2°/0°-18	13.0-30.5	"	"	5.1	510	1276	3760	100
MAT2°/0°-19	9.0-26.5	"	"	7.4	510	870	5400	100

TABLE XXXIV - Continued

Specimen Number	Average Bond-Line Thickness (10^{-3} in.)	Cross-Head Speed (in./min)	Test Temp. (°F)	ϵ_1 (10^{-3})	ϵ_2 (10^{-3})	ϵ_3 (10^{-3})	Stress Level (% σ_F)
MAT3-13	7.7	0.02	72	0.55	0.16	0.39	83
MAT1-12	10.0	"	"	0.40	0.30	0.10	85
MAT3-14	7.1	"	"	0.80	0	0.80	82
MAT3-11	8.7	"	"	0.30	0	0.30	82
MAT2°/2°-X1	14.3-49.3	"	"	0.35	0	0.35	72
MAT2°/2°-X5	10.7-45.7	"	"	0.20	0.20	0	80
MAT1°/1°-18	12.0-29.5	"	"	0.35	0.3	0.05	87
MAT1°/1°-19	11.2-28.7	"	"	0.50	0	0.50	84
MAT2°/0°-11	5.4-22.9	"	"	0.70	0.4	0.3	95
MAT2°/0°-12	6.0-23.5	"	"	0.30	0.17	0.13	75
MAT3-15	8.3	0.02	160	0.90	0	0.90	80
MAT1-13	10.3	"	"	0.90	0.3	0.60	83
MAT2°/2°-X6	9-44	"	"	0.30	0	0.30	77
MAT2°/2°-X7	8.6-43.6	"	"	0.40	0	0.40	81

TABLE XXXIV - Continued

Specimen Number	Average Bond-Line Thickness (10^{-3} in.)	Cross-Head Speed (in./min)	Test Temp. (°F)	ϵ_1 (10^{-3})	ϵ_2 (10^{-3})	ϵ_3 (10^{-3})	Stress Level (% σ_F)
MAT1°/1°-20	8.8-26.3	0.02	160	0.92	0.2	0.72	78
MAT1°/1°-21	4.3-21.8	"	"	1.20	0	1.20	85
MAT2°/0-14	4.7-22.2	"	"	0.92	0	0.92	71
MAT2°/0-16	7.3-24.8	"	"	0.40	0.07	0.33	72
MAT3-15	7.9	0.002	160	1.00	0	1.00	92
MAT3-16	8.2	"	"	0.90	0.1	0.80	85
MAT2°/2°-12	6.5-41.5	"	"	1.30	0.1	1.20	78
MAT2°/2°-13	3.2-38.2	"	"	0.90	0	0.90	87
MAT1°/1°-22	8.2-25.7	"	"	0.30	0	0.30	82
MAT1°/1°-23	12.0-29.5	"	"	0.56	0	0.56	74
MAT2°/0°-18	13.0-30.5	"	"	0.82	0.8	0.74	85
MAT2°/0°-19	9.0-26.5	"	"	0.47	0	0.47	57

TABLE XXXV. TENSILE SUMMARY, METLBOND 329, ALUMINUM, PHASES VII AND VIII

Bond-Line Configuration	Cross-Head Speed (in./min)	Test Temp. (^{o}F)	Elastic Tensile Modulus (10^5 psi)	Precision Elastic limit (psi)	Microyield Stress (psi)	Fracture Stress σ_F (psi)	ϵ_1 (10^{-3})	ϵ_2 (10^{-3})	Stress Level (% σ_F)
0/0	0.02	72	8.0±1.1	2270±760	3210±585	4760±240	0.60±.19	0.23±.07	≈ 83
2°/2°	"	"	8.7±.2	1780±130	2550± 0	5470±970	0.28±.08	0.10±.1	≈ 76
1°/1°	"	"	7.9±1.4	1850±60	2550±250	4150±80	0.43±.08	0.15±.15	≈ 86
2°/0°	"	"	8.5±.8	1470±310	2475± 55	4335±535	0.50±.2	0.29±.11	≈ 85
0/0	0.02	160	5.8±1	1785±515	2680±640	5965±165	0.90±0	0.15±.15	≈ 82
2°/2°	"	"	6.9±.8	957±64	1530±130	4545±125	0.35±.05	0	≈ 79
1°/1°	"	"	6.4±.1	1315±245	2140±50	4420±420	1.06±.14	0.1±.1	≈ 81
2°/0°	"	"	7.0±1.3	1018±252	1655±385	5350±350	0.66±.26	0.03±.03	≈ 71
0/0	0.002	160	4.1±0	703±62	1700±300	4130± 50	0.95±.05	0.05±.05	≈ 88
2°/2°	"	"	6.5±1	765± 255	1400±380	4205±135	1.1±.2	0.05±.05	≈ 82
1°/1°	"	"	6.9±.7	1015±165	1645±395	4900± 50	0.43±.13	0	≈ 78
2°/0°	"	"	6.3±1.2	510± 0	1073±203	4580±820	0.65±.18	0.4±.4	≈ 71

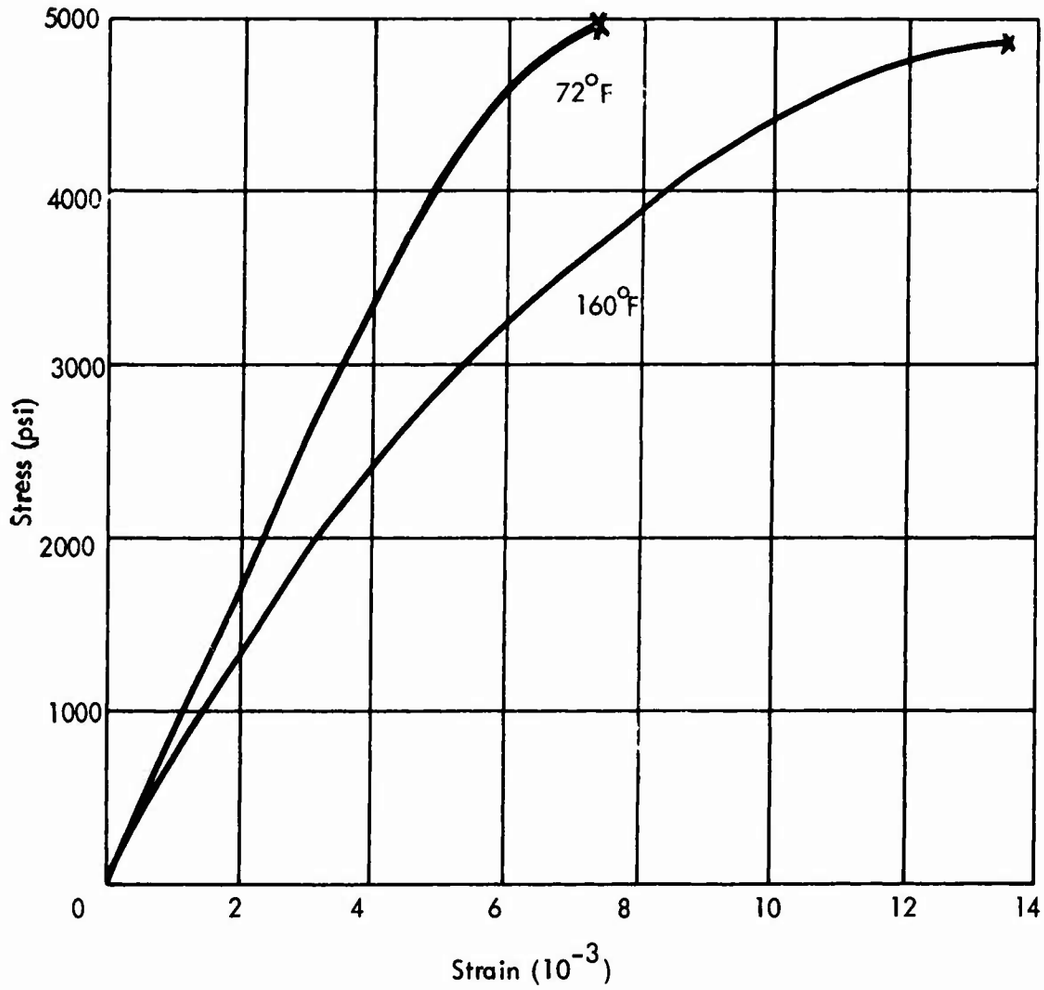

Figure 16. Tensile Tests, Metlbond 329, Aluminum, Cross-Head Speed - 0.02 in./min, 0°/0°.

TABLE XXXVI. SHEAR, METLBOND 329, ALUMINUM, PHASE VII AND VIII

Specimen Number	Average Bond-Line Thickness (10^{-3} in.)	Cross-Head Speed (in./min)	Test Temp. (°F)	Elastic Shear Modulus (10^5 psi)	Precision Elastic Limit (psi)	Microyield Stress (psi)	Fracture Stress τ_F (psi)	Fracture Mode (% cohesive)
MAS11-12	7.4	0.5	72	3.3	970	3680	7160	10
MAS11-13	6.7	"	"	3.2	390	1160	7000	50
MAS22'/22'-9	8.9-47.3	"	"	4.3	490	1560	7560	100
MAS22'/22'-X6	8.2-46.6	"	"	3.5	612	1360	7950	50
MAS11'/11'-10	10.8-30.0	"	"	3.6	582	930	7520	50
MAS11'/11'-11	12.5-31.7	"	"	3.6	292	865	6220	50
MAS22'/0-20	12.4-31.6	"	"	3.4	252	1550	5340	100
MAS22'/0-21	9.8-29.0	"	"	4.0	300	485	5050	50
MAS12-5	10.2	0.5	160	3.2	388	583	7200	50
MAS11-14	5.2	"	"	3.0	310	485	6700	100
MAS22'/22'-8	12.5-50.9	"	"	3.5	300	533	6200	100
MAS22'/22'-10	7.6-46.0	"	"	3.8	272	373	5150	50
MAS11'/11'-9	7.7-25.9	"	"	2.6	320	535	6300	60
MAS11'/11'-X6	10.8-30.0	"	"	3.5	262	570	5100	1000

TABLE XXXVI - Continued

Specimen Number	Average Bond-Line Thickness (10^{-3} in.)	Cross-Head Speed (in./min)	Test Temp. (°F)	Elastic Shear Modulus (10^5 psi)	Precision Elastic Limit (psi)	Microyield Stress (psi)	Fracture Stress τ_F (psi)	Fracture Mode (% cohesive)
MAS22¹/0-17	14.7-33.9	0.5	160	2.6	250	780	4770	100
MAS22¹/0-18	8.2-27.4	"	"	2.5	194	445	5280	85
MAS12-6	8.2	0.05	160	3.5	292	580	9200	50
MAS11-14	6.0	"	"	3.1	291	670	8250	100
MAS22¹/22¹-X5	10.9-49.3	"	"	3.4	388	770	6200	20
MAS22¹/22¹-X7	10.1-48.5	"	"	2.3	292	485	4320	50
MAS11¹/11¹-X7	10.7-29.9	"	"	3.5	242	388	6450	100
MAS11¹/11¹-X8	11.8-31.0	"	"	3.2	350	775	4880	100
MAS22¹/0-9	7.8-27.0	"	"	3.8	388	778	6300	100
MAS22¹/0-19	10-29.2	"	"	2.0	190	583	5600	70

TABLE XXXVI - Continued

Specimen Number	Average Bond-Line Thickness (10^{-3} in.)	Cross-Head Speed (in./min)	Test Temp. (°F)	γ_1 (10^{-3})	γ_2 (10^{-3})	γ_3 (10^{-3})	Stress Level (% τ_F)
MAS11-12	7.4	0.5	72	0.7	0	0.7	63
				1.8	0	1.8	89
MAS11-13	6.7	"	"	3.0	0.6	2.4	72
				4.0	1.1	2.9	93
MAS22'/22'-9	8.9-47.3	"	"	2.4	0.8	1.6	75
MAS22'/22'-X6	8.2-46.6	"	"	0.8	0	0.8	75
MAS11'/11'-10	10.8-30.0	"	"	2.0	0.8	1.2	71
MAS11'/11'-11	12.5-31.7	"	"	1.0	0	1.0	75
MAS22'/0-20	12.4-31.6	"	"	2.0	0	2.0	77
MAS22'/0-21	9.8-29.0	"	"	0.4	0	0.4	32
MAS12-5	10.2	0.5	160	6.7	1.0	5.7	68
				9.5	1.9	7.6	81
MAS11-14	5.2	"	"	2.3	0.9	1.4	56
MAS22'/22'-8	12.5-50.9	"	"	2.5	1.2	1.3	77
MAS22'/22'-10	7.6-46.0	"	"	0.9	0.2	0.7	50

TABLE XXXVI - Continued

Specimen Number	Average Bond-Line Thickness (10^{-3} in.)	Cross-Head Speed (in./min)	Test Temp. (°F)	γ_1 (10^{-3})	γ_2 (10^{-3})	γ_3 (10^{-3})	Stress Level (% τ_F)
MAS11'/11'-9	7.7-25.9	0.5	160	2.4	0.8	1.6	70
MAS11'/11'-X6	10.8-30.0	"	"	3.8	0	3.8	76
MAS22'/0-17	14.7-33.9	"	"	1.0	0.5	0.5	63
MAS22'/0-18	8.2-27.4	"	"	2.4	0.8	1.6	60
MAS12-6	8.2	0.05	160	3.7	1.5	2.2	53
MAS11-14	6.0	"	"	5.2	1.3	3.9	71
MAS22'/22'-X5	10.9-49.3	"	"	1.2	0.3	0.9	50
MAS22'/22'-X7	10.1-48.5	"	"	1.4	0.3	1.1	72
MAS11'/11'-X7	10.7-29.9	"	"	1.7	0.4	1.3	50
MAS11'/11'-X8	11.8-31.0	"	"	1.3	0.8	0.5	70
MAS22'/0-9	7.8-27.0	"	"	1.8	0	1.8	77
MAS22'/0-19	10-29.2	"	"	2.4	0.6	1.8	35

TABLE XXXVII. SHEAR SUMMARY, METLBOND 329, ALUMINUM, PHASES VII AND VIII

Bond-Line Configuration	Cross-Head Speed (in./min)	Test Temp. (^{o}F)	Elastic Shear Modulus (10^5 psi)	Precision Elastic Limit (psi)	Microyield Stress (psi)	Fracture Stress τ_F (psi)	γ_1 (10^{-3})	γ_2 (10^{-3})	Stress Level (%τ_F)
0/0	0.5	72	3.3±.1	680±290	2420±1260	7080±80	1.9±1.1	0.3±.3	≈ 80
22'/22'	"	"	3.9±.4	551± 61	1460±100	7755±195	1.6±.8	0.4±.4	75
11'/11'	"	"	3.6±0	437± 145	898± 32	6870±650	1.5±.5	0.4±.4	≈ 73
22'/0	"	"	3.7±.3	276± 24	1018±532	5195±145	1.2±.8	0	≈ 50
0/0	0.5	160	3.1±.1	349±39	534±49	6950±250	4.5±2.2	0.95±.05	≈ 68
22'/22'	"	"	3.7±.2	286± 14	453±80	5675±525	1.7±.8	0.7±.5	≈ 73
11'/11'	"	"	3.1±.5	291±29	553±17	5700±600	3.1±.7	0.4±.4	≈ 63
22'/0	"	"	2.6±.1	222± 28	613±167	5025±255	1.7±.7	0.7±.2	≈ 61
0/0	0.05	160	3.3±.2	292±1	625± 45	8725±475	4.5±.8	1.4±.1	≈ 62
22'/22'	"	"	2.9±.6	340± 48	628±142	5260±940	1.3±.1	0.3±0	≈ 61
11'/11'	"	"	3.4±.2	296± 54	582± 193	5665±785	1.5±.2	0.6±.2	≈ 60
22'/0	"	"	2.9±.9	289±99	682±96	5950±350	2.1±.3	0.3±.3	≈ 56

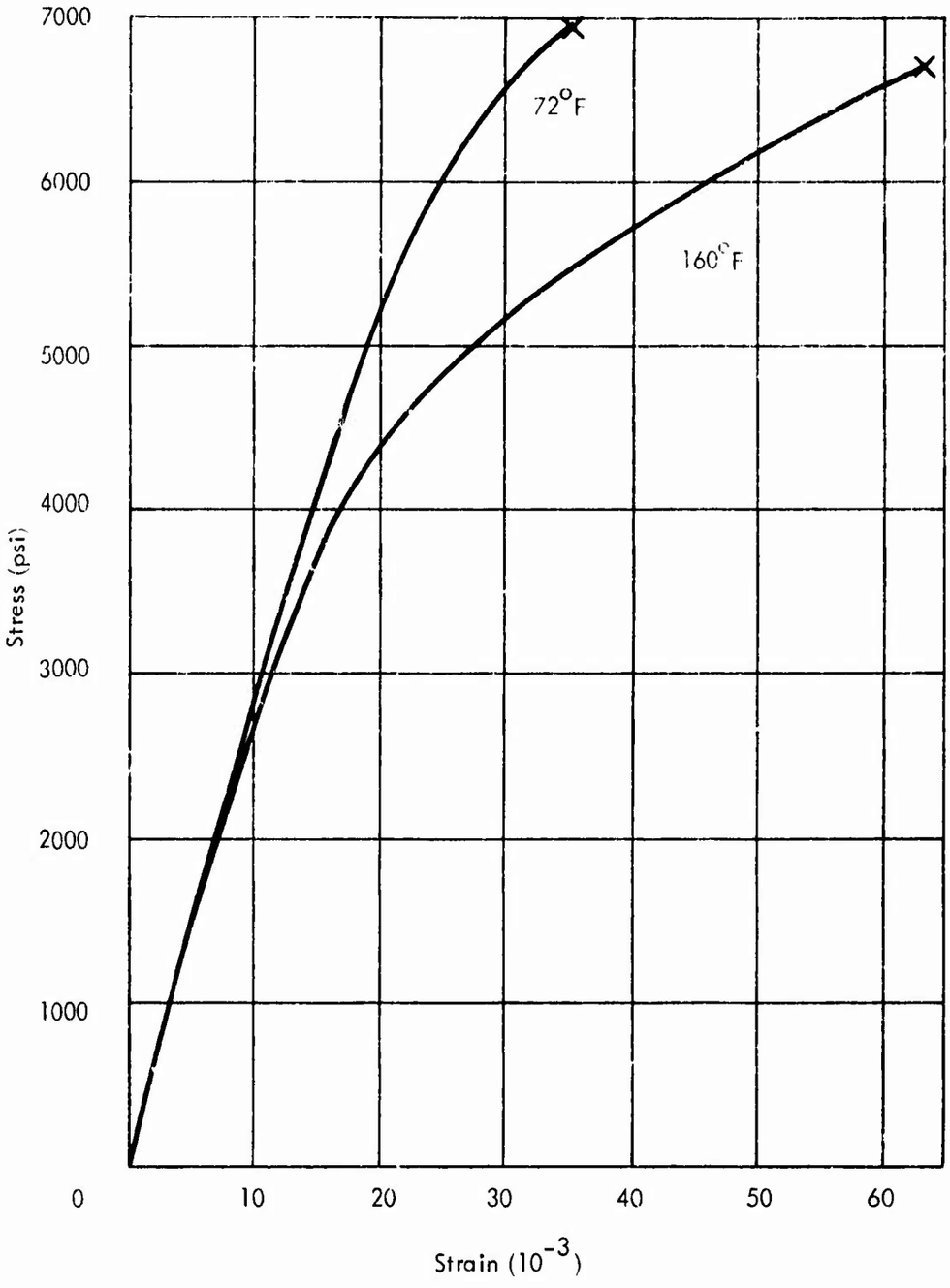

Figure 17. Shear Tests, Metlbond 329, Aluminum, Cross-Head Speed - 0.5 in./min, $0^{\circ}/0^{\circ}$.

As with the tensile results, raising the test temperature lowers the modulus, the precision elastic limit and the microyield stress; increases the viscoelastic flow; and does not significantly affect the fracture behavior. The magnitude of these effects was smaller in the case of tensile tests than it was for the shear tests. Introducing a tapered bond line appears to raise the modulus, lower the strength levels, and diminish the viscoelastic flow. Based on average values, lowering the strain rate, in addition to raising the test temperature, has a negligible effect on the properties. The average shear modulus for the Phase VII results was 3.6×10^5 psi. Raising the test temperature to 160°F decreased this value only 13 percent to 3.12×10^5 psi. Lowering the strain rate by a factor of ten did not introduce any further changes in the shear modulus. Values for the P.E.L. and τ_{mys} decreased in absolute value and percentage of the fracture stress when the test temperature was raised. At 72°F, the P.E.L. was 7 percent and the τ_{mys} was 22 percent of τ_F. At 160°F, these percentages were 5 and 10, respectively, for the P.E.L. and the τ_{mys}. At the higher temperature, the viscoelastic strain at unloading, γ_1, was nearly doubled that for tests at 72°F. The recovered strain, γ_2, as a percentage of γ_1 increased at 160°F and was raised even more with the lower strain rate.

Lap Shear Tests

The base-line tests at 72°F with a cross-head speed of 0.5 in./min had an average fracture stress of 2375 psi, with 100 percent cohesive failure. When the test temperature was raised to 160°F, an average value of 2395 psi was observed. Lowering the cross-head speed to 0.05 in./min at 160°F resulted in an average fracture stress of 2435 psi, again with 100 percent cohesive failure. These test results are presented in Table XXXVIII.

Within the ranges of temperature and strain rate used in these two phases, it was shown that test temperature was more effective in modifying the properties than was changing the strain rate. The property changes were relatively small for the increase of 88°F in test temperature.

PHASE IX, AGEING/ENVIRONMENT

For this phase of the investigation, two batches of FM1000 were stored in different environments. One batch was kept in a controlled environment maintained at 68°F with a relative humidity of 45 percent. Tensile specimens were prepared and tested after 4 months' exposure. After 8 and 12 months' exposure, additional tensile specimens and some lap shear specimens were prepared and tested. The second batch of FM1000 was stored in an uncontrolled environment in which both the temperature and humidity fluctuated from day to day over ranges of 72° to 75°F and 20 to 60 percent relative humidity. After 4 months in this uncontrolled

TABLE XXXVIII. LAP SHEAR, METLBOND 329, ALUMINUM, PHASES VII AND VIII

Specimen Number	Bond-Line Thickness (10^{-3} in.)	Cross-Head Speed (in./min)	Test Temp. (°F)	Fracture Stress (psi)	Fracture Mode (% cohesive)
MAL1	10.0	0.5	72	2300	100
MAL2	10.0	"	"	2450	100
MAL3	8.0	0.5	160	2400	100
MAL4	10.0	"	"	2390	100
MAL5	9.0	0.05	160	2480	100
MAL6	9.0	"	"	2390	100

environment, specimens were prepared for tensile and lap shear tests. The manufacturer's warranty for FM1000 is 6 months from date of shipment when stored below 85°F. All tests were made using the standard experimental conditions of Phase II with only uniform bond-line thicknesses (no tapers).

Tensile Tests

The test results for the tensile specimens are shown in Table XXXIX and summarized in Table XXXX. Within the experimental scatter, ageing in the controlled environment did not appreciably alter the mechanical properties for up to 8 months' exposure. However, the material aged 12 months in the controlled environment underwent marked decreases in properties. The tensile modulus dropped from 6.3 to 2.5×10^5 psi and the fracture stress was lowered to 7100 psi from 10,650 psi. It appears that the 4 months' exposure to the uncontrolled environment lowered the elastic tensile modulus but did not affect the other properties to any great extent.

Lap Shear Tests

The test results for lap shear specimens aged 8 months in a controlled environment and 4 months in an uncontrolled environment are shown in Table XXXXI. In contrast to the tensile results, there was a marked deterioration in the properties as a result of ageing. The fracture stress dropped 55 percent after 4 months' exposure to the uncontrolled environment. For the controlled environment, after 8 months the fracture stress dropped 68 percent; after 12 months there was a 42 percent decrease. The fracture mode was somewhat less cohesive in nature after the ageing. An additional set of experiments was performed (see Table XXXXI). Lap shear specimens were cured and then aged 4 months in the uncontrolled environment with no deterioration in properties. In fact, the fracture stress was higher than for freshly bonded specimens (8125 psi as compared to 7075 psi).

TABLE XXXIX. TENSILE, FM1000, TITANIUM, PHASE IX

Specimen Number	Average Bond-Line Thickness (10^{-3} in.)	Cross-Head Speed (in./min)	Test Temp. (°F)	Elastic Tensile Modulus (10^5 psi)	Precision Elastic Limit (psi)	Microyield Stress (psi)	Fracture Stress σ_F (psi)	Fracture Mode (% cohesive)
FTT9-1	7.5	0.02	72	6.0	1280	2960	8800	75
FTT9-2	8.1	"	"	7.5	1480	2300	10600	90
FTT12-3	7.9	"	"	5.5	1780	4040	10700	75
Aged 4 Months in Controlled Environment (68°F with a relative humidity of 45%)								
FTT1-2	4.3	0.02	72	4.9	1020	1780	10200	80
FTT1-3	2.4	"	"	5.1	764	1270	11500	70
Aged 8 Months in Controlled Environment (68°F with a relative humidity of 45%)								
FTT12-Y2	5.7	0.02	72	6.5	1800	3570	10850	70
FTT2-Y3	14.2	"	"	5.7	1800	3550	7250	50
Aged 4 Months in Uncontrolled Environment								
FTT2-X1	7.4	0.02	72	5.4	1780	4600	10450	80
FTT12-X3	7.1	"	"	4.2	720	1780	9700	85

TABLE XXXIX - Continued

Specimen Number	Average Bond-Line Thickness (10^{-3} in.)	Cross-Head Speed (in./min)	Test Temp. (^{o}F)	Elastic Tensile Modulus (10^{5} psi)	Precision Elastic Limit (psi)	Microyield Stress (psi)	Fracture Stress σ_F (psi)	Fracture Mode (% cohesive)
Aged 12 Months in Controlled Environment (68^{o}F with a relative humidity of 45%)								
FTT6-X3	5.9	0.02	72	2.8	510	1530	7700	75
FTT11-X3	6.5	"	"	2.3	440	1530	6500	30

TABLE XXXIX - Continued

Specimen Number	Average Bond Line Thickness (10^{-3} in.)	Cross Head Speed (in./min)	Test Temp. (°F)	ϵ_1 (10^{-3})	ϵ_2 (10^{-3})	ϵ_3 (10^{-3})	Stress Level (% σ_F)
FTT9-1	7.5	0.02	72	1.60	0.80	0.20	84
FTT9-2	8.1	"	"	1.60	-	-	86
FTT12-3	7.9	"	"	0.65	0.05	0.60	76
Aged 4 Months in Controlled Environment (68°F with a relative humidity of 45%)							
FTT1-2	4.3	0.02	72	0.9	nil	0.9	80
FTT1-3	2.4	"	"	3.0	1.0	2.0	85
Aged 8 Months in Controlled Environment (68°F with a relative humidity of 45%)							
FTT12-Y2	5.7	0.02	72	1.20	0.30	0.90	80
FTT2-Y3	14.2	"	"	0.22	0	0.22	85
Aged 4 Months in Uncontrolled Environment							
FTT2-X1	7.4	0.02	72	0.8	0	0.8	80
FTT12-X3	7.1	"	"	1.30	1.0	0.30	80

TABLE XXXIX - Continued

Specimen Number	Average Bond-Line Thickness (10^{-3} in.)	Cross-Head Speed (in./min)	Test Temp. (°F)	ϵ_1 (10^{-3})	ϵ_2 (10^{-3})	ϵ_3 (10^{-3})	Stress Level (% σ_F)
Aged 12 Months in Controlled Environment (68°F with a relative humidity of 45%)							
FTT6-X3	5.9	0.02	72	2.4	0	-	85
FTT11-X3	6.5	"	"	14.0	0	-	85

TABLE XXXX. TENSILE SUMMARY, FM1000, TITANIUM, PHASE IX

Remarks	Cross-Head Speed (in./min)	Test Temp. (°F)	Elastic Tensile Modulus (10^5 psi)	Precision Elastic Limit (psi)	Microyield Stress (psi)	Fracture Stress σ_F (psi)	ϵ_1 (10^{-3})	ϵ_2 (10^{-3})	Stress Level (% σ_F)
Fresh Adhesive	0.02	72	6.3± 1.0	1510±250	3100±870	10030±950	1.6	0.8	84*
Aged 4 months in controlled environment	"	"	5.0±.1	890±130	1525±255	10850±650	1.95±1.05	0.5±.5	≈83
Aged 8 months in controlled environment	"	"	6.1±.4	1800±0	3560±10	9050±1800	0.71±.5	0.1±.1	≈83
Aged 4 months in uncontrolled environment	"	"	4.8±.6	1250±530	3190±1400	10075±375	1.0±.2	0.5±.5	80
Aged 12 months in controlled environment	"	"	2.5±.3	475±35	1530±0	7100±600	8.2±5.8	0	85

* only one datum point

TABLE XXXXI. LAP SHEAR SUMMARY, FM1000, TITANIUM, PHASE IX

Cross-Head Speed (in./min)	Fracture Stress (psi)	Fracture Mode (% cohesive)	Remarks
0.5	7075 ± 300	75	Fresh adhesive
0.5	2290 ± 170	50	Aged 8 months in controlled environment
0.5	3880 ± 1100	50	Aged 4 months in uncontrolled environment
0.5	8125 ± 125	50	Aged 4 months in controlled environment after curing
0.5	4100±450	0	Aged 12 months in controlled environment

SUMMARY OF RESULTS

The results of this research program will be summarized by phases, including major property values (average) and the influence of the principal experimental variables. The effects of introducing nonuniform bond-line configurations will be listed separately, again by phases.

Phase I, Base-Line Data

Properties of FM1000 on aluminum adherends (standard tests):

Tensile	Shear	Lap Shear
$E^* = 5.0 \times 10^5$ psi	$G = 1.43 \times 10^5$ psi	fracture = 6750 psi
P.E.L. = 870psi ($0.08\sigma_F$)	P.E.L. = 320psi ($0.05\tau_F$)	
$\sigma_{mys} = 1580$psi ($0.15\sigma_F$)	$\tau_{mys} = 620$psi ($0.06\tau_F$)	
$\sigma_F = 10{,}800$psi	$\tau_F = 9500$psi	
$\epsilon_1 = 1.48 \times 10^{-3}$ (@ $0.8\sigma_F$)	$\gamma = 5.2 \times 10^{-3}$ (@ $0.5\tau_F$)	

Deviations from elastic flow occurred at very low stress levels (for shear, about half that for tensile). Viscoelastic flow was considerably greater for shear than for tension.

Phase II, Adherend Material

Properties of FM1000 on titanium adherends (standard tests):

Tensile	Shear	Lap Shear
$E^* = 5.9 \times 10^5$ psi	$G = 1.48 \times 10^5$ psi	fracture = 7075 psi
P.E.L. = 810 psi	P.E.L. = 246 psi	
$\sigma_{mys} = 1785$ psi	$\tau_{mys} = 530$ psi	
$\sigma_F = 10{,}160$ psi	$\tau_F = 7900$ psi	
$\epsilon_1 = 1.23 \times 10^{-3}$	$\gamma_1 = 4.4 \times 10^{-3}$	

Titanium adherends raised the tensile modulus 18 percent but did not appreciably change the other properties.

Phase III, Cryogenic

Properties of FM1000 on titanium adherends (-65°F):

Tensile	Shear	Lap Shear
$E^* = 7.3 \times 10^5$ psi	$G = 1.98 \times 10^5$ psi	fracture = 8435 psi
P.E.L. = 2500 psi	P.E.L. = 1860 psi	
$\sigma_{mys} = 5460$ psi	$\tau_{mys} = 3120$ psi	
$\sigma_F = 15,000$ psi	$\tau_F = 13,400$ psi	
ϵ_1 = nil	γ_1 = nil	

Properties of FM1000 aluminum adherends (-65°F):

Tensile	Shear	Lap Shear
$E^* = 7.15 \times 10^5$ psi	$G = 1.9 \times 10^5$ psi	fracture = 8000 psi
P.E.L. = 3750 psi	P.E.L. = 525 psi	
$\sigma_{mys} = 8030$ psi	$\sigma_{mys} = 1470$ psi	
$\sigma_F = 17,120$ psi	$\sigma_F = 13,260$ psi	
ϵ_1 = nil	γ_1 = nil	

At -65°F, all the strength properties were increased in value and there was no viscoelastic flow.

Phase IV, Strain Rate

Properties of FM1000 on aluminum adherends (low strain rate):

Tensile	Shear	Lap Shear
$E^* = 5.0 \times 10^5$ psi	$G = 1.55 \times 10^5$ psi	fracture = 5600 psi
P.E.L. = 810 psi	P.E.L. = 290 psi	
$\sigma_{mys} = 1570$ psi	$\tau_{mys} = 510$ psi	
$\sigma_F = 9100$ psi	$\tau_F = 8100$ psi	
$\epsilon_1 = 1.38 \times 10^{-3}$	$\gamma_1 = 10.7 \times 10^{-3}$	

Properties of FM1000 on aluminum adherends (high strain rate):

Tensile	Shear	Lap Shear
$E^* = 6.1 \times 10^5$ psi	$G = 1.8 \times 10^5$ psi	fracture = 7300
P.E.L. = 1510 psi	P.E.L. = 340 psi	
$\sigma_{mys} = 3250$ psi	$\tau_{mys} = 770$ psi	
$\sigma_F = 10,700$ psi	$\tau_F = 8720$ psi	
$\epsilon_1 = 0.52 \times 10^{-3}$	$\gamma_1 = 8.1 \times 10^{-3}$	

The lower strain rate did not appreciably change the Phase I properties; however, the higher strain rate raised E and G and the strength levels and diminished the viscoelastic flow.

Phase V, Cryogenic/Strain Rate

Properties of FM1000 aluminum adherends (low temperature, high strain rate):

Tensile	Shear	Lap Shear
$E^* = 8.6 \times 10^5$ psi	$G = 2.15 \times 10^5$ psi	fracture = 8200 psi
P.E.L. = 3420 psi	P.E.L. = 700 psi	
$\sigma_{mys} = 10,100$ psi	$\tau_{mys} = 2370$ psi	
$\sigma_F = 17,900$ psi	$\tau_F = 13,200$ psi	
ϵ_1 = nil	γ_1 = nil	

This combination of experimental variables produced the highest strength levels for any of the FM1000 tests; the effects were the greatest for the tensile tests.

Phase VI, Bond-Line Thickness

Properties of EC2214 on aluminum adherends (thin bond-line):

Tensile	Shear	Lap Shear
$E^* = 0.86 \times 10^6$ psi	$G = 3.4 \times 10^5$ psi	fracture = 5950 psi
P.E.L. = 2350 psi	P.E.L. = 385 psi	
$\sigma_{mys} = 4820$ psi	$\tau_{mys} = 1375$ psi	
$\sigma_F = 10,350$ psi	$\tau_F = 9330$ psi	
$\epsilon_1 = 0.65 \times 10^{-3}$	$\gamma_1 = 3.1 \times 10^{-3}$	

Properties of EC2214 on aluminum adherends (thick bond-line):

Tensile	Shear	Lap Shear
$E^* = 0.96 \times 10^6$ psi	$G = 3.2 \times 10^5$ psi	fracture = 5550 psi
P.E.L. = 2230 psi	P.E.L. = 277 psi	
$\sigma_{mys} = 4290$ psi	$\tau_{mys} = 940$ psi	
$\sigma_F = 10,480$ psi	$\tau_F = 8560$ psi	
$\epsilon_1 = 0.32 \times 10^{-3}$	$\gamma_1 = 3.82 \times 10^{-3}$	

The effects due to bond-line thickness were indeterminate for this system.

Phases VII and VIII, High Temperature/Strain Rate

Properties of Metlbond 329 on aluminum adherends (standard strain rate, 72°F):

Tensile	Shear	Lap Shear
$E^* = 8.3 \times 10^5$ psi	$G = 3.6 \times 10^5$ psi	fracture = 2375 psi
P.E.L. = 1840 psi	P.E.L. = 486 psi	
$\sigma_{mys} = 2700$ psi	$\tau_{mys} = 1450$ psi	
$\sigma_F = 4680$ psi	$\tau_F = 6730$ psi	
$\epsilon_1 = 0.45 \times 10^{-3}$	$\gamma_1 = 1.6 \times 10^{-3}$	

Properties of Metlbond 329 on aluminum adherends (standard strain rate, 160°F):

Tensile	Shear	Lap Shear
$E^* = 6.5 \times 10^5$ psi	$G = 3.12 \times 10^5$ psi	fracture = 2395 psi
P.E.L. = 1270 psi	P.E.L. = 287 psi	
$\sigma_{mys} = 2000$ psi	$\tau_{mys} = 538$ psi	
$\sigma_F = 5070$ psi	$\tau_F = 5830$ psi	
$\epsilon_1 = 0.74 \times 10^{-3}$	$\gamma_1 = 2.75 \times 10^{-3}$	

Properties of Metlbond 329 on aluminum adherends (low strain rate, 160°F):

Tensile	Shear	Lap Shear
$E^* = 5.95 \times 10^5$ psi	$G = 3.12 \times 10^5$ psi	fracture = 2435 psi
P.E.L. = 750 psi	P.E.L. = 304 psi	
σ_{mys} = 1450 psi	τ_{mys} = 630 psi	
σ_F = 4450 psi	τ_F = 6400 psi	
$\epsilon_1 = 0.78 \times 10^{-3}$	$\gamma_1 = 2.35 \times 10^{-3}$	

The higher test temperature lowered the modulus values and decreased the strength levels. Reducing the strain rate accentuated that trend.

Phase IX, Ageing/Environment

Tensile properties of FM1000 on titanium adherends:

	Fresh Adhesive	Aged 4 Months Controlled	Aged 8 Months Controlled	Aged 4 Months Uncontrolled	Aged 12 Months Controlled
E* (psi)	6.3×10^5	5.0×10^5	6.1×10^5	4.8×10^5	2.5×10^5
P.E.L.	1510 psi	890 psi	1800 psi	1250 psi	475 psi
σ_{mys}	3100 psi	1525 psi	3560 psi	3190 psi	1530 psi
σ_F	10,030 psi	10,850psi	9050 psi	10,075psi	7100 psi
ϵ_1	1.26×10^{-3}	1.95×10^{-3}	0.71×10^{-3}	1.0×10^{-3}	8.2×10^{-3}
lap shear fracture	7075 psi	-	2290 psi	3880 psi	4100 psi

The effects due to ageing were more pronounced for the lap shear specimens than for the tensile tests.

Nonuniform Bond-Line Effects

The effects due to introducing nonuniform bond-line configurations are summarized in Table XXXXII. The most striking influence of nonuniformity was the large reduction in viscoelastic strain (both ϵ_1 and γ_1). Generally the modulus values were raised, with only small changes in the strength levels. The fracture stress values were not significantly changed.

TABLE XXXXII. EFFECTS OF NONUNIFORM BOND LINES

PHASE	TENSILE					SHEAR				
	E^*	P.E.L.	σ_{mys}	σ_F	ϵ_1	G	P.E.L.	τ_{mys}	τ_F	γ_1
I (Al) Base-Line	N	L	L	N	L	R	R	N	N	L*
II (Ti) Adherend	N	L	L	N	N	R	L	L	L	L
III (Ti) Cryogenic (Al)	N R	N R	N N	N R	- -	R N	R N	L N	N N	- -
IV (Al) Strain Rate	R	N	N	N	R @ low $\dot{\epsilon}$ L @ high $\dot{\epsilon}$	R	N	N	N	L* @ both $\dot{\gamma}$
V (Al) Cryogenic/Strain Rate	R	L	N	N	-	R	N	L	L	-
VI (Al) Bond-Line Thickness Thin Thick	- -	R L	N L	N N	L* L*	N N	L N	L L	N N	L* L*
VII (Al) High Temp. VIII (Al) High Temp/Strain Rate	R	L	L	L	L	R	L	L	L	L

L* = strongly lowered L = lowered N = not changed R = raised

CONCLUSIONS

Based on the test results and their interpretation, the following conclusions have been drawn:

1. Tapered bond lines do not degrade the basic properties of the adhesive, the fracture stress is not reduced, the mode of failure is not changed, and the values for the precision elastic limit and microyield stress remain largely unchanged. Some property values are improved, such as the modulus, which is usually slightly increased. The largest improvement is a marked reduction of viscoelastic strain following a load-unload cycle.

2. Poor bonding and curing practices and out-of-date adhesive have the most damaging effects on bonded joint properties.

3. Deviations from perfectly elastic behavior occur at surprisingly low stress values. However, much of that strain is recovered within two minutes after unloading.

4. The elastic limits are much lower for shear loading than for tensile loading, and the viscoelastic strain is greater for shear (γ_1) than for tension (ϵ_1).

5. Within the range of variables used here, temperature had a larger influence on the properties than did the change in strain rate.

6. Raising the test temperature has the same general effects as decreasing the strain rate. Conversely, a lower test temperature causes the same kind of changes as raising the strain rate. Both sets of effects are due to modifications in the viscoelastic strain mechanisms.

7. Temperature excursions below the curing temperature do not change the room-temperature property values.

8. Ageing of FM1000 for 12 months at 68°F with a relative humidity of 45 percent produced a marked decrease in the tensile properties.

LITERATURE CITED

1. Hughes, E.J., Rutherford, J.L., Bossler, F.C., CAPACITANCE METHODS FOR MEASURING PROPERTIES OF ADHESIVES IN BONDED JOINTS, Rev. Sci. Inst., Vol. 39, No. 5, May 1968.

2. Bossler, F.C., Franzblau, M.C., Rutherford, J.L., TORSION APPARATUS FOR MEASURING SHEAR PROPERTIES OF ADHESIVE BONDED JOINTS, Brit. Jour. Sci. Inst. (J. of Phys. E), Vol. 1, Series 2, 1968.

3. Rutherford, J.L., Bossler, F.C., Hughes, E.J., ON MEASURING THE PROPERTIES OF ADHESIVES IN BONDED JOINTS, Society Aerospace and Material Process Engineers, 14th Nat. Symp., Nov. 1968.

Unclassified

Security Classification

DOCUMENT CONTROL DATA - R & D

(Security classification of title, body of abstract and indexing annotation must be entered when the overall report is classified)

1. ORIGINATING ACTIVITY (Corporate author)	2a. REPORT SECURITY CLASSIFICATION
Kearfott Division Singer-General Precision, Inc. Little Falls, New Jersey	Unclassified 2b. GROUP

3. REPORT TITLE

Study of the Performance of Adhesive Bonded Joints

4. DESCRIPTIVE NOTES (Type of report and inclusive dates)

Final Report; 12 June 1969 through 12 June 1970

5. AUTHOR(S) (First name, middle initial, last name)

Harold K. Shen and John L. Rutherford

6. REPORT DATE	7a. TOTAL NO. OF PAGES	7b. NO. OF REFS
November 1970	147	3

8a. CONTRACT OR GRANT NO.	9a. ORIGINATOR'S REPORT NUMBER(S)
DAAJ02-69-C-0094	USAAVLABS Technical Report 70-65
b. PROJECT NO. Task 1F162204A17001	
c.	9b. OTHER REPORT NO(S) (Any other numbers that may be assigned this report)
d.	Final Report RC 70-3

10. DISTRIBUTION STATEMENT

This document is subject to special export controls, and each transmittal to foreign governments or foreign nationals may be made only with prior approval of U.S. Army Aviation Materiel Laboratories, Fort Eustis, Virginia 23604.

11. SUPPLEMENTARY NOTES	12. SPONSORING MILITARY ACTIVITY
	U.S. Army Aviation Materiel Laboratories Fort Eustis, Va.

13. ABSTRACT

The purpose of this work was to observe the effects of selected experimental and material variables on the performance of metal/metal adhesive bonded joints. Three adhesives were used: FM1000, EC2214 and Metlbond 329 with aluminum and titanium adherends. The major experimental variables were test temperature and strain rate. Material variables included composition of adhesive, adherend material, bond-line thickness and tapered bond lines. The following properties were determined for tensile and shear loading: modulus, microyield stress, precision elastic limit, viscoelastic flow, and fracture behavior. Lap shear properties were also measured. The strains were determined using a high sensitivity capacitance-type extensometer.

It was found that the tapered bond lines did not degrade the properties; in fact, the viscoelastic flow was considerably reduced. The adhesives at 72°F, and higher, were elastic only up to about 5 to 15 percent of the fracture stress. The elastic limits were lower and the viscoelastic flow was higher for shear loading than for tension. Raising the test temperature and lowering the strain rate produce similar effects. Temperature cycles below the curing temperature did not influence the room-temperature properties. Poor bonding procedures and out-of-date adhesives provided the most damaging effects on the properties.

DD FORM 1 NOV 68 1473 REPLACES DD FORM 1473, 1 JAN 64, WHICH IS OBSOLETE FOR ARMY USE.

Unclassified

Security Classification

Unclassified
Security Classification

14. KEY WORDS	LINK A		LINK B		LINK C	
	ROLE	WT	ROLE	WT	ROLE	WT
Adhesives						
Adhesive-bonded joints						
Micromechanical properties						
Epoxy adhesives						
Extensometer						
Aerospace technology						
Microstrain techniques						
Thin film joints						
Tensile modulus						
Shear modulus						
Precision elastic limit						
Fracture stress						
Mode of fracture						
Elastic deformation						
Tapered joints						
Viscoelasticity						
Lap shear						
Strain rate						
Bond-line thickness						
Cross-head speed						

Unclassified
Security Classification